This Dissertation

entitled

EVENT TRIGGERED STATE ESTIMATION AND CONTROL WITH LIMITED COMMUNICATION

typeset with NDdiss2$_\varepsilon$ v3.2013 (2013/04/16) on June 14, 2013 for

Lichun Li

This LaTeX 2$_\varepsilon$ classfile conforms to the University of Notre Dame style guidelines as of Fall 2012. However it is still possible to generate a non-conformant document if the instructions in the class file documentation are not followed!

> Be sure to refer to the published Graduate School guidelines at `http://graduateschool.nd.edu` as well. Those guidelines override everything mentioned about formatting in the documentation for this NDdiss2$_\varepsilon$ class file.

It is YOUR responsibility to ensure that the Chapter titles and Table caption titles are put in CAPS LETTERS. This classfile does *NOT* do that!

This page can be disabled by specifying the "`noinfo`*" option to the class invocation.* (i.e.,`\documentclass[...,noinfo]{nddiss2e}`)

This page is *NOT* part of the dissertation/thesis. It should be disabled before making final, formal submission, but should be included in the version submitted for format check.

NDdiss2$_\varepsilon$ documentation can be found at these locations:

`http://www.gsu.nd.edu`
`http://graduateschool.nd.edu`

EVENT TRIGGERED STATE ESTIMATION AND CONTROL WITH LIMITED COMMUNICATION

A Dissertation

Submitted to the Graduate School
of the University of Notre Dame
in Partial Fulfillment of the Requirements
for the Degree of

Doctor of Philosophy

by

Lichun Li

Michael Lemmon, Director

Graduate Program in Department of Electrical Engineering
Notre Dame, Indiana

June 2013

EVENT TRIGGERED STATE ESTIMATION AND CONTROL WITH LIMITED COMMUNICATION

Abstract

by

Lichun Li

Control systems are becoming more efficient, more sustainable and less costly by the convergence with networking and information technology. The limitation of transmission frequency and instantaneous bit-rate on most networks, however, can degrade or even destroy control systems. To maintain system performance with the limited transmission frequency and limited instantaneous bit-rate, event triggered transmission, with which transmission is triggered by a certain event, is proposed. Our research is to analytically examine the tradeoff among system performance, transmission frequency, and instantaneous bit-rate in event triggered systems.

We first study the optimal communication rule which minimizes mean square state estimation error with limited transmission frequency. It is shown that the optimal communication rule is event triggered transmission. Because the optimal event trigger is difficult to compute, computationally efficient suboptimal event trigger is presented. Our simulation results show that we can compute tighter upper bounds on the suboptimal costs and tighter lower bounds on the optimal costs than prior work, while guaranteeing comparative actual costs. Based on the same idea, computationally efficient weakly coupled suboptimal event triggers are also designed for output feedback control systems to minimize the mean square state with limited transmission frequency.

The work above, however, only considers limited transmission frequency. We, then, consider both the limited transmission frequency and limited instantaneous bit-rate in event triggered control systems to guarantee input-to-state stability and resilience, respectively. To guarantee input-to-state stability, a minimum inter-sampling interval and a sufficient instantaneous bit-rate are provided. Besides, we also give a sufficient condition of efficient attentiveness, i.e. longer inter-sampling interval and lower instantaneous bit-rate can be achieved when the system state gets closer to the origin. To guarantee resilience to transient unknown magnitude disturbance, detailed algorithms and required sufficient instantaneous bit-rate are presented. Our simulation results demonstrate the resilience of event triggered systems to transient unknown magnitude disturbances.

CONTENTS

FIGURES

TABLES

CHAPTER 1

INTRODUCTION

The use of networking and information technology in control systems is making our world *smart*. *'Smart grid'* is expected to address the major challenges, such as generation diversifications, demand response, energy conservation, environmental compliance, and so on, of the existing electricity grid [28, 18]. *'Smart manufacturing system'* promises to reduce time-to-market, drive greater exports due to lower production costs, and minimize energy use and materials while maximizing environmental sustainability [58]. *'Smart health-care system'* provides continuous monitoring of patients, and minimizes the need of care-givers and helps the chronically ill and elderly to survive an independent life [1]. *'Smart farms'* optimally and sustainably manage the water and land resources in agriculture [68].

While the integration of networking and information technology into control systems has the potential to reduce cost, increase operational efficiency, and promote sustainability, there are two challenges in NIT-enabled control systems. The first challenge is *the limited transmission frequency*. Many NIT-enabled control systems make use of wireless sensor networks which usually has limited power [2, 10, 55]. Since data transmission consumes significantly more energy than data processing [50], the transmission frequency needs to be trimmed to prolong the network lifetime. The second challenge is *the limited instantaneous bit-rate*. Networks, especially wireless networks, have limited bandwidth, which means that there are only finite number of bits in one packet, and this packet is transmitted with non-negligible delay. Since both the limited transmission frequency and the limited instantaneous rate can dam-

age or degrade control systems [23], how to maintain system performance with limited communication becomes a knotty problem.

To address this knotty problem, event triggered transmission was raised. Instead of deciding the transmission times ahead of time as is done with periodic transmission, event triggered transmission uses on line information to detect the advent of an event which triggers a transmission. There has been numerous experimental results to show shown that the event triggered transmission can significantly reduce the transmission frequency while maintaining comparable system performance as periodic transmission [5, 6, 59, 64, 15, 3, 44, 67, 63]. But little substantive work analytically investigate the tradeoff between system performance and transmission frequency, and the challenge of limited instantaneous bit-rate was totally ignored by the prior work. *Our research is to analytically examine the tradeoff among system performance, transmission frequency, and instantaneous bit-rate in event triggered state estimation and control systems.*

One of the interesting questions about the tradeoff is what the best system performance is for given limited transmission frequency. This question was first studied in [29, 54] for minimum mean square state estimation error problem in finite horizon during which only a finite number of transmissions were allowed. This problem was treated as an optimal problem in a Markov decision process [53, 25], and the decision to be made at each step is whether to transmit data. By dynamic programming, both [29] and [54] showed that the optimal communication rule was event triggered. At the same time, [70] explored the infinite horizon case. Instead of restricting the number of transmissions over a finite horizon, [70] assumed a cost for each transmission, and studied the optimal stochastic communication rule which minimized the average mean square state estimation error discounted by the transmission cost. In this case, the decision to be made at each step is the probability of transmission. The optimal communication rule was shown, again, to be event triggered.

The optimal event trigger, however, is difficult to compute because of the curse of dimensionality in dynamic programming. So, computationally efficient suboptimal event trigger is of interest. Most prior work approximated the value function with a quadratic function or a set of quadratic functions, and then used the LMI toolbox to efficiently compute the suboptimal event trigger [40, 35, 14, 12]. Although upper bounds on the suboptimal cost were always provided, only [14] characterized how far away its suboptimal cost was from the optimal cost by providing a lower bound on the optimal cost. Even in this case, the lower bound on the optimal cost is only effective for stable systems.

Instead of using quadratic functions, we used polynomials to approximate the value functions, and provided computationally efficient suboptimal event trigger, an upper bound on the suboptimal cost and a lower bound on the optimal cost [39, 37], which will be presented in Chapter 2. These computationally efficient event trigger and bounds on the costs are computed by searching for the solution of a set of linear polynomial inequalities. The linear polynomial inequalities are transformed to a semi-definite programming through the sum of squares decomposition of polynomials [11], and hence efficiently solved. Our simulation results show that we can compute tighter upper bounds on the suboptimal costs and tighter lower bounds on the optimal costs than the prior work [14, 12, 35], while guaranteeing comparative actual costs as the prior work [14, 12, 35].

After introducing the computationally efficient suboptimal event trigger for state estimation problem, we will introduce *computationally efficient* suboptimal event triggers for observer based output feedback control problem in Chapter 3 based on our work in [36, 42]. The suboptimal event triggers are weakly coupled, which means that the event trigger at the sensor and the event trigger at the controller are based on local information only, the transmission at the sensor does not necessarily trigger the transmission at the controller, and vice versa. This weakly coupled event trigger

design represents an advance over the recent work in event-triggered output feedback control where transmission from the controller subsystem was tightly coupled to the receipt of event-triggered sensor data [16], especially in multi-sensor networked control systems.

All the work above only analyzes the tradeoff between system performance and transmission frequency. The influence of limited instantaneous bit-rate is ignored. To analyze the tradeoff among system performance, transmission frequency and instantaneous bit-rate, Chapter 4 and 5 explicitly consider not only inter-sampling interval, but also quantization and network delay to achieve input-to-state stability (ISS) and resilience, respectively.

Event triggered systems usually generate sporadic data packets. If properly designed, longer inter-sampling interval and lower instantaneous bit-rate can be achieved if the system state gets closer to the origin. This property is called *efficient attentiveness*. Since for most of the time, the system state lies in a neighborhood of its equilibrium, efficiently attentive event triggered systems only require infrequent transmission and low instantaneous bit-rate to maintain system performance. Efficient attentiveness, however, is not a necessary property of event triggered systems, a counter example was provided in [38].

Chapter 4 concludes our research in [66, 41, 43], provides a sufficient condition to guarantee efficient attentiveness, and obtains the minimum inter-sampling interval and a sufficient instantaneous bit-rate to guarantee ISS. Quantization error and the acceptable delay that preserving ISS are explicitly studied. Different from the prior work which considered constant bounded delay [71, 72, 20, 33], the acceptable delay we present is state dependent. In our simulation, the required instantaneous bit-rate increases sharply as the inter-sampling interval increases. This fact indicates that with limited bandwidth, we should not only focus on lengthening inter-sampling interval, but also need to guarantee that the channel bandwidth satisfies the required

instantaneous bit-rate.

Efficiently attentive event triggered systems can have long inter-sampling interval when the system state is close to its equilibrium. A prime concern about this long inter-sampling interval is whether event triggered control systems are resilient to unexpected disturbances which appear between two consecutive transmissions. By 'resilience', we mean that the system's ability to return to its operational normalcy in the presence of unexpected disturbances.

Chapter 5 addresses the resilience issue in an event triggered scalar nonlinear system with transient unknown magnitude disturbances. When the system is in normal situation, a necessary instantaneous bit-rate and a sufficient instantaneous bit-rate are given to assure uniform boundedness. If the system was linear, it was shown that the sufficient bit-rate achieves the necessary bit-rate. When the system is hit by transient unknown magnitude disturbances, a sufficient instantaneous bit-rate is provided to guarantee resilience, i.e. return to a neighborhood of the origin in a finite time.

CHAPTER 2

MINIMUM MEAN SQUARE STATE ESTIMATION ERROR WITH LIMITED TRANSMISSION FREQUENCY

2.1 Introduction

Because of the very limited bandwidth in wireless channels, most wireless networked control systems have communication constraints, especially when the sensors are battery driven. Since wireless communication is a major source of power consumption [55, 57, 2], efficient management of wireless communication is very important to extend the working life of the whole wireless networked control systems.

To efficiently manage the wireless communication, some prior work [30, 54] searched for the optimal communication rule which minimized the mean square state estimation error under the communication constraint that only a limited number of transmissions were allowed in a finite horizon. The optimal communication rule was shown to be event triggered. Under Event triggered communication rule, transmission occurs only if some event occurs. Prior work in [5, 6, 59, 64, 45, 3, 24, 15] has shown the advantage of event triggered communication over periodic communication on reducing transmission frequency while maintaining system performance. The optimal event trigger, however, is computationally complicated. This computational complexity limited [30] and [54] to scalar cases. At the same time, [70] studied the optimal communication rule which minimized the average mean square state estimation error discounted by the transmission cost in infinite horizon. The optimal communication rule was still event triggered, and difficult to compute.

Because of the computational complexity of the optimal event trigger, computationally efficient suboptimal event triggers are of interest. For finite horizon cases, [40] provided a quadratic suboptimal event trigger which involved backward recursive matrix multiplication. For infinite horizon cases, [14] also provided a quadratic suboptimal event trigger, but this quadratic suboptimal event trigger was only for stable systems. Later, [12] and [35] presented suboptimal event triggers for both stable and unstable systems based on linear matrix inequalities (LMI). Although all these prior work [40, 14, 12, 35] gave upper bounds on their suboptimal costs, only [14] characterized how far away its suboptimal cost was from the optimal cost by giving a lower bound on the optimal cost, and this lower bound was only effective in stable systems.

This chapter presents not only computationally efficient suboptimal event trigger and an upper bound on its cost, but also computationally efficient lower bound on the optimal cost. All of them are effective for both stable and unstable systems, and computed based on linear polynomial inequalities. Linear polynomial inequalities can be transformed to a semi-definite programming (SDP) based on sums of squares (SOS) decomposition of polynomials through SOSTOOLS [52], and hence efficiently solved by SeDuMi [8] or SDPT3 [62]. Our simulation results show that we can compute tighter upper bounds on the suboptimal costs and tighter lower bounds on the optimal costs than the prior work [14, 12, 35], while guaranteeing comparative actual costs as the prior work [14, 12, 35].

Later, we apply the polynomial event triggers to an 8 dimensional 3 degree of freedom (3DOF) helicopter. To our best knowledge, this is the first time the suboptimal event trigger has been applied to a system whose dimension is greater than 2. Our simulation results show that with polynomial event triggers, the 3DOF helicopter tracked the reference signal with small overshoot and no steady error. This event triggered helicopter used less communication resource than periodically triggered he-

licopter with comparable performance, and bore the same amount of transmission delay as the periodically triggered helicopter while maintaining the system performance.

2.2 Background on Average Optimality for Markov Control Processes

This section presents the existing work on *average optimality* for *Markov control processes*, since this existing work is the basis for the main results in this chapter.

A **Markov control process**, which is also called *Markov decision process* [**?**] or *controlled Markov process* [17], is a stochastic dynamical system specified by the five-tuple [4, 25]

$$\{\mathbf{X}, \mathbf{A}, \{A(x)|x \in \mathbf{X}\}, Q(\cdot|x \in \mathbf{X}, a \in \mathbf{A}), c\}\,, \tag{2.1}$$

where

- $\mathbf{X}$ is a Borel space (e.g. $\mathbb{R}^n$, finite set, and countable set), called the *state space*;
- $\mathbf{A}$ is a Borel space, called the *action space*;
- $A(x)$ is a non-empty measurable subset of $\mathbf{A}$, denoting the set of all feasible actions when the system is in state $x \in \mathbf{X}$. Suppose that the set of *feasible state-action pairs*

  $$\mathbf{K} = \{(x, a)|x \in \mathbf{X}, a \in A(x)\}$$

  is also a Borel space;
- Q is a conditional probability function on $\mathbf{X}$ given $\mathbf{K}$, called the *transition law*. Let D be a Borel set of $\mathbf{X}$, and $\{x(t), t \in \mathbb{N}_0\}$ and $\{a(t), t \in \mathbb{N}_0\}$ be stochastic processes. $Q(D|x(t), a(t)) = P(x(t+1) \in D|x(t), a(t))$, where P is the cumulative probability function.
- $c : \mathbf{K} \to \mathbb{R}$ is the (measurable) *one-stage cost function*.

Given a Markov control process described as above, an action at step t is decided based on all the history state and action information. Let $\mathbf{H}(t)$ denote the *admissible*

history up to time t. It is defined as

$$\mathbf{H}(0) = \mathbf{X}, \mathbf{H}(t+1) = \mathbf{H}(t) \times \mathbf{K}, \forall t \in \mathbb{N}_0.$$

An element $h(t)$ of $\mathbf{H}(t)$ is a vector of the form

$$h(t) = (x(0), a(0), \ldots, x(t-1), a(t-1), x(t)).$$

An **admissible control strategy** or **policy** is a sequence $\pi = \{\pi(\cdot, t|\cdot), t \in \mathbb{N}_0\}$ of stochastic kernel $\pi(t)$ on the action space $\mathbf{A}$ given $\mathbf{H}(t)$ satisfying the constraint

$$\pi(A(x(t)), t|h(t)) = 1, \forall h(t) \in \mathbf{H}(t), t \in \mathbb{N}_0. \tag{2.2}$$

The set of all policies is denoted by Π.

Generally, the action $a(t)$ is a random variable in action space $\mathbf{A}$. $\pi(\cdot, t|h(t))$ characterize the probability distribution of $a(t)$ given $h(t)$. Equation (2.2) indicates that all possible actions produced by an (admissible) policy π are in the feasible action set $A(x(t))$.

A specific case is that A policy becomes deterministic and stationary. A policy π is said to be a **deterministic stationary policy** if there is a function $f : \mathbf{X} \to \mathbf{A}$ with $f(x) \in A(x)$ for all $x \in \mathbf{X}$ such that

$$\pi(f(x(t)), t|h(t)) = \pi(f(x(t))|x(t)) = 1, \forall h(t) \in \mathbf{H}(t), \forall t \in \mathbb{N}_0.$$

f is said to be a deterministic stationary rule.

Given a Markov control process and a policy π, the expected long-run **average**

cost incurred by π is given by

$$V(\pi, x) = \limsup_{N\to\infty} E\left[\frac{1}{N}\sum_{t=0}^{N-1} c(x(t), a(t))\right],$$

where $a(t)$ is the action taken at step t, and the average optimal value function $V^*(x)$ is as follows:

$$V^*(x) = \inf_{\pi\in\Pi} V(\pi, x).$$

First, we state the conditions for the existence of an average optimal deterministic stationary policy. The first condition is a Lyapunov-like condition.

Assumption 2.2.1 (**Lyapunov-like condition**). *1. There exist constants $b > 0$ and $\beta \in (0, 1)$, and a (measurable) function $\omega(x) \geq 1$ for all $x \in \mathbf{X}$ such that*

$$\int_{\mathbf{X}} \omega(y)Q(dy|x, a) \leq \beta\omega(x) + b, \forall (x, a) \in \mathbf{K}.$$

2. There exists a constant $M > 0$, such that $|c(x, a)| \leq M\omega(x)$ for all $(x, a) \in \mathbf{K}$.

The second condition is a continuity condition on the action space.

Assumption 2.2.2 (**Continuity condition on action space**). *For any state $x \in \mathbf{X}$,*

1. The feasible action set $A(x)$ is compact.

2. The one-state cost function $c(x, a)$ is lower semi-continuous in $a \in A(x)$;

3. The function $a \mapsto \int_{\mathbf{X}} \upsilon(y)Q(dy|x, a)$ is continuous on $A(x)$ for all bounded measurable functions υ on $\mathbf{X}$.

Remark 2.2.3. *Assumption 2.2.2 holds when $A(x)$ is finite for all $x \in \mathbf{X}$.*

For the function $\omega > 1$ in Assumption 2.2.1, let us first define a Banach space

$\mathbf{B}_\omega(\mathbf{X})$ as

$$\mathbf{B}_\omega(\mathbf{X}) = \{\nu : \sup_{x\in\mathbf{X}} \omega(x)^{-1}|\nu(x)| < \infty\}.$$

The third condition is a uniform boundedness condition on parameter α which is described as the following.

Assumption 2.2.4 (**Uniform boundedness condition w.r.t.** α)**.** *There exist two functions* $\nu_1,\ \nu_2 \in B_\omega(\mathbf{X})$*, and some state* $x_0 \in \mathbf{X}$*, such that*

$$\nu_1(x) \le h_\alpha(x) \le \nu_2(x), \forall x \in \mathbf{X}, \forall \alpha \in (0,1),$$

where $h_\alpha(x) = V_\alpha^*(x) - V_\alpha^*(x_0)$*, and* $V_\alpha^*(x) = \min_{a\in A(x)} E\left[\sum_{t=0}^{\infty} \alpha^t c(x(t), a(t))\right]$ *is the minimum discounted cost satisfying*

$$V_\alpha^*(x) = \min_{a\in A(x)} \left\{ c(x,a) + \alpha \int_{\mathbf{X}} V_\alpha^*(y) Q(dy|x,a) \right\}, \tag{2.3}$$

for all $x \in \mathbf{X}$*.*

We now give the main results about average optimality. Please check Theorem 4.1 of [22] for the proofs of Lemma 2.2.5 and Corollary 2.2.6 and 2.2.7.

Lemma 2.2.5 (**Average optimality**)**.** *Under Assumption 2.2.1, 2.2.2, and 2.2.4, the following assertions hold.*

1. *There exist a unique constant* J^**, two functions* h_1^**,* h_2^**, and a deterministic stationary rule* f^**, such that for all* $x \in \mathbf{X}$ *the* two average cost optimality inequalities *hold.*

$$J^* + h_1^*(x) \le \min_a \left\{ c(x,a) + \int_{\mathbf{X}} h_1^*(y) Q(dy|x,a) \right\} \tag{2.4}$$

$$J^* + h_2^*(x) \ge \min_a \left\{ c(x,a) + \int_{\mathbf{X}} h_2^*(y) Q(dy|x,a) \right\} \tag{2.5}$$

$$= c(x, f^*(x)) + \int_{\mathbf{X}} h_2^*(x) Q(dy|x, f^*(x)) \tag{2.6}$$

2. $J^* = V^*(x)$ *for all* $x \in \mathbf{X}$.

3. *Any deterministic stationary rule* f *realizing the minimum of (2.5) is average optimal; thus,* f^* *in (2.6) is a deterministic stationary policy for the average cost problem.*

Corollary 2.2.6 (**Lower bounds on optimal costs**). *Under Assumption 2.2.1, 2.2.2, and 2.2.4, the following assertions hold.*

1. *There exist a constant* $\underline{J}$ *and a function* h_1*, such that for all* $x \in \mathbf{X}$

$$\underline{J} + h_1(x) \leq \min_{a \in A(x)} \left\{ c(x,a) + \int_{\mathbf{X}} h_1(y) Q(dy|x,a) \right\}.$$

2. $J^* \geq \underline{J}$.

Corollary 2.2.7 (**Suboptimal event triggers and the corresponding upper bounds**). *Under Assumption 2.2.1, 2.2.2, and 2.2.4, the following assertions hold.*

1. *There exist a constant* $\overline{J}$*, a function* h_2*, and a deterministic stationary rule* f*, such that for all* $x \in \mathbf{X}$

$$\begin{aligned} \overline{J} + h_2(x) \geq & \min_{a \in A(x)} \left\{ c(x,a) + \int_{\mathbf{X}} h_2(x) Q(dy|x,a) \right\} \\ = & c(x, f(x)) + \int_{\mathbf{X}} h_2(x) Q(dy|x, f(x)). \end{aligned}$$

2. $V(f,x) \leq \overline{J}$.

Remark 2.2.8. *Similar results to that of Corollary 2.2.6 and 2.2.7 can also be found in [13].*

2.3 Background on SOSTOOLS

Our suboptimal event triggers are computed based on the solution of a set of polynomial inequalities. Since SOSTOOLS automatically transforms polynomial inequalities to a semi-definite program (SDP) based on the sums of squares decomposition (SOS) of polynomials, we can use SOSTOOLS to efficiently compute the

suboptimal event trigger. In this section, we presents a brief review of the basic idea of **SOSTOOLS**.

Let $\mathbf{x} \in \mathbb{R}^n$ and $\alpha_i \in \mathbb{R}^n$. $\mathbf{x}^{\alpha_i} = \mathbf{x}_1^{\alpha_{i,1}} \cdot \ldots \cdot \mathbf{x}_n^{\alpha_{i,n}}$. A polynomial $p(\mathbf{x})$ of N terms can be expressed as

$$p(\mathbf{x}) = \sum_{i=1}^{N} a_i \mathbf{x}^{\alpha_i}.$$

A polynomial $p(\mathbf{x})$ is a **sum of squares** (SOS), if there exist polynomials $f_1(\mathbf{x}), \ldots, f_m(\mathbf{x})$ such that

$$p(\mathbf{x}) = \sum_{i=1}^{m} f_1^2(\mathbf{x}).$$

This SOS condition is equivalent to the existence of a positive semi-definite matrix B such that [11, 51, 49]

$$p(\mathbf{x}) = \overline{\mathbf{x}}^T B \overline{\mathbf{x}},$$

where $\overline{\mathbf{x}}$ is some properly chosen vector of monomials with $\overline{\mathbf{x}}_i = \mathbf{x}^{\beta_i}$. At this point, the **SOS decomposition** of the polynomial $p(\mathbf{x})$ is the same as finding a symmetric matrix B such that

$$\sum_{\beta_i + \beta_j = \alpha_k} B_{i,j} = a_k, \text{for all } k = 1, \ldots, N,$$

$$B \geq 0.$$

This is a SDP problem, and hence can be efficiently solved by SeDuMi [8] or SDPT3 [62].

Based on the SOS decomposition and the SDP, **SOSTOOLS** automatically converts polynomial inequalities to SDP, calls the SDP solver (SeDumi or SDPT3), and

converts the SDP solution back to the solution of the original polynomial inequalities. The basic feasibility problem that the SOSTOOLS solves is formulated as finding polynomials $p_i(\mathbf{x})$ for $i = 1, 2, \ldots, N$, such that

$$a_{0,j}(\mathbf{x}) + \sum_{i=1}^{N} p_i(\mathbf{x}) a_{i,j}(\mathbf{x}) = 0, \text{ for } j = 1, 2, \ldots, \hat{J} \tag{2.7}$$

$$a_{0,j}(\mathbf{x}) + \sum_{i=1}^{N} p_i(\mathbf{x}) a_{i,j}(\mathbf{x}) \geq 0, \text{ for } j = \hat{J}+1, \ldots, J, \tag{2.8}$$

where $a_{i,j}(\mathbf{x})$ are given scalar constant coefficient polynomials.

SOSTOOLS also solves the problem of optimizing of an objective function which is linear in the coefficients of $p_i(x)$'s. This optimization problem is formulated as searching for $p_i(x)$ for $i = 1, 2, \ldots, N$ that

$$\min_{c} w^T c \tag{2.9}$$

$$\text{subject to: equation (2.7) and (2.8)},$$

where w is a given weight vector, and c is a vector consisting of the coefficients of $p_i(x)$'s.

To define and solve an SOS programming using SOSTOOLS, please check Chapter 2 of [52].

2.4 Event Triggered State Estimation problem

Consider a state estimation system shown in Figure 2.1. The plant is a discrete time, linear, time invariant system described by the following difference equation.

$$x(k) = Ax(k-1) + w(k-1),$$
$$y(k) = Cx(k) + v(k), \text{for } k = 1, 2, \ldots, \infty.$$

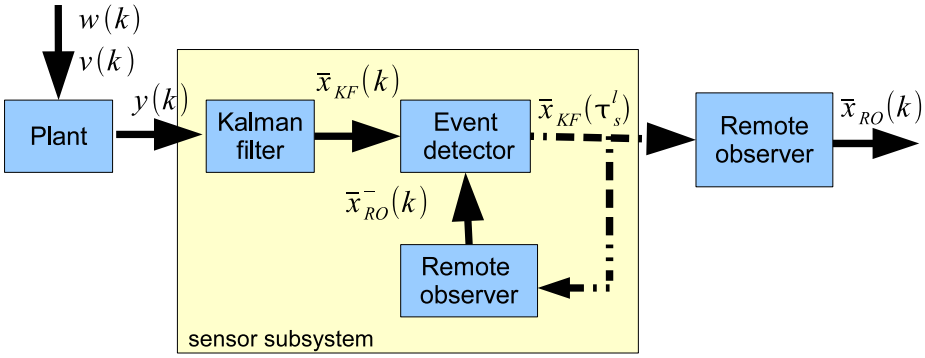

Figure 2.1. Structure of the event triggered state estimation systems

where $x \in \mathbb{R}^n$ is the state with its initial condition Gaussian distributed with mean μ_0 and variance π_0, $y \in \mathbb{R}^p$ is the measurement, $w \in \mathbb{R}^n$ is a zero mean white Gaussian noise process with variance W, and $v \in \mathbb{R}^p$ is another zero mean white Gaussian noise process with variance V. These two noise processes and the initial state are independent with each other.

The measurements are first processed by a Kalman filter

$$\overline{x}_{KF}(k) = A\overline{x}_{KF}(k-1) + L\left[y(k) - CA\overline{x}_{KF}(k-1)\right] \tag{2.10}$$

where L is the Kalman gain. The steady state estimation error $\overline{e}_{KF}(k) = x(k) - \overline{x}_{KF}(k)$ is a Gaussian random variable with zero mean and variance Q. Besides a Kalman filter, a remote observer is also built in the sensor subsystem to generate an *a priori* remote state estimate $\overline{x}^-_{RO}$. The gap $e^-_{KF,RO}(k) = \overline{x}_{KF}(k) - \overline{x}^-_{RO}(k)$ is, then, used by the event detector to decide whether to transmit the current $\overline{x}_{KF}(k)$ to the remote observer. Let $a_s(k) = 1$ indicate the decision of transmitting $\overline{x}_{KF}(k)$, and 0 otherwise. We force $a_s(k) = 1$ if $\|e^-_{KF,RO}(k)\| > \theta$ for a large positive constant θ.

The remote observer produces an *a posteriori* remote state estimate $\overline{x}_{RO}(k)$ based

on the following difference equation.

$$\overline{x}_{RO}^{-}(k) = A\overline{x}_{RO}(k-1), \tag{2.11}$$

$$\overline{x}_{RO}(k) = \begin{cases} \overline{x}_{RO}^{-}(k), & \text{if } a_s(k) = 0; \\ \overline{x}_{KF}(k), & \text{if } a_s(k) = 1\ , \end{cases} \tag{2.12}$$

Let us define the remote state estimation error $e_{RO}(k)$ as

$$e_{RO}(k) = x(k) - \overline{x}_{RO}(k).$$

The average cost in this event triggered state estimation problem is

$$J(\{a_s(k)\}_{k=0}^{\infty}) = \lim_{N\to\infty} \frac{1}{N} \sum_{k=0}^{N-1} E\left(c(e_{RO}(k), a_s(k))\right), \tag{2.13}$$

where the cost function

$$c(e_{RO}(k), a_s(k)) = \|e_{RO}(k)\|_Z^2 + a_s(k)\lambda, \tag{2.14}$$

$\|e_{RO}(k)\|_Z^2 = e_{RO}(k)^T Z e_{RO}(k)$ with a given semi-positive definite $n \times n$ matrix Z, and λ is the communication price for one transmission.

Noticing that $e_{KF,RO}(k)$ is orthogonal to the filtered state error $e_{KF}(k)$ (please check Lemma A.0.1 in Appendix A for the proof), together with the dynamic behavior of $\overline{x}_{KF}$ and $\overline{x}_{RO}^{-}$, the average cost is rewritten as

$$J(\{a_s(k)\}_{k=0}^{\infty}) = \lim_{N\to\infty} \frac{1}{N} \sum_{k=0}^{N-1} E\left(c_n(e_{KF,RO}^{-}(k), a_s(k))\right) + trace(QZ),$$

where

$$c_n(e^-_{KF,RO}(k), a_s(k)) = a_s(k)\lambda + (1 - a_s(k))\|e^-_{KF,RO}(k)\|^2_Z.$$

Our objective is to find a transmission rule to minimize the average cost $J(\{a_s(k)\}_{k=0}^{\infty})$, i.e.

$$J^* = \min_{\{a_s(k)\}_{k=0}^{\infty}} J(\{a_s(k)\}_{k=0}^{\infty}). \tag{2.15}$$

2.5 The Optimal Event Trigger

This optimal problem was solved in [70], but the optimal solution is difficult to compute. For the completeness of this paper, we state the optimal solution in [70] without proof.

Theorem 2.5.1. *Let*

$$T_h(s,l) = E\left(h(e^-_{KF,RO}(k+1))|e^-_{KF,RO}(k) = s, a_s(k) = l\right),$$

where $s \in \mathbb{R}^n$ *and* $l \in \{0,1\}$.

1. *There exist a unique constant* ρ^* *and a function* h^*, *such that for all* $s \in \mathbb{R}^n$

$$\rho^* + h^*(s) = \min\left\{\|s\|^2_Z + T_{h^*}(s,0), \lambda + T_{h^*}(s,1)\right\}, \tag{2.16}$$

2. *The optimal cost* $J^* = \rho^* + trace(QZ)$.

3. *The optimal event trigger is*

$$a^*_s(k) = \begin{cases} 1, & \text{if } V_0(e^-_{KF,RO}(k)) \geq V_1(e^-_{KF,RO}(k)) \text{ or } \|e^-_{KF,RO}(k)\| > \theta, \\ 0, & \text{otherwise.} \end{cases}$$

where $V_0(s) = \|s\|^2_Z + T_{h^*}(s,0)$, *and* $V_1(s) = \lambda + T_{h^*}(s,1)$.

Remark 2.5.2. *It is hard to find a solution to equation (2.16). Although we can iteratively compute the solution of equation (2.16) by value iteration [21] or policy*

iteration [47, 26], the computational complexity increases exponentially with respect to the state dimension.

2.6 A Computationally Efficient Lower Bound on The Optimal Cost

Although the optimal cost is difficult to compute, we can efficiently compute a lower bound on the optimal cost based on SOSTOOLS. This section first gives a theorem about the lower bound on the optimal cost, and then discusses how to use SOSTOOLS to compute the largest lower bound on the optimal cost.

Theorem 2.6.1. *If there exists a constant ρ_1 and a polynomial function h_1, such that for all $s \in \mathbb{R}^n$*

$$\rho_1 + h_1(s) \leq \|s\|_Z^2 + T_{h_1}(s,0), \tag{2.17}$$

$$\rho_1 + h_1(s) \leq \lambda + T_{h_1}(s,1), \tag{2.18}$$

then $J^* \geq \underline{J}^* = \rho_1 + trace(QZ)$.

Proof. Equation (2.17) and (2.18) indicate that

$$\begin{aligned}
&\rho_1 + h_1(e^-_{KF,RO}(k)) \\
\leq &\min_{a_s(k)\in\{0,1\}} c_n(e^-_{KF,RO}(k), a_s(k)) + T_{h_1}(e^-_{KF,RO}(k), a_s(k)) \\
\leq &c_n(e^-_{KF,RO}(k), a_s(k)) + T_{h_1}(e^-_{KF,RO}(k), a_s(k))
\end{aligned}$$

The expected values of both sides of the above inequality satisfy

$$\begin{aligned}
&\rho_1 + E(h_1(e^-_{KF,RO}(k))) \\
\leq &E(c_n(e^-_{KF,RO}(k), a_s(k))) + E(h_1(e^-_{KF,RO}(k+1))).
\end{aligned}$$

Varying k from 0 to N, and adding all these inequalities together, we have, for all

feasible $\{a_s(k)\}_{k=0}^N$,

$$\begin{aligned}\rho_1 \leq & \frac{\sum_{k=0}^N E(c_n(e^-_{KF,RO}(k), a_s(k)))}{N} \\ & + \frac{E(h_1(e^-_{KF,RO}(N+1))) - E(h_1(e^-_{KF,RO}(0)))}{N}.\end{aligned} \tag{2.19}$$

Since $a_s(k)$ is forced to be 1 if $\|e^-_{KF,RO}(k)\| > \theta$, from equation (2.11) and (2.12), it is easy to see that

$$\|e^-_{KF,RO}(k)\| \leq \theta, \text{for all } k = 0, 1, \cdots .$$

Since h_1 is a polynomial, we know that $E(h_1(e^-_{KF,RO}(k))) < \infty$ for all $k = 0, 1, \cdots$, and

$$\rho_1 \leq \lim_{N\to\infty} \frac{1}{N} \sum_{k=0}^{N} E(c_n(e^-_{KF,RO}(k), a_s(k))),$$

for all feasible $\{a_s(k)\}_{k=0}^\infty$.

Therefore, $\rho_1 + traceQZ \leq J^*$. □

Remark 2.6.2. *Equation (2.17) and (2.18) are polynomial inequalities whose coefficients are linear combinations of the coefficients of h_1. It is easy to get the dynamic behavior of $e^-_{KF,RO}$ from equation (3.2), (2.11) and (2.12) as the following.*

$$e^-_{KF,RO}(k+1) = (1 - a_s(k))Ae^-_{KF,RO}(k) + L\tilde{y}(k) \tag{2.20}$$

where $\tilde{y}(k) = CAe_{KF}(k) + Cw(k) + v(k+1)$ is a zero mean Gaussian random variable with covariance $Y = CAQA^TC^T + CWC^T + V$.

Therefore, $T_{h_1}(s, 0) = E(h_1(s'))$ where s' is a Gaussian random variable with mean As and covariance Y, and $T_{h_1}(s, 1) = E(h_1(s'))$ where s' is a zero mean Gaussian random variable with covariance Y.

According to the Isserlis' theorem [1], $T_{h_1}(s,0)$ *and* $T_{h_1}(s,1)$ *are polynomials whose coefficients are linear combinations of the coefficients of* h_1.

So, Equation (2.17) and (2.18) are both polynomial inequalities whose coefficients are linear combinations of the coefficients of h_1.

Remark 2.6.3. *Since equation (2.17) and (2.18) are polynomial inequalities whose coefficients are linear combinations of the coefficients of* h_1*, the largest lower bound on the optimal cost can be efficiently computed by the following SOS programming.*

$$\min -\rho_1 \tag{2.21}$$

subject to: (2.17) and (2.18)

2.7 A Computationally Efficient Suboptimal Event Trigger

The last section talks about how to compute the largest lower bound on the optimal cost based on SOSTOOLS, but does not provide a computationally effective suboptimal event trigger. In this section, a suboptimal event trigger and an upper bound on its cost are provided, and an SOS based algorithm is given to efficiently search for the smallest upper bound on the suboptimal cost.

Theorem 2.7.1. *Let* $s^\phi = [s_1^\phi \ s_2^\phi \ \dots \ s_n^\phi]^T$*, where* $s \in \mathbb{R}^n$ *and* ϕ *is a positive integer. Given a positive constant* d*, and positive integers* ϕ *and* δ*, if there exist a constant* ρ_2*, and a* positive definite *polynomial function* h_2 *such that the following inequalities*

[1] [Isserlis' theorem:] If $(x_1, \dots, x_{2n})$ is a zero mean multivariate normal random vector, then

$$E(x_1 x_2 \cdots, x_{2n}) = \sum \prod E(x_i x_j),$$
$$E(x_1 x_2 \cdots, x_{2n-1}) = 0,$$

where the notation $\sum \prod$ means summing over all distinct ways of partitioning $x_1, \dots, x_{2n}$ into pairs. [31]

hold for all $s \in \mathbb{R}^n$,

$$(\|s\|_z^2 + T_{h_2}(s,0)) \left(1 - \frac{\|s^\phi\|_Z^2 - d}{500d}\right) \leq \rho_2 + h_2(s) \tag{2.22}$$

$$(\lambda + T_{h_2}(s,1))(\|s^\phi\|_Z^2 + \|s^{\phi+\delta}\|_Z^2) \leq (\rho_2 + h_2(s))(d + \|s^{\phi+\delta}\|_Z^2) \tag{2.23}$$

then there exists a suboptimal event trigger

$$a_{s,2}(k) = \begin{cases} 1, & \text{if } \bar{V}_0(e^-_{KF,RO}(k)) \geq \bar{V}_1(e^-_{KF,RO}(k)) \text{ or } \|e^-_{KF,RO}(k)\| > \theta, \\ 0, & \text{otherwise.} \end{cases}$$

where $\bar{V}_0(s) = \|s\|_Z^2 + T_{h_2}(s,0)$, *and* $\bar{V}_1(s) = \lambda + T_{h_2}(s,1)$, *and the suboptimal cost satisfies*

$$J(\{a_{s,2}(k)\}_{k=0}^\infty) \leq \overline{J} = \rho_2 + trace(QZ).$$

Proof. Rewrite equation (2.23) as

$$(\lambda + T_{h_2}(s,1)) \left(1 + \frac{\|s^\phi\|_Z^2 - d}{d + \|s^{\phi+\delta}\|_Z^2}\right) \leq \rho_2 + h_2(s). \tag{2.24}$$

It is easy to find that no matter whether $\|s^\phi\|_Z^2 - d \geq 0$ is true, equation (2.22) and (2.24) indicate that

$$\begin{aligned} \rho_2 + h_2(s) \geq & \min_{a_s(k)} \left\{\bar{V}_0(s), \bar{V}_1(s)\right\} \\ = & c_n(s, a_{s,2}(k)) + T_{h_2}(s, a_{s,2}(k)) \end{aligned}$$

Following the same steps in the proof of Theorem 2.6.1, we have

$$\rho_2 \geq \lim_{N\to\infty} \frac{1}{N} \sum_{k=0}^{N} E(c_n(e^-_{KF,RO}(k), a_{s,2}(k))),$$

and $J(\{a_{s,2}(k)\}_{k=0}^\infty) \leq \rho_2 + trace(QZ)$. □

Remark 2.7.2. *Equation (2.22) and (2.23) are polynomial inequalities whose coefficients are linear combinations of the coefficients of h_2. From Remark 2.6.2, we know that $T_{h_2}(s,0)$ and $T_{h_2}(s,1)$ are both polynomials whose coefficients are linear combinations of the the coefficients of h_2. Since $1-\frac{\|s^{\phi}\|_Z^2-d}{500d}$, $\|s^{\phi}\|_Z^2+\|s^{\phi+\delta}\|_Z^2$, and $d+\|s^{\phi+\delta}\|_Z^2$ are all given constant coefficient polynomials, equation (2.22) and (2.23) are polynomial inequalities whose coefficients are linear combinations of the coefficients of h_2.*

Remark 2.7.3. *Since equation (2.22) and (2.23) are polynomial inequalities whose coefficients are linear combinations of the coefficients of h_2, h_2 and ρ_2, $a_{s,2}$ and $\overline{J}$ can be efficiently computed using SOSTOOLS by solving the following SOS programming.*

$$\min \rho_2 \tag{2.25}$$

subject to: (2.22) and (2.23).

Remark 2.7.4. *The degree, ϕ and δ, of the constant coefficient polynomials $1-\frac{\|s^{\phi}\|_Z^2-d}{500d}$, $\|s^{\phi}\|_Z^2+\|s^{\phi+\delta}\|_Z^2$, and $d+\|s^{\phi+\delta}\|_Z^2$ should be chosen as large as possible as long as the computation time is not too long. Generally speaking, higher ϕ and δ can provide smaller ρ_2 for h_2 with the same degree, but consumes more computation effort. So, ϕ and δ can be chosen to be large enough such that the computation time is not too long.*

Remark 2.7.5. *The positive scalar constant, d, in the constant coefficient polynomials $1-\frac{\|s^{\phi}\|_Z^2-d}{500d}$ and $d+\|s^{\phi+\delta}\|_Z^2$ is chosen through Lipschitz optimization such that ρ_2 computed according to equation (2.25) is minimized. Built upon Lipschitz optimization, DIRECT algorithm [19] is a matlab based function which is used in our algorithm to search for the scalar constant d^* which provides the smallest ρ_2.*

Algorithm 2.7.6 (Compute the suboptimal event trigger)**.**

1. *Initialization*

   i *Provide system parameters: A, C, W, V, L, Q, Z, and λ.*

   ii *Provide parameters in equation (2.22) and (2.23): ϕ, δ.*

   iii *Initialize an SOS programming using toolbox 'SOSTOOLS'.*

   - *Declare scalar decision variables: ρ_2, s_1, $\ldots$, s_n ($s = [s_1, \ldots, s_n]^T$ denotes $e^-_{KF,RO}(k)$ in equation (2.22) and (2.23)).*
   - *Declare a polynomial variable: h_2.*
   - *Compute $T_{h_2}(s, 0)$ and $T_{h_2}(s, 1)$ using the Isserlis' theorem.*

2. *Use DIRECT function to search interval $[0, 5\lambda]$ for the d^* which provides the smallest ρ_2.*

3. *Solve the SOS programming (2.25) with $d = d^*$.*

4. *Compute the suboptimal event trigger: $s^T Z s + E_{h_2}(As) - \lambda - E_{h_2}(0) > 0$.*

5. *Compute the upper bound on the suboptimal cost: $\rho_2 + trace(QZ)$.*

6. *Return.*

2.8 Mathematical Examples

The last two sections propose SOS programs to efficiently compute a lower bound on the optimal cost, and a suboptimal event trigger and an upper bound on its cost. This section will use two examples to show that SOS program (2.21) and (2.25) can compute tighter lower bound on the optimal cost and tighter upper bound on the suboptimal cost than the prior work [14, 12, 35], while guaranteeing almost the same actual cost as the prior work [14, 12, 35].

2.8.1 Stable system

Consider a marginally stable system as below

$$x(k+1) = \begin{bmatrix} 1 & 0 \\ 0 & 1 \end{bmatrix} x(k) + w(k)$$

$$y(k) = x(k),$$

with covariance matrix $W = \begin{bmatrix} 0.03 & -0.02 \\ -0.02 & 0.04 \end{bmatrix}$, the weight matrix $Z = \begin{bmatrix} 2 & 1 \\ 1 & 2 \end{bmatrix}$, and the communication price $\lambda = 20$. This is the same example used in [14], and we would like to compare our results with the results in [14] and [35].

The SOS program (2.21) was first used to compute a lower bound $\underline{J}$ on the minimum cost. In this program, h_1 was set to be a polynomial which contained all possible monomials whose degrees were no greater than D_1. We varied D_1 from 1 to 8, and the computed largest lower bounds are shown in the top plot of Figure 2.2. We find when the degree of h_1 was increased to be 4, the lower bound provided by the SOS program (2.21) was larger than the lower bound provided by [14] by about 2 times, while [35] did not talk about how to compute a lower bound on the optimal cost.

We, then, use SOS program (2.25) to compute a suboptimal event trigger and an upper bound on its cost. In this program, h_2 was set to be a polynomial which contained all possible monomials whose degrees were even and no greater than D_2. let $\phi = 3$ and $\delta = 1$. The constant d is chosen using the DIRECT optimization algorithm. The degree of h_2, D_2, was varied from 1 to 8, and the computed upper bounds on the suboptimal cost are shown in the middle plot of Figure 2.2. We see that when the degree of h_2 was increased to 6, the upper bound on the suboptimal cost was smaller than the upper bounds provided by [14] and [35].

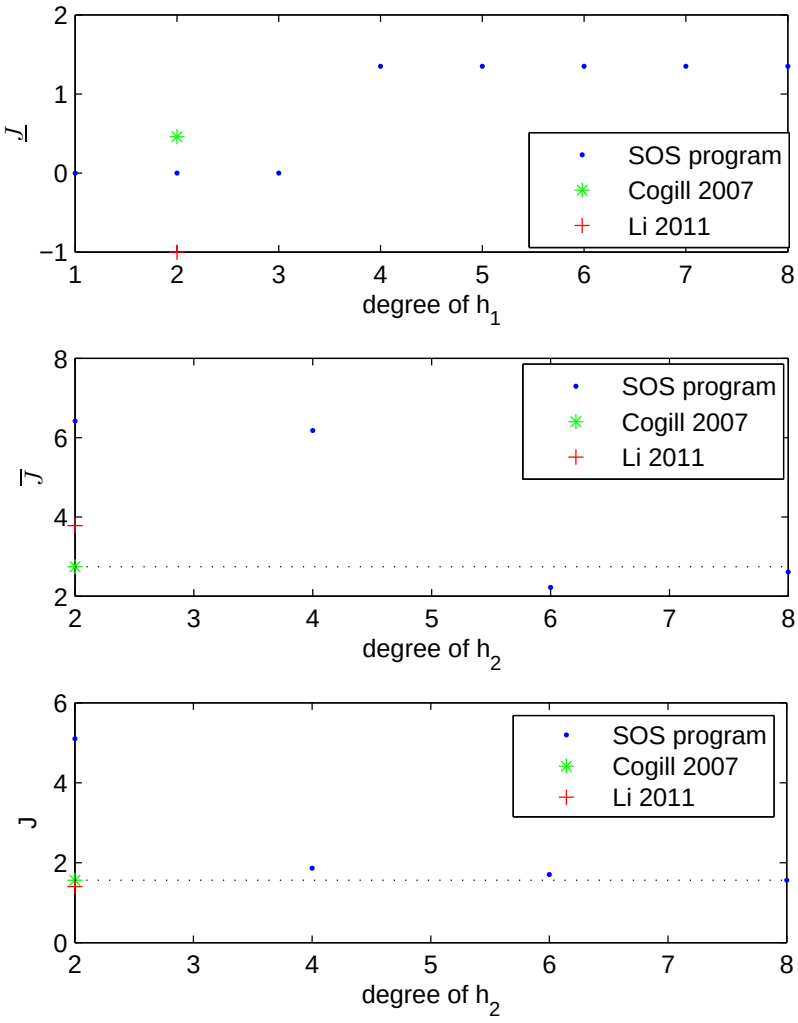

Figure 2.2. Results for the stable system. Negative values indicate no feasible solution or not available.

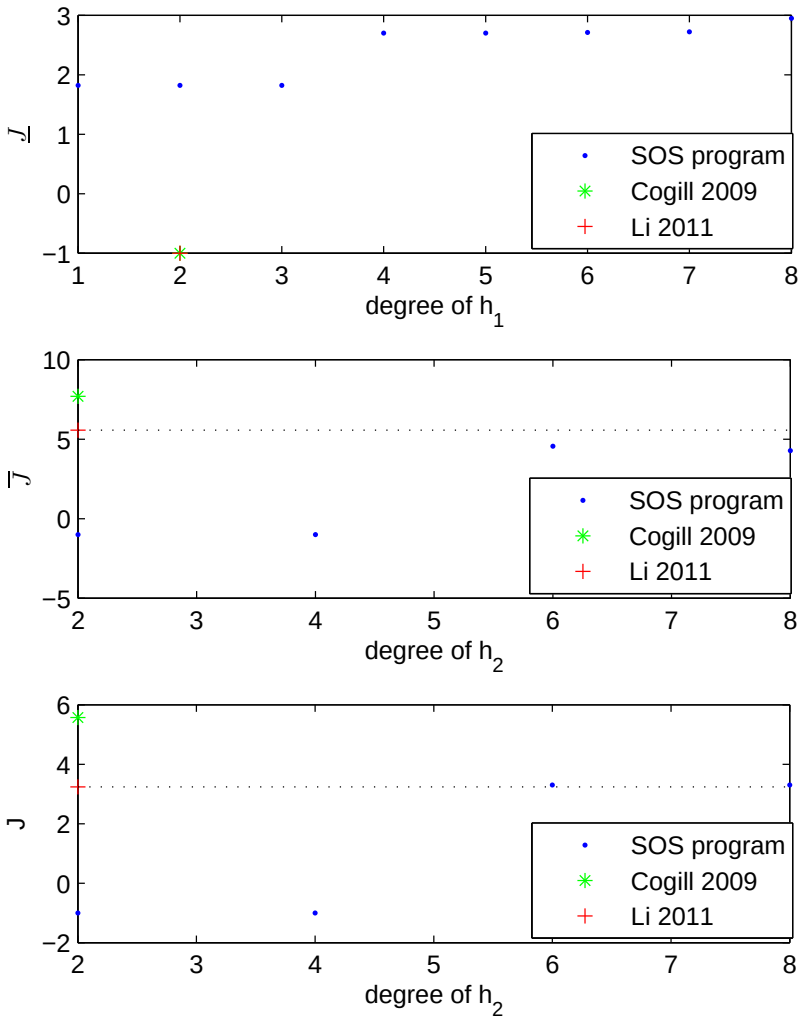

Figure 2.3. Results for the unstable system. Negative values indicate no feasible solution or not available.

The suboptimal event triggers were, then, used in the state estimation system, and the actual costs are given in the bottom plot of Figure 2.2. We find that when the degree of h_2 was increased to 6, the actual cost is almost the same as the actual costs provided by [14] and [35].

2.8.2 Unstable system

Next, we consider an unstable system.

$$x(k+1) = \begin{bmatrix} 0.95 & 1 \\ 0 & 1.01 \end{bmatrix} x(k) + w(k)$$
$$y(k) = \begin{bmatrix} 0.1 & 1 \end{bmatrix} x(k) + v,$$

with the covariance matrix $W = \begin{bmatrix} 0.2 & 0 \\ 0 & 0.2 \end{bmatrix}$ and $V = 0.3$, the weight matrix $Z = \begin{bmatrix} 1 & 0 \\ 0 & 1 \end{bmatrix}$, and the communication price $\lambda = 5$.

With the same steps as we did for the stable system, we computed the lower bound $\underline{J}$ on the minimum cost while varying the degree of h_1 from 1 to 8. The results are given in the top plot of Figure 2.3. We see that when the degree of h_1 is greater than 4, the lower bound on the optimal cost is always greater than 2.7, while there is no prior work provided lower bounds on the optimal cost for unstable systems.

Follow the same steps as what we did for the stable system, we computed the suboptimal event trigger, and the upper bound $\overline{J}$ on its cost. In this case, the degree ϕ and δ in equation (2.22) and (2.23) is set to be 6 and 1, respectively. We varied the degree of h_2 from 2 to 8, the upper bounds on the suboptimal costs are given in the middle plot of Figure 2.3. We see that when the degree of h_2 was increased to 6, the upper bounds on the suboptimal costs are smaller than the upper bounds provided

by both [12] and [35].

The suboptimal event triggers were, then, applied to the state estimation system. The actual costs are shown in the bottom plot of Figure 2.3. We see that when the degree of h_2 is greater than 6, the actual costs are almost the same as the actual cost given by [35], and are less than the actual cost provided by [12].

2.9 Application in a $QUANSER^{©}$ 3DOF Helicopter

This section applies the suboptimal event trigger computed from Algorithm 2.7.6 to a 8 dimensional nonlinear 3DOF helicopter. Subsection 2.9.1 introduces the nonlinear model of the 3DOF helicopter, linearization of this nonlinear model and the controllers we will use for the 3DOF helicopter. Subsection 2.9.2 explains how we design the suboptimal event triggers for this 3DOF helicopter. The experiment results are given in subsection 2.9.3.

2.9.1 $QUANSER^{©}$ 3DOF Helicopter

Figure 2.4 gives the basic schematic of the 3DOF helicopter. The 3DOF helicopter consists of three subsystems: elevation (ϵ), pitch (ρ) and travel (γ). Elevation is the angle between the main beam and the horizontal axis, pitch is the angle that the motor beam moves around the main beam, and travel is the angle that the main beam moves around the vertical axis. T_f and T_b are the front and back thrusts generated by the DC motors. Our objective is to control the 3DOF helicopter to follow a commanded elevation ϵ_r and a commanded travel rate $\dot{\gamma}_r$.

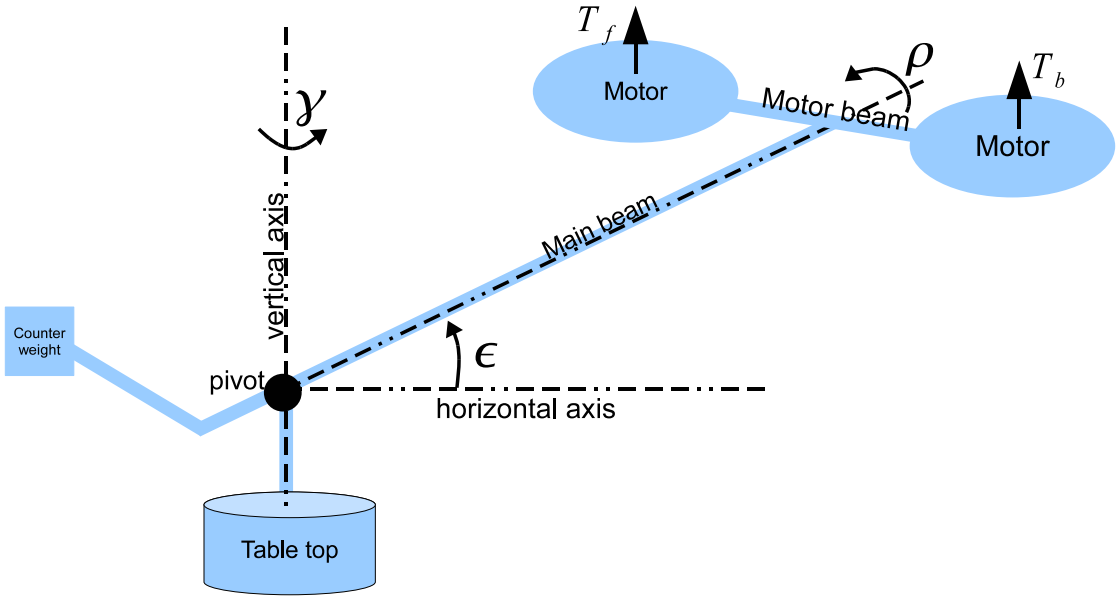

Figure 2.4. Schematic of the 3DOF helicopter.

l_a	0.67 m	ϵ_0	-0.136 rad
l_h	0.177 m	c_ϵ	0.18 $kg.m^2/s$
l_w	0.48 m	c_ρ	0.003 $kg.m^2/s$
d	0.04 m	c_γ	0.25 $kg.m^2/s$
M	1.4611 kg	$c_{\gamma\rho}$	0.003 $kg.m^2/s$
m	2 kg	J_ϵ	3.5 $kg.m^2$
M_bf	0.29 kg	J_ρ	0.01 $kg.m^2$
g	9.8 m/s^2	J_γ	4 $kg.m^2$

TABLE 2.1

3DOF helicopter parameter values

The system dynamic is described by the following equations [7].

$$\begin{aligned} J_\epsilon \ddot{\epsilon_m} =& -\sqrt{((ml_w - Ml_a)g)^2 + ((m+M)gd)^2}\sin(\epsilon_m) \\ & + T_{col}\cos(\rho)(l_a + d\tan(\epsilon_m + \epsilon_0)) - c_\epsilon \dot{\epsilon}_m, \\ J_\rho \ddot{\rho} =& T_{cyc} l_h - M_{bf} g d \sin(\rho) - c_\rho \dot{\rho} + c_{\gamma\rho}\dot{\gamma}, \\ J_\gamma \ddot{\gamma} =& -l_a T_{col}\sin\rho\cos\epsilon - c_\gamma \dot{\gamma}, \end{aligned}$$

and the elevation, pitch and travel rate can be directly measured with the measurement noises to be white zero mean Gaussian, and the variances of the measurement noises are 1.857×10^{-6}, 1.857×10^{-6}, and 1.857×10^{-6}, respectively.

In this model, $\epsilon_m = \epsilon - \epsilon_0$, m is the gross counter weight at the tail, M is the gross weight at the head, $M_{bf} = m_b + m_f$ is the sum mass of the two motors, l_w is the length from the pivot to the tail while l_a is the length from the pivot to the head, d is some adjusted length with respect to the elevation, g is the gravity acceleration, $T_{col} = T_f + T_b$ and $T_{cyc} = T_b - T_f$ are the collective and cyclic thrusts, $c_\epsilon\dot{\epsilon}$, $c_\rho\dot{\rho}$, $c_{\gamma\rho}\dot{\gamma}$, $c_\gamma\dot{\gamma}$ are the drags generated by air due to the change of elevation, pitch and travel, and J_ϵ, J_ρ and J_γ are the inertia moments for elevation, pitch and travel respectively. The parameter values are given in Table 2.1.

Neglecting the non-dominant terms and under the assumption that $\sin(\rho) \approx \rho$ and $\sin(\epsilon_m) \approx \epsilon_m$, the model of 3DOF helicopter can be linearized as

$$J_\epsilon \ddot{\epsilon}_m = -\sqrt{((ml_w - Ml_a)g)^2 + ((m+M)gd)^2}\epsilon_m - c_\epsilon\dot{\epsilon}_m + l_a u_{\epsilon_m} \tag{2.26}$$

$$J_\rho \ddot{\rho} = -M_{bf} g d\rho - c_\rho\dot{\rho} - c_{\gamma\rho}\dot{\gamma} + l_h u_\rho \tag{2.27}$$

$$J_\gamma \ddot{\gamma} = -c_\gamma\dot{\gamma} - l_a u_\gamma, \tag{2.28}$$

where u_{ϵ_m}, u_ρ and u_γ are the control inputs for elevation, pitch and travel subsystems

satisfying

$$u_{\epsilon_m} = T_{col}\cos(\rho), \tag{2.29}$$

$$u_{\rho} = T_{cyc}, \tag{2.30}$$

$$u_{\gamma} = T_{col}\rho\cos(\epsilon). \tag{2.31}$$

The control laws of these control inputs are

$$u_{\epsilon_m} = [7\ 44\ 68][\int_0^t \epsilon_m(s) - \epsilon_r(s)ds\ \epsilon_m(t) - \epsilon_r(t)\ \dot{\epsilon}_m(t)]^T, \tag{2.32}$$

$$u_{\rho} = [3.5\ 30\ 20][\int_0^t \rho(s) - \rho_r(s)ds\ \rho(t) - \rho_r(t)\ \dot{\rho}(t)]^T, \tag{2.33}$$

$$u_{\gamma} = [25\ 3][\gamma(t) - \gamma_r(t)\ \dot{\gamma}(t) - \dot{\gamma}_r(t)]^T, \tag{2.34}$$

where ρ_r is the reference pitch signal which will be explained later.

To compute the collective and cyclic thrusts T_{col} and T_{cyc}, we first compute the control inputs u_{ϵ_m}, u_{ρ} and u_{γ} according to equation (2.32), (2.33) and (2.34) respectively, and then compute T_{col}, T_{cyc} and ρ_r based on the following equations which are derived from equation (2.29), (2.30 and (2.31).

$$\begin{aligned} T_{col} &= u_{\epsilon_m}/\cos(\rho), \\ T_{cyc} &= u_{\rho}, \\ \rho_r &= u_{\gamma}/(T_{col}\cos(\epsilon)). \end{aligned}$$

2.9.2 Design of the event triggered 3DOF helicopter.

From equation (2.26), (2.27) and (2.28), we can see that the helicopter system is decomposed into 2 decoupled subsystems: elevation subsystem and pitch-travel subsystems. For each subsystem, we will design a Kalman filter, a remote observer and a suboptimal event trigger. The structure of the whole closed loop system can

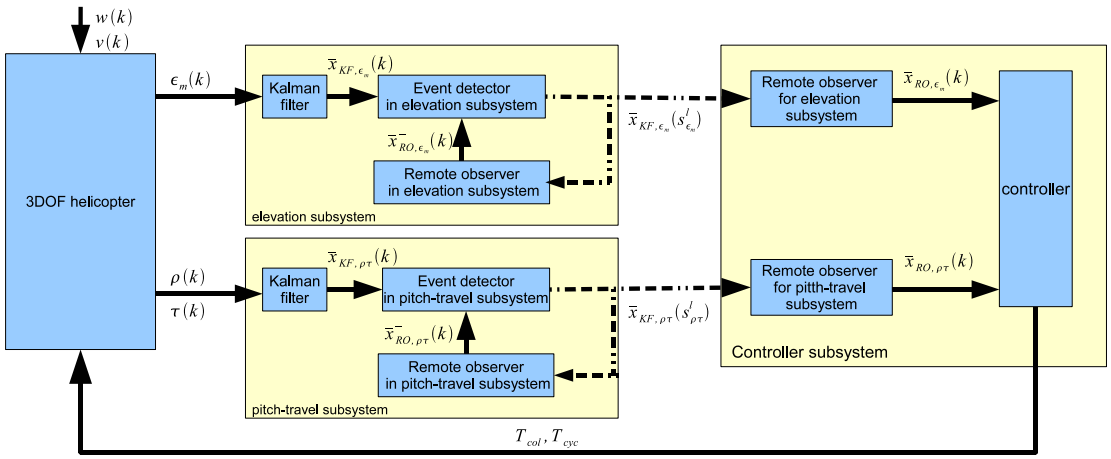

Figure 2.5. Structure of event triggered 3DOF helicopter

be found in Figure 2.5.

2.9.2.1 Design of the elevation subsystem

The elevation subsystem is discretized with period $0.005s$, and the discrete model of the elevation subsystem is

$$x_{\epsilon_m}(k+1) = \begin{bmatrix} 1 & 0.005 & 1.25e-5 \\ 0 & 1 & 0.004999 \\ 0 & -0.001956 & 0.9997 \end{bmatrix} x_{\epsilon_m}(k) + \begin{bmatrix} 3.988e-9 \\ 2.393e-60.000957 \end{bmatrix} u_{\epsilon_m} + w_{\epsilon_m}$$

$$y_{\epsilon_m}(k) = \begin{bmatrix} 1 & 0 & 0 \\ 0 & 1 & 0 \end{bmatrix} x_{\epsilon_m}(k) + v_{\epsilon_m},$$

where $x_{\epsilon_m}(k) = [\int_0^{0.005k} \epsilon_m(s)ds \ \epsilon_m(0.005k) \ \dot{\epsilon}_m(0.005k)]^T$, the variances of w_{ϵ_m} and v_{ϵ_m} are $diag([8e-3 \ 1e-12 \ 3.1e-4])$ and $diag([01.86e-6])$, respectively.

subsystem	elapsed time for operating 2.25	upper bound $\overline{J}$	lower bound on minimum cost $\underline{J}^*$	$\frac{\overline{J}}{\underline{J}^*}$
elevation	$\approx$ 40s	0.20	0.076	2.65
pitch-travel	$\approx$ 630	0.67	0.16	4.18

TABLE 2.2

Upper bound on the suboptimal cost and lower bound on the minimum cost

By solving the discrete linear Riccati equation, we have the Kalman filter gain as

$$L_{\epsilon_m} = \begin{bmatrix} 1 & 0.0016 \\ 0 & 0.3563 \\ 0 & 10.77 \end{bmatrix}.$$

Algorithm 2.7.6 was, then, used to compute a suboptimal event trigger. Let the weight matrix $Z = diag([1\ 6\ 1])$, $\lambda = 1$, $\phi = 2$, $\delta = 1$. h_2 was chosen to be a polynomial which contains all possible monomials whose degree is even and no greater than 10.

A lower bound on the minimum cost was computed based on the SOS programming 2.21. In this Algorithm, h_1 was chosen to be a polynomial which contains all possible monomials whose degree is no greater than 10.

The related results about the upper bound on the suboptimal cost and lower bound on the minimum cost are given in Table 2.2. From the last column of this table, we find that the upper bound on the suboptimal cost is 2.65 times of the lower bound on the optimal cost, which is considered to be acceptable.

2.9.2.2 Design of the pitch-travel subsystem

With the period to be $0.005s$, the discrete model of the pitch-travel subsystem is given below.

$$x_{\rho\tau}(k+1) = \begin{bmatrix} 1 & 0.005 & 1.249e-5 & 0 & 6.247e-11 \\ 0 & 0.9999 & 0.004996 & 0 & 3.748e-8 \\ 0 & -0.05679 & 0.9984 & 0 & 1.499e-005 \\ 0 & 0 & 0 & 1 & 0.004999 \\ 0 & 0 & 0 & 0 & 0.9997 \end{bmatrix} x_{\rho\tau}(k)$$

$$+ \begin{bmatrix} 3.686e-7 & -1.308e-14 \\ 0.0002211 & -1.046e-11 \\ 0.08843 & -6.277e-9 \\ 0 & -2.094e-6 \\ 0 & -0.0008374 \end{bmatrix} \begin{bmatrix} u_\rho \\ u_\tau \end{bmatrix} + w_{\rho\tau}$$

$$y_{\rho\tau}(k) = \begin{bmatrix} 1 & 0 & 0 \\ 0 & 1 & 0 \end{bmatrix} x_{\rho\tau}(k) + v_{\rho\tau},$$

where $x_{\rho\tau}(k) = [\int_{s=0}^{0.005k} \rho(s)ds \ \rho(0.005k) \ \dot{\rho}(0.005k) \ \tau(0.005k) \ \dot{\tau}(0.005k)]^T$. The variances of $w_{\rho\tau}$ and $v_{\rho\tau}$ are $diag([1e{-}3 \ 1e{-}12 \ 2e{-}4 \ 1e{-}12 \ 5.4e{-}4])$ and $diag([0 \ 1.86e{-}6 \ 1.86e-6])$, respectively.

The Kalman gain can be computed by solving the discrete linear Riccati equation.

For the pitch-travel subsystem, the Kalman gain is

$$L_{\epsilon_m} = \begin{bmatrix} 1 & 0.0015 & 0 \\ 0 & 0.3177 & 0 \\ 0 & 8.68 & 0 \\ 0 & 0 & 0.4083 \\ 0 & 0 & 13.837 \end{bmatrix}.$$

We, then, used Algorithm 2.7.6 to compute a suboptimal event trigger. Let the weight matrix $Z = diag([1\ 6\ 1\ 1\ 6])$, $\lambda = 1$, $\phi = 2$, $\delta = 1$. Here, we chose h_2 such that there was no cross terms between the pitch state and the travel state, and all possible monomials whose degree was even and no greater than 4 were included.

A lower bound on the minimum cost was also computed based on the SOS programming 2.21. In this algorithm, h_1 was chosen such that it contained all polynomials, except cross terms between the pitch state and the travel state, whose degree is no greater than 8. The related results about the upper bound on the suboptimal cost and the lower bound on the minimum cost is shown in the second row of Table 2.2. From the last column, we see that the upper bound on the suboptimal cost is 4.18 times of the lower bound on the minimum cost, which is considered to be acceptable.

2.9.3 Experimental results for the event triggered 3DOF helicopter and periodically triggered 3DOF helicopter

We first ran the event triggered 3DOF helicopter system for 90 seconds, and then ran a periodically triggered 3DOF helicopter system for 90 seconds. When we ran the periodically triggered 3DOF helicopter system, we adjusted the periods of the elevation subsystem and pitch-travel subsystem until the performance was similar to the performance of the event triggered 3DOF helicopter.

sampling method	delay: s	elevation	pitch-travel	total
polynomial event trigger	0.005	1	53	54
periodic triggering		1	300	301
polynomial event trigger	0.01	1	48	49
periodic triggering		1	300	301
polynomial event trigger	0.02	1	2422	2423
periodic triggering		1	300	301

TABLE 2.3

Transmission times using event triggering and periodic triggering with different delays.

2.9.3.1 Transmission times and performance with $0.005s$ delay

The transmission times for both event triggered and periodically triggered helicopter are shown in Table 2.3. In this experiment, the transmission delay is set to be $0.005s$, from the last column, we can see that the total transmission times of event triggered helicopter is less than 0.2 times of the transmission times of the periodically triggered helicopter.

Figure 2.6 shows the inter-sampling intervals of even triggered helicopter with x-axis indicating time and y-axis indicating inter-sampling intervals measured by second. Let us first look at the inter-sampling intervals (circles) of pitch-travel subsystem. The most frequent transmissions occurred during the intervals $[15s, 20s]$, $[32s, 42s]$ and $[55s, 60s]$. Compared with the middle plot of Figure 2.7, we see that these intervals are those when the travel subsystem was in transient processes. We, then, look at the inter-sampling intervals (dot) of elevation subsystem, and find that

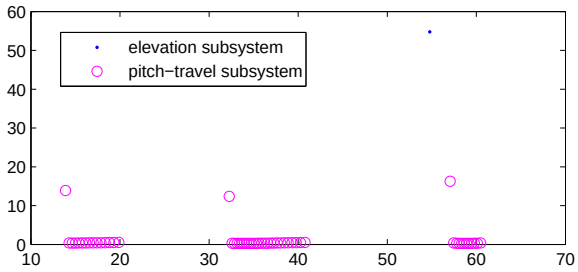

Figure 2.6. Inter-sampling intervals of event triggered 3DOF helicopter.

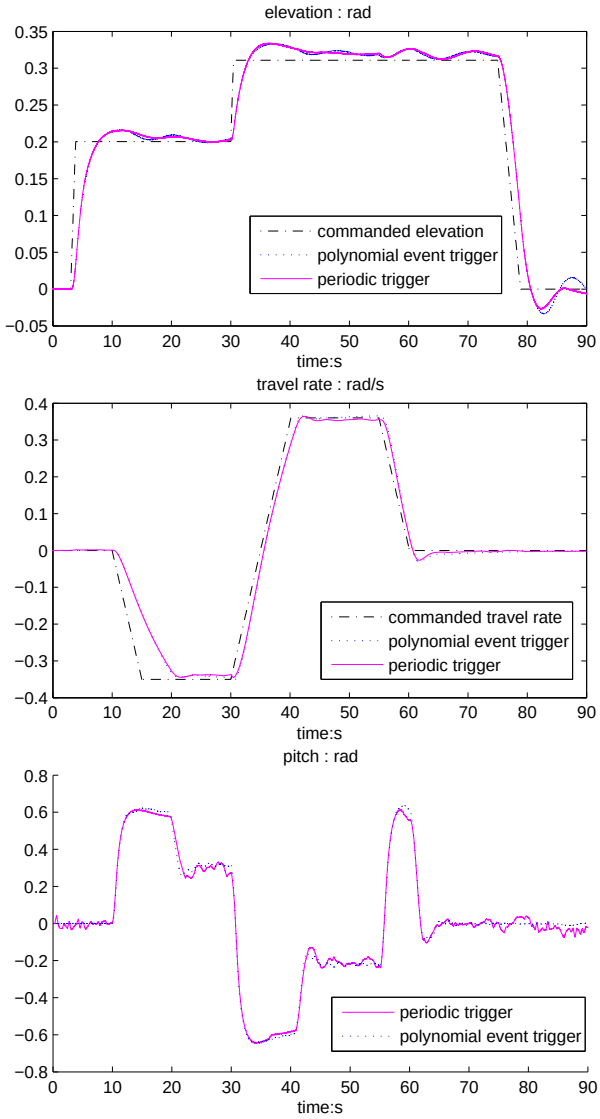

Figure 2.7. The elevation, travel rate and pitch performance of the event triggered 3DOF helicopter and periodically triggered 3DOF helicopter.

there was only one transmission in the elevation subsystem. Notice that the elevation subsystem is stable and only coupled with pitch subsystem (see equation (2.26)). So, if the remote state estimate of pitch is accurate enough, the remote state estimate of elevation will be accurate enough and there will be very few transmissions in the elevation subsystem.

The system performances are shown in Figure 2.7. The top plot is the system performance of elevation subsystem, with x-axis indicating time and y-axis indication elevation measured by rad. We can see that event triggered helicopter (dotted line) and periodically triggered helicopter (solid line) has similar elevation performance, and both of them track the commanded signal (dash dotted line) with small overshoot and no steady state error. The middle plot is the performance of travel rate measured by rad/s, with x-axis indicating time and y-axis indicating travel rate. From the middle plot, we see that event triggered helicopter (dotted line) and periodically triggered helicopter (solid line) has similar performance, and both of them track the commanded signal (dash dotted line) with small overshoot and no steady state error. The bottom plot is the performance of pitch measured by rad, with x-axis indication time and y-axis indication pitch angle. We see that the event triggered helicopter (dotted line) and the periodically triggered helicopter (solid line) have similar pitch performance, and both of them only have small oscillation. Overall, we can say that the event triggered helicopter and the periodically triggered helicopter have similar performance.

2.9.3.2 Transmission times and performances with 0.01s and 0.02s delay

In this experiment, we first set the transmission delay to be 0.01s, and then set the transmission delay to be 0.02s to see how the system performances of event triggered helicopter and periodically triggered helicopter decay with respect to transmission delays.

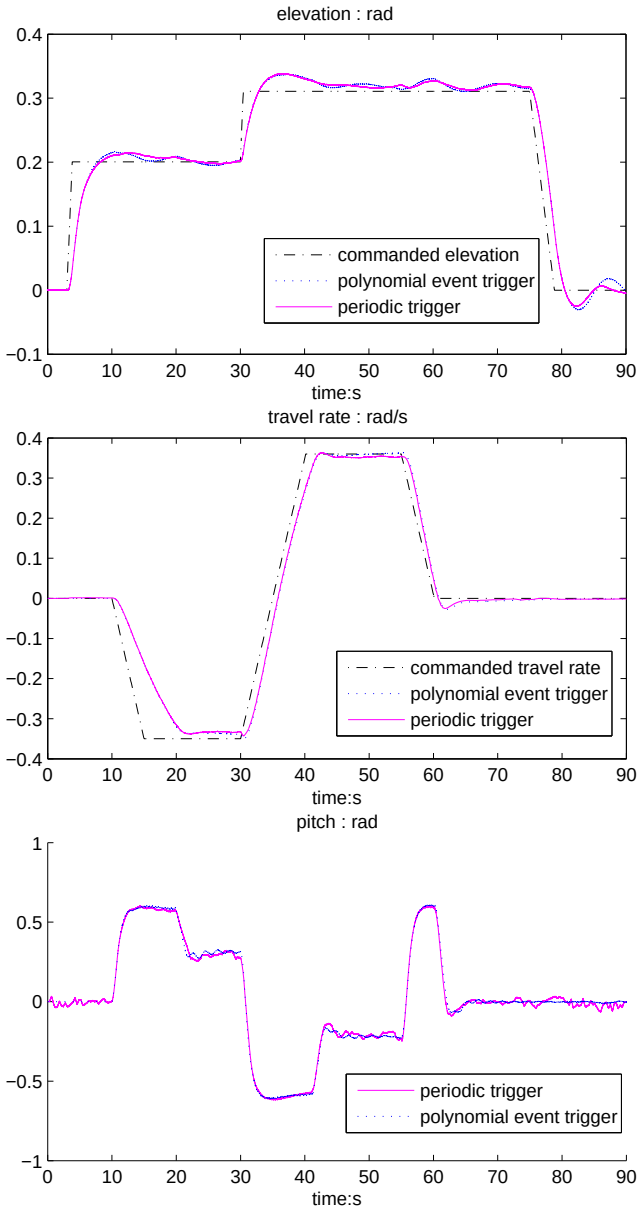

Figure 2.8. System performance with 0.01s delay

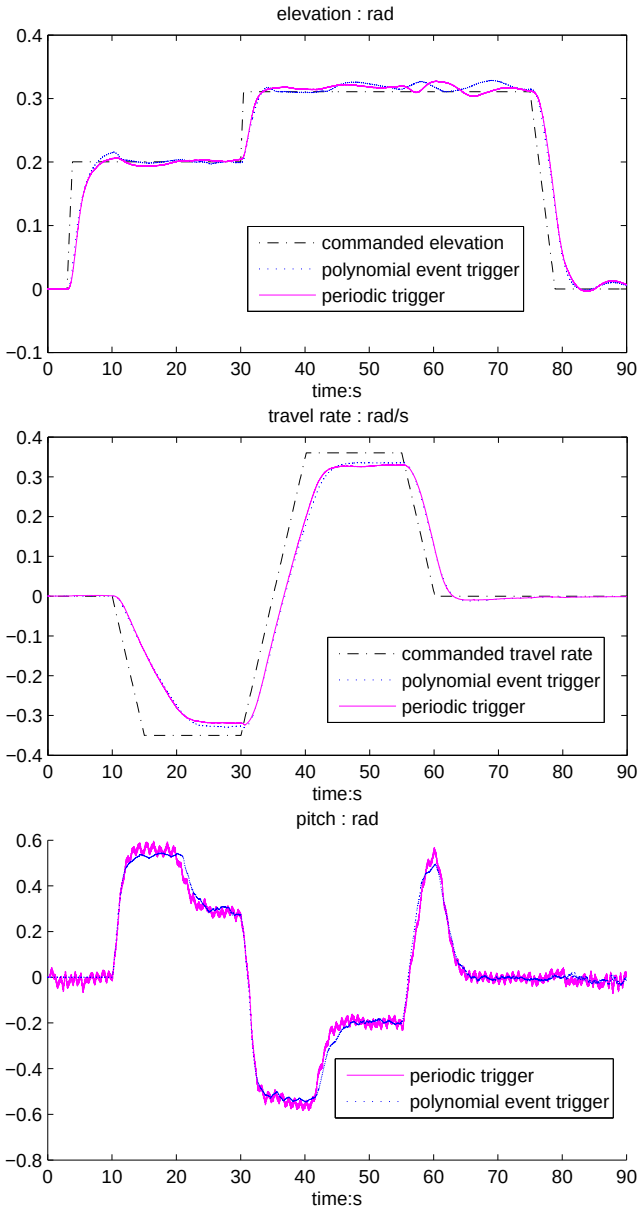

Figure 2.9. System performance with 0.02s delay

In the presence of 0.01s delay, the system performances of both event triggered 3DOF helicopter and periodically triggered 3DOF helicopter are shown in Figure 2.8. The top plot is the performance of the elevation subsystem, the middle plot is the performance of travel rate, and the bottom plot is the performance of pitch. In these three plots, solid lines are performances of periodically triggered helicopter, dotted lines are performances of event triggered helicopter, and dash dotted lines are commanded signals. From the three plots of Figure 2.8, we can see that in the presence of 0.01s delay, the performance of event triggered helicopter is similar to the performance of periodically triggered helicopter, and both of them tracked the commanded elevation and travel rate with small overshoot and no steady state error with small oscillation in the pitch angle. Now, let us look at the transmission times of both event triggered helicopter and periodically triggered helicopter. The transmission times are shown in the 3rd and 4th row of Table 2.3. We see that compared with the periodically triggered helicopter system, the total transmission times in the event triggered helicopter system is about 0.2 of the total transmission times in the periodically triggered helicopter system. Therefore, we conclude that when the transmission delay is 0.01s, the event triggered helicopter and the periodically triggered helicopter achieved similar performances while the event triggered helicopter transmitted less than the periodically triggered helicopter.

When the transmission delay is 0.02s, the system performances are shown in Figure 2.9 with dotted lines indicating performances of the event triggered helicopter, solid line indicating performances of the periodically triggered helicopter, and dash dotted line indicating commanded signals. The top two plots are the performances of elevation and travel rate, respectively. We see that event triggered helicopter and periodically triggered helicopter had similar elevation and travel rate performance. While both event triggered system and periodically triggered system tracked the commanded elevation with small overshoot and no steady state error, there existed

steady state errors in travel rate for both event triggered system and periodically triggered system. The bottom plot shows the performances of pitch. we can see that the event triggered helicopter had smaller oscillation in pitch than the periodically triggered helicopter. The transmission times of event triggered helicopter and the periodically triggered helicopter are given in the 5th and 6th row of Table 2.3. We see that in event triggered system, while the transmission times of elevation subsystem remained at the same level, the transmission times of the pitch-travel subsystem increase to 2422 from 54 (0.005s delay) and 49 (0.01s delay). This is because the pitch angle kept oscillating, which means that the pitch subsystem was always in a transient process. So, the pitch-travel subsystem kept transmitting information during the whole running horizon. From Table 2.3, we see that event triggered helicopter transmitted more than the periodically triggered helicopter, and the total transmission times of event triggered helicopter is about 8 times of the transmission times of the periodically triggered helicopter. From Figure 2.9 and Table 2.3, we conclude that when the transmission delay is 0.02s, the event triggered helicopter had better performance than the periodically triggered helicopter, but consumed more communication resource than the periodically triggered helicopter.

2.10 Conclusion

This chapter provides computationally efficient, SOS programming based algorithms to compute suboptimal event triggers, upper bounds on the suboptimal costs, and lower bounds on the optimal costs. These SOS programming based algorithms are effective for both stable and unstable systems. Our simulation results show that SOS program (2.21) and (2.25) can compute tighter lower bound on the optimal cost and tighter upper bound on the suboptimal cost than the prior work [14, 12, 35], while guaranteeing almost the same actual cost as the prior work [14, 12, 35]. The algorithms are, then, applied to an 8 dimensional nonlinear 3DOF helicopter. The

simulation results show that the event triggered helicopter uses less communication resource than periodically triggered helicopter to achieve similar performance, and tolerates the same amount of delay. To our best knowledge, this is the first time the approximation of the optimal event trigger has been applied to a system whose dimension is greater than 2.

CHAPTER 3

MINIMUM MEAN SQUARE STATE WITH LIMITED TRANSMISSION FREQUENCY

In last chapter, computationally efficient suboptimal event trigger is designed to minimize the estimation error of the remote state estimate. In this chapter, we use this remote state estimate to compute a control input, and then design an event trigger for the remote controller to decide when to transmit the control input back to the plant such that the mean square state is minimized. The proposed triggering events only rely on local information so that the transmissions from the sensor and controller subsystems are not necessarily synchronized. This represents an advance over recent work in event-triggered output feedback control where transmission from the controller subsystem was tightly coupled to the receipt of event-triggered sensor data. The paper presents an upper bound on the optimal cost attained by the closed-loop system. Simulation results demonstrate that transmissions between sensors and controller subsystems are not tightly synchronized. These results are also consistent with derived upper bounds on overall system cost.

3.1 Introduction

Most prior work in the event triggering literature discusses state feedback control and state estimation. This work has traditionally assumed a single feedback link in the system. It has only been very recently that researchers have turned to study event-triggered output feedback control where there are separate communication channels from sensor to controller and controller to actuator. If we design triggering events

for both communication channels, an interesting question to ask is how these two triggering events are coupled with each other.

Some of the work in event triggered output feedback systems hid this question by assuming that only part of the control loop was closed over communication channel, i.e. either sensor-to-controller link or controller-to-actuator link is connected directly [34, 71, 48]. Another work in [16] assumed very strong coupling between the triggering rules of sensor-to-controller link and controller-to-actuator link. They required that the transmission in one link triggered the transmission in the other link, so transmissions in both communication channels are synchronized.

This synchronization is not necessary. This chapter examines a *weakly coupled* event triggered system. We study optimal event triggers that minimize the mean square cost of the system state discounted by the communication cost in both links. By realizing that the remote state estimate is orthogonal to the remote state estimation error, the optimal cost of the output feedback system is decomposed into the optimal cost of a state estimation problem and the optimal cost of a state feedback problem. This paper first gives the optimal event-triggers for both the state estimation problem and the state feedback problem. Because of the computational complexity of the optimal event triggers, computationally efficient *suboptimal* event triggers and the upper bounds on associated costs are, then, provided.

Compared with the synchronized design, there are two advantages of this weakly coupled design, especially in large scale multi-sensor systems. *The first advantage* is that this weakly coupled design has the potential to reduce the communication cost a lot in large scale multi-sensor systems. With weakly coupled design, sensors only transmit information when the remote estimation error is large enough, and the controller only transmit information when the remote state estimate and the actual control input are large enough. With synchronized design, when the controller transmits its control signal, all sensors have to transmit sensor information, even

though some of the sensors may have just finished their transmissions. At the same time, in a large scale multi-sensor system, the controller receives information from all the sensors. It is very possible that several sensor signals arrive in a short time. With synchronized design, the controller has to transmit very similar control signals several times in a short time. All these cases in synchronized design is a waste of communication resources, which can be easily avoided by the weakly coupled design. *The second advantage* of the weakly coupled design is to reduce the scheduling burden of the controller with synchronized design in large scale multi-sensor systems. With synchronized design, as the number of sensors increases, the transmission frequency of the controller also increases, and the controller has to schedule the transmission tasks more and more often, which increases the scheduling burden of the controller. While with the weakly coupled design, since the controller only transmits when the remote state estimate and the control signal are large enough, the controller will not schedule the transmission tasks more frequently, as long as the dynamic of the system, the system noises and the measurement noises remain at the same level. So, compared with synchronized design, the weakly coupled design reduces the scheduling burden of the controller in large scale multi-sensor systems.

3.2 Problem Statement

Consider a system shown in Figure 3.1. The plant is a discrete time linear time invariant system described by the following difference equation.

$$x(k) = Ax(k-1) + Bu_a(k-1) + w(k-1),$$
$$y(k) = Cx(k) + v(k), \forall k = 1, 2, \cdots,$$

where $x \in \mathbb{R}^n$ is the state with its initial condition Gaussian distributed with mean μ_0 and variance π_0, $y \in \mathbb{R}^p$ is the measurement, $u_a \in \mathbb{R}^m$ is the control input applied

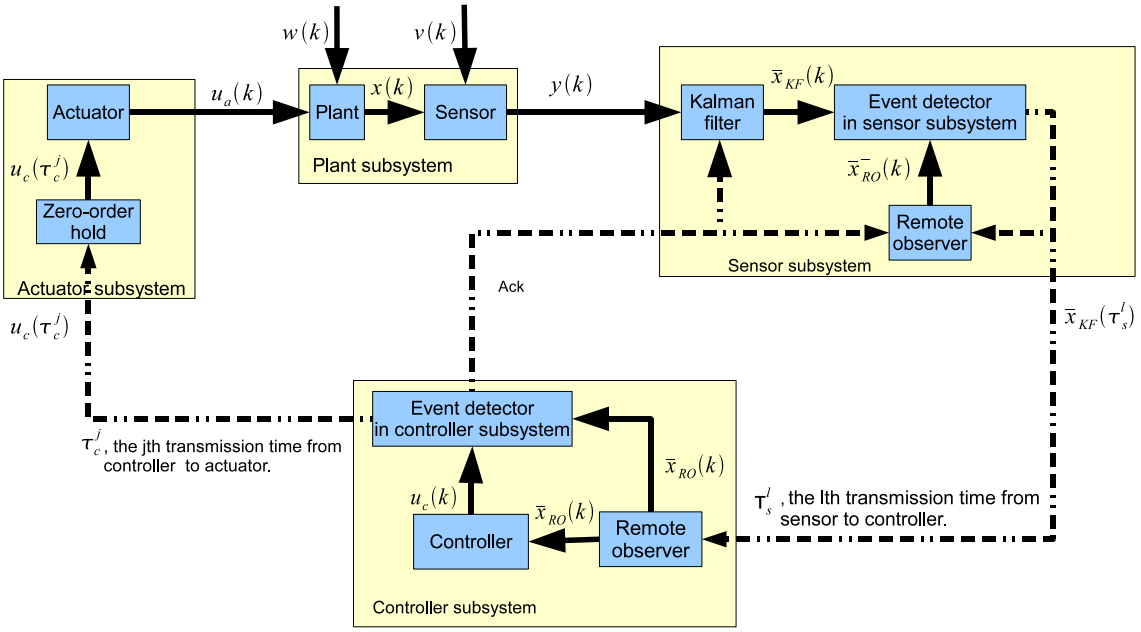

Figure 3.1. Structure of the event triggered output feedback control systems

to the plant, $w \in \mathbb{R}^n$ is a zero mean white Gaussian noise process with variance W, $v \in \mathbb{R}^p$ is another zero mean white Gaussian noise process with variance V. These two noise processes and the initial state are independent with each other.

The sensor subsystem decides when to transmit information to the controller subsystem. The measurements are first processed by a Kalman filter

$$\overline{x}_{KF}(k) = A\overline{x}_{KF}(k-1) + Bu_a(k-1) + L\left[y(k) - C(A\overline{x}_{KF}(k-1) + Bu_a(k-1))\right],$$

where $L = AXC^T(CXC^T+V)^{-1}$, and X satisfies the discrete linear Riccati equation

$$AXA^T - X - AXC^T(CXC^T + V)^{-1}CXA^T + W = 0.$$

The steady state estimation error $\overline{e}_{KF}(k) = x(k) - \overline{x}_{KF}(k)$ is a Gaussian random variable with zero mean and variance $Q = (I - LC)X$. The *remote observers* in

both sensor and controller subsystems generate an *a priori* remote state estimate $\overline{x}_{RO}^{-}(k)$ and an *a posteriori* remote state estimate $\overline{x}_{RO}(k)$. The gap $e_{KF,RO}^{-}(k) = \overline{x}_{KF}(k) - \overline{x}_{RO}^{-}(k)$ is, then, used by the event detector to decide whether to transmit the current $\overline{x}_{KF}(k)$ to the remote observer. Let $a_s(k) = 1$ indicate the decision of transmitting $\overline{x}_{KF}(k)$, and 0 otherwise. We force $a_s(k) = 1$ if $\|e_{KF,RO}^{-}(k)\| > \theta_s$ for a large positive constant θ_s. The lth transmission time of the sensor subsystem is denoted as τ_s^l.

The controller subsystem produces the control input, and decides when to transmit the current control input. The remote observer takes the form of

$$\overline{x}_{RO}^{-}(k) = A\overline{x}_{RO}(k-1) + Bu_a(k-1), \text{ with } \overline{x}^{-}(0) = \mu_0 \tag{3.1}$$

$$\overline{x}_{RO}(k) = \begin{cases} \overline{x}_{RO}^{-}(k), & \text{if } a_s(k) = 0; \\ \overline{x}_{KF}(k), & \text{if } a_s(k) = 1\ , \end{cases} \tag{3.2}$$

It is easy to show through mathematical induction that this is the minimum mean square estimate of x based on all history information of the controller (please check Lemma A.0.2 in Appendix for the proof). The *controller* generates a control input

$$u_c(k) = K\overline{x}_{RO}(k),$$

where K is the controller gain. The *event detector in the controller subsystem*, then, uses the augmented vector $[\overline{x}_{RO}(k)\ u_a(k-1)]^T$ to decide whether to transmit the current control input $u_c(k)$ to the plant. Let $a_c(k) = 1$ indicate the decision of transmitting $u_c(k)$, and 0 otherwise. We force $a_c(k) = 1$ if $\|[\overline{x}_{RO}(k)\ u_a(k-1)]^T)\| > \theta_c$ for a large positive constant θ_c. Once the controller subsystem decides to transmit $u_c(k)$, an *acknowledgement* is also transmitted to the sensor subsystem. The jth transmission time from controller to actuator is denoted by τ_c^j.

When $u_c(\tau_c^j)$ is transmitted, the actuator subsystem updates $u_a(k)$ to be $u_c(\tau_c^j)$,

and holds this value until the next transmission occurs. $u_a(k)$, then, satisfies

$$u_a(k) = u_c(\tau_c^j), \forall k = \tau_c^j, \ldots, \tau_c^{j+1} - 1. \tag{3.3}$$

The average cost is defined as

$$J(\{a_s(k)\}_{k=0}^{\infty}, \{a_c(k)\}_{k=0}^{\infty}) = \lim_{N\to\infty} \frac{1}{N} \sum_{k=0}^{N-1} E\left(c(x(k), a_s(k), a_c(k))\right),$$

where the cost function

$$c(x(k), a_s(k), a_c(k)) = \|x(k)\|_Z^2 + \lambda_s a_s(k) + \lambda_c a_c(k),$$

where $Z \in \mathbb{R}^{n\times n}$ is a positive definite matrix, $\|x(k)\|_Z^2 = x^T Z x$, λ_s and λ_c are the communication prices for transmissions over the sensor-to-controller link and controller-to-actuator link, respectively.

Our objective is to find transmission rules for both the sensor subsystem and the controller subsystem to minimize the average cost $J(\{a_s(k)\}_{k=0}^{\infty}, \{a_c(k)\}_{k=0}^{\infty})$, i.e.

$$J^* = \min_{\{a_s(k)\}_{k=0}^{\infty}, \{a_c(k)\}_{k=0}^{\infty}} J(\{a_s(k)\}_{k=0}^{\infty}, \{a_c(k)\}_{k=0}^{\infty}).$$

3.3 Decomposition of the average cost

This section shows that the average cost J can be decomposed into a state estimation cost and a control cost.

Let $\overline{e}_{RO}(k) = x(k) - \overline{x}_{RO}(k)$ be the remote state estimation error, and we have the following lemma.

Lemma 3.3.1. *$\overline{e}_{RO}(k)$ is orthogonal to $\overline{x}_{RO}(k)$ for all $k \in \mathbb{Z}^+$.*

Proof. From Lemma A.0.2, we know that $\overline{x}_{RO}(k)$ is a minimum mean square estimate

of the system state $x(k)$, and hence the remote state estimation error $\overline{e}_{RO}(k)$ is orthogonal to $\overline{x}_{RO}(k)$. □

Based on the Lemma 3.3.1, the average cost is decomposed into a state estimation cost and a control cost.

Theorem 3.3.2. *The average cost*

$$J(\{a_s(k)\}_{k=0}^{\infty}, \{a_c(k)\}_{k=0}^{\infty}) = J_s(\{a_s(k)\}_{k=0}^{\infty}) + J_c(\{a_c(k)\}_{k=0}^{\infty}),$$

where

$$J_s(\{a_s(k)\}_{k=0}^{\infty}) = \lim_{N\to\infty} \frac{1}{N} \sum_{k=0}^{N-1} E\left[\|\overline{e}_{RO}(k)\|_Z^2 + \lambda_s a_s(k)\right],$$
$$J_c(\{a_c(k)\}_{k=0}^{\infty}) = \lim_{N\to\infty} \frac{1}{N} \sum_{k=0}^{N-1} E\left[\|\overline{x}_{RO}(k)\|_Z^2 + \lambda_c a_c(k).\right]$$

Proof. According to Lemma 3.3.1, the average cost $J(\{a_s(k)\}_{k=0}^{\infty}, \{a_c(k)\}_{k=0}^{\infty})$ is rewritten as

$$\begin{aligned} J(\{a_s(k)\}_{k=0}^{\infty}, \{a_c(k)\}_{k=0}^{\infty}) = \lim_{N\to\infty} \frac{1}{N} \sum_{k=0}^{N-1} E\big(&\|\overline{e}_{RO}(k)\|_Z^2 + \lambda_s a_s(k) \\ &+\|\overline{x}_{RO}(k)\|_Z^2 + \lambda_c a_c(k)\big) \\ =&J_s(\{a_s(k)\}_{k=0}^{\infty}) + J_c(\{a_c(k)\}_{k=0}^{\infty}). \end{aligned}$$

□

$J_s(\{a_s(k)\}_{k=0}^{\infty})$ relies on the remote state estimation error and the communication price between sensor and controller, and is called the *state estimation cost*. $J_c(\{a_c(k)\}_{k=0}^{\infty})$ relies on the remote state estimate and the communication price between controller and actuator, and is called the *control cost*.

Remark 3.3.3. *Both the state estimation cost and the control cost depend on the communication decision $a_s(k)$ in the sensor subsystem. It is easy to see that the state estimation cost J_s relies on $a_s(k)$. The control cost J_c also relies on $a_s(k)$, because J_c must be computed with respect to the remote state estimate, $\overline{x}_{RO}(k)$, which is related to $a_s(k)$ according to equation (2.12). To emphasize the dependence of the control cost on the communication decision $a_s(k)$ in the sensor subsystem, we rewrite the the control cost as $J_c(\{a_s(k)\}_{k=0}^{\infty}) = J_c(\{a_s(k)\}_{k=0}^{\infty}, \{a_c(k)\}_{k=0}^{\infty})$.*

Let $a_s^\dagger$ be the optimal transmission rule that minimizes J_s with the corresponding optimal cost $J_s^\dagger$, and $a_c^\dagger$ be the controller's optimal communication strategy that minimizes the controller cost J_c based on $a_s^\dagger$ with the corresponding control cost $J_c^\dagger(a_s^\dagger)$. Since J_s and J_c are coupled, we see that the minimum cost J^* is bounded above by

$$J^* \leq J(a_s^\dagger, a_c^\dagger) = J_s^\dagger + J_c^\dagger(a_s^\dagger). \tag{3.4}$$

3.4 The Optimal Event Triggers

This section provides the optimal communication rule $a_s^\dagger$ for the sensor subsystem and the optimal communication rule $a_c^\dagger$ for the controller subsystem based on $a_s^\dagger$.

3.4.1 The Optimal Event Trigger in The Sensor Subsystem

Let $e_{KF,RO}(k) = \overline{x}_{KF}(k) - \overline{x}_{RO}(k)$ be the *a posteriori* gap between the filtered state and the remote state estimate. Noticing that $e_{KF,RO}(k)$ is orthogonal to the filtered state error $e_{KF}(k)$ (please check Lemma A.0.1 in Appendix for the proof), together with the dynamic behavior of $\overline{x}_{KF}$ and $\overline{x}_{RO}^-$, the estimation cost is rewritten

as

$$J_s(\{a_s(k)\}_{k=0}^{\infty}) = \lim_{N\to\infty} \frac{1}{N} \sum_{k=0}^{N-1} E\left(c_s(e^-_{KF,RO}(k), a_s(k))\right) + trace(QZ),$$

where

$$c_s(e^-_{KF,RO}(k), a_s(k)) = a_s(k)\lambda_s + (1 - a_s(k))\|e^-_{KF,RO}(k)\|^2_Z.$$

Theorem 2.5.1 in the last chapter has given the optimal transmission rule for the state estimation problem. For the convenience of readers, we restate the lemma as below.

Lemma 3.4.1. *Let*

$$T^s_h(s,\ell) = E\left(h(e^-_{KF,RO}(k+1))|e^-_{KF,RO}(k) = s, a_s(k) = \ell\right),$$

where $s \in \mathbb{R}^n$ *and* $\ell \in \{0,1\}$.

1. *There exist a unique constant* $\rho^\dagger_s$ *and a function* $h^\dagger_s$, *such that for all* $s \in \mathbb{R}^n$

$$\rho^\dagger_s + h^\dagger_s(s) = \min\left\{\|s\|^2_Z + T_{h^\dagger_s}(s,0), \lambda_s + T_{h^\dagger_s}(s,1)\right\}, \tag{3.5}$$

2. *The optimal cost* $J^\dagger_s = \rho^\dagger_s + trace(QZ)$.

3. *The optimal event trigger is*

$$a^\dagger_s(k) = \begin{cases} 1, & \text{if } V_{s,0}(e^-_{KF,RO}(k)) \geq V_{s,1}(e^-_{KF,RO}(k)) \text{ or } \|e^-_{KF,RO}(k)\| > \theta_s, \\ 0, & \text{otherwise.} \end{cases}$$

where $V_{s,0}(s) = \|s\|^2_Z + T_{h^\dagger_s}(s,0)$, *and* $V_{s,1}(s) = \lambda_s + T_{h^\dagger_s}(s,1)$.

3.4.2 The Optimal Event Trigger in The Controller Subsystem

Using the same technique as in Theorem 2.5.1, we derive the optimal transmission rule for the controller subsystem assuming that $a^\dagger_s$ is used as the triggering set in the

sensor subsystem.

Lemma 3.4.2. *Let* $\phi(k) = [\overline{x}_{RO}(k)\ \overline{x}_{KF}(k)\ u_a(k-1)]^T$ *be an augmented state. Define an operation* $T_h^c(s,\ell)$ *as*

$$T_h^c(s,\ell) = E\left(h(\phi(k+1))|\phi(k) = s, a_c(k) = \ell\right),$$

where $s \in \mathbb{R}^{2n+m}$ *and* $\ell \in \{0,1\}$*. Given* $a_s^\dagger$*, the following statements are true.*

1. *There exist a unique constant* $\rho_c^\dagger$ *and a function* $h_c^\dagger$*, such that for all* $s \in \mathbb{R}^{2n+m}$

$$\rho_c^\dagger + h_c^\dagger(s) = \min\left\{\|s\|_Z^2 + T_{h_c^\dagger}(c,0), \lambda_c + T_{h_c^\dagger}(s,1)\right\}, \tag{3.6}$$

2. *The optimal cost* $J_c^\dagger = \rho_c^\dagger$*.*
3. *The optimal event trigger is*

$$a_c^\dagger(k) = \begin{cases} 1, & \text{if } V_{c,0}(e^-_{KF,RO}(k)) \geq V_{c,1}(e^-_{KF,RO}(k)) \\ & \text{or } \|[\overline{x}_{RO}(k)\ u_a(k-1)]^T\| > \theta_c, \\ 0, & \text{otherwise.} \end{cases}$$

where $V_{c,0}(s) = \|s\|_Z^2 + T_{h_c^\dagger}(s,0)$*, and* $V_{c,1}(s) = \lambda + T_{h_c^\dagger}(s,1)$*.*

3.4.3 Upper Bound on The Cost of The Optimal Triggering Sets

From equation (3.4), Lemma 3.4.1 and 3.4.2, we obtain the following upper bound on J^*.

Theorem 3.4.3. *Given* $a_s^\dagger$ *and* $a_c^\dagger$ *defined in Lemma 3.4.1 and 3.4.2, respectively. The optimal cost of the closed loop system* J^* *satisfies*

$$J^* \leq \rho_s^\dagger + trace(QZ) + \rho_c^\dagger.$$

3.5 Suboptimal Event Triggers

As what was mentioned in Remark 2.5.2 in the last section, equation (3.5) and (3.6) are difficult to compute. With the concern about the computational complexity

of the optimal event triggers, we turn to a more computationally tractable approach for determining approximations to the optimal event triggers in this section.

3.5.1 A Suboptimal Event Trigger in The Sensor Subsystem

To find the suboptimal triggering set in the sensor subsystem, we first give the following lemma which is a direct result from Theorem 1 of [13].

Lemma 3.5.1. *Given a transmission rule a_s, if there exists a function $h_s : \mathbb{R}^n \to \mathbb{R}$ bounded from below and a finite constant ρ_s such that for any $s \in \mathbb{R}^n$,*

$$\rho_s + h_s(s) \geq c_s(s, a_s) + T^s_{h_s}(s, a_s(k)) \tag{3.7}$$

then

$$J_s(\{a_s(k)\}_{k=0}^{\infty}) \leq \rho_s + trace(QZ). \tag{3.8}$$

Based on lemma 3.5.1, we can identify a suboptimal triggering set in quadratic form, and the upper bound on this suboptimal triggering set is also given.

Lemma 3.5.2. *Given a suboptimal event trigger for the sensor subsystem as the following.*

$$a_s(k) = \begin{cases} 1, & \text{if } \|e^-_{KF,RO}(k)\|^2_{H_s} \geq \lambda_s - \zeta_s \text{ or } \|e^-_{KF,RO}(k)\| > \theta_s, \\ 0, & \text{otherwise.} \end{cases} \tag{3.9}$$

where the $n \times n$ matrix $H_s \geq 0$ satisfies

$$\frac{A^T H_s A}{1+\delta_s^2} - H_s + \frac{Z}{1+\delta_s^2} \leq 0, \tag{3.10}$$

for some $\delta_s^2 \geq 0$, and $\zeta_s = \frac{\delta_s^2 \lambda_s + tr(H_s R)}{1+\delta_s^2}$, where $R = L(CAQA^TC^T + CWC^T + V)L^T$,

then

$$J_s(\{a_s(k)\}_{k=0}^{\infty}) \leq \min\{tr(H_sR) + \zeta_s, \lambda_s\} + tr(QZ) \tag{3.11}$$

Proof. To find an upper bound on the cost of triggering set defined in equation (3.9), we need to find a bounded function h_s and a finite constant ρ_s such that equation (3.7) is satisfied.

Now, let's define h_s as

$$h_s(e^-_{KF,RO}(k)) = \min\{\|e^-_{KF,RO}(k)\|^2_{H_s} + \zeta_s, \lambda_s\},$$

and ρ_s as

$$\rho_s = E(h_s(e^-_{KF,RO}(k+1))|e_{KF,RO}(k) = 0). \tag{3.12}$$

In the case of $\|e^-_{KF,RO}(k)\|^2_{H_s} \leq \lambda_s - \zeta_s$, no transmission occurs at step k, so the right hand side of equation (3.7) satisfies the following equations.

$$\begin{aligned}
&E\left(h_s(e^-_{KF,RO}(k+1))|e^-_{KF,RO}(k), S_s\right) + c_s\left(e^-_{KF,RO}, S_s\right)\\
=&E\left(h_s(e^-_{KF,RO}(k+1))|e_{KF,RO}(k) = e^-_{KF,RO}(k)\right) + \|e^-_{KF,RO}\|^2_Z\\
\leq&\|e^-_{KF,RO}\|^2_{A^TH_sA} + tr(H_sR) + \zeta_s + \|e^-_{KF,RO}\|^2_Z\\
\leq&\|e^-_{KF,RO}(k)\|^2_{H_s} + \|e^-_{KF,RO}(k)\|^2_{A^TH_sA-H_s+Z} + \zeta_s + tr(H_sR)\\
\leq&\|e^-_{KF,RO}(k)\|^2_{H_s} + \zeta_s + \delta_s^2(\lambda_s - \zeta_s) + tr(H_sR)\\
=&h_s(e^-_{KF,RO}(k)) + \zeta_s\\
\leq&h_s(e^-_{KF,RO}(k)) + \rho_s.
\end{aligned}$$

The second step is taken by the fact that $E(\min(f,g)) \leq \min(E(f), E(g))$, the fourth step is derived from equation (3.10) and the fact that $\|e^-_{KF,RO}(k)\|^2_{H_s} \leq \lambda_s - \zeta_s$, and

the fifth step is derived from how we define the ζ_s.

In the case of $\|e^-_{KF,RO}(k)\|^2_{H_s} > \lambda_s - \zeta_s$, transmission occurs. The right side of inequality (3.7) satisfies

$$\begin{aligned}
&E\left(h_s(e^-_{KF,RO}(k+1))|e^-_{KF,RO}(k), S_s\right) + c_s\left(e^-_{KF,RO}, S_s\right) \\
=&E\left(h_s(e^-_{KF,RO}(k+1))|e_{KF,RO}(k) = 0\right) + \lambda_s \\
=&\rho_s + h_s(e^-_{KF,RO}(k))
\end{aligned}$$

Since the inequality (3.7) holds in both conditions, from Lemma 3.5.1, we have $J_s(\{a_s(k)\}_{k=0}^{\infty}) \leq \min\{tr(H_sR) + \zeta_s, \lambda_s\} + tr(QZ)$ □

Remark 3.5.3. *For any A and Z, there must exist a positive definite matrix H_s and a constant δ_s such that equation (3.10) holds. It is easy to see that we can always choose δ_s^2 big enough (e.g square of the largest singular value of A) so that $\frac{A}{\sqrt{1+\delta_s^2}}$ is stable, and hence for any positive definite Z, there is a positive definite matrix H_s satisfying equation (3.10).*

Remark 3.5.4. *With fixed δ_s, Equation (3.10) is a linear matrix inequality, and hence can be efficiently solved. According to our experience, to obtain as small as possible upper bound on the suboptimal cost, δ_s should be chosen as small as possible while equation (3.10) is feasible.*

3.5.2 A Suboptimal Event Trigger in Controller Subsystem

Similar to the derivation of the suboptimal event trigger in the sensor subsystem, the subsection provides a suboptimal event trigger in the controller subsystem and an upper bound on the suboptimal cost.

Define $c_c\left(\overline{x}_{RO}(k), a_c\right) = \|\overline{x}_{RO}\|^2_Z + \lambda_c a_c(k)$.

Lemma 3.5.5. *Given any communication rule a_c, if there exists a function $h_c : \mathbb{R}^n \times \mathbb{R}^m \to \mathbb{R}$ bounded from below and a finite constant ρ_c such that*

$$\rho_c + h_c\left(\phi(k)\right) \geq c_c\left(\overline{x}_{RO}(k), S_c\right) + T^c_{h_c}(\phi(k), a_c(k)), \tag{3.13}$$

then $J_c(\{a_c(k)\}_{k=0}^{\infty}) \leq \rho_c$.

Based on Lemma 3.5.5, the suboptimal event trigger in the controller subsystem and its upper bound are provided in the following Lemma.

Lemma 3.5.6. *Given the transmission rule a_s in the sensor subsystem defined in Equation (3.9). Let $A_u = \begin{bmatrix} A & B \\ 0 & I \end{bmatrix}$, $A_c = \begin{bmatrix} A+BK & 0 \\ K & 0 \end{bmatrix}$, $Z_a = \begin{bmatrix} Z & 0 \\ 0 & 0 \end{bmatrix}$, and $H_s = P_{Hs}^T P_{Hs}$. Given the suboptimal event trigger for the controller subsystem as the following.*

$$a_c(k) = \begin{cases} 1, & \text{if } \left\| \begin{bmatrix} \overline{x}_{RO}(k) \\ u_a(k-1) \end{bmatrix} \right\|^2_{H_c} + \zeta_c \leq \|\overline{x}_{RO}(k)\|^2_Z + \lambda_c \\ & \text{or } \|[\overline{x}_{RO}(k)\ u_a(k-1)]^T\| > \theta_c, \\ 0, & \text{otherwise.} \end{cases} \tag{3.14}$$

where $H_c \geq Z_a$ and controller gain K satisfy

$$A_u^T H_c A_u + (1+\delta_c^2)(Z_a - H_c) \leq 0, \tag{3.15}$$

$$A_c^T H_c A_c + (1-\rho_c^2)(Z_a - H_c) \leq 0, \tag{3.16}$$

for some constant $\delta_c^2 \geq 0$ and $0 \leq \alpha_c^2 \leq 1$, and

$$\zeta_c = \frac{\delta_c^2 + \alpha_c^2 - 1}{\delta_c^2 + \alpha_c^2} \lambda_c. \tag{3.17}$$

The controller cost satisfies

$$J_c(\{a_s(k)\}_{k=0}^{\infty}, \{a_c(k)\}_{k=0}^{\infty}) \leq \frac{\delta_c^2}{\delta_c^2 + \alpha_c^2}\lambda_c + \overline{\sigma}((P_{Hs}^T)^{-1} H_{c,lu} P_{Hs}^{-1})(\lambda_s - \zeta_s), \tag{3.18}$$

where $\overline{\sigma}(\cdot)$ *indicates the greatest singular value, and* $H_{c,lu}$ *is the left upper* $n \times n$ *sub-matrix of* H_c*.*

Proof. According to Lemma 3.5.5, as long as we can find a function h_c bounded from below and a finite constant ρ_c such that the inequality (3.13) is satisfied, Lemma 3.5.6 is true.

Let's define

$$h_c\left(\overline{x}_{RO}(k), u_a(k-1)\right) = \left\| \begin{bmatrix} \overline{x}_{RO}(k) \\ u_a(k-1) \end{bmatrix} \right\|_{H_c}^2 + \zeta_c,$$

and

$$\rho_c = \frac{\delta_c^2}{\delta_c^2 + \alpha_c^2}\lambda_c + \overline{\sigma}((P_{Hs}^T)^{-1} H_{c,lu} P_{Hs}^{-1})(\lambda_s - \zeta_s).$$

First, we consider the case when $\left\| \begin{bmatrix} \overline{x}_{RO}(k) \\ u_a(k-1) \end{bmatrix} \right\|_{H_c}^2 + \zeta_c \leq \|\overline{x}_{RO}(k)\|_Z^2 + \lambda_c$. In this case, the controller subsystem doesn't transmit. The right hand side of equation

(3.13) is

$$
\begin{aligned}
&\leq \begin{bmatrix} \overline{x}_{RO}(k) \\ u_a(k-1) \end{bmatrix}^T A_u^T H_c A_u \begin{bmatrix} \overline{x}_{RO}(k) \\ u_a(k-1) \end{bmatrix} + \overline{\sigma}((P_{Hs}^T)^{-1} H_{c,lu} P_{Hs}^{-1})(\lambda_s - \zeta_s) + \zeta_c \\
&\quad + \begin{bmatrix} \overline{x}_{RO}(k) \\ u_a(k-1) \end{bmatrix}^T Z_a \begin{bmatrix} \overline{x}_{RO}(k) \\ u_a(k-1) \end{bmatrix} \\
&\leq \rho_c + f_c \left(\begin{bmatrix} \overline{x}_{RO}(k) \\ u_a(k-1) \end{bmatrix} \right)
\end{aligned}
$$

The first inequality is from equation (3.9), and the second inequality is from equation (3.15) and (3.17).

The second case is when $\left\| \begin{bmatrix} \overline{x}_{RO}(k) \\ u_a(k-1) \end{bmatrix} \right\|_{H_c}^2 + \zeta_c > \|\overline{x}_{RO}(k)\|_Z^2 + \lambda_c$. In this case, the controller subsystem transmits information. So the right hand side of equation (3.13) is

$$
\begin{aligned}
&\leq \begin{bmatrix} \overline{x}_{RO}(k) \\ u_a(k-1) \end{bmatrix}^T A_c^T H_c A_c \begin{bmatrix} \overline{x}_{RO}(k) \\ u_a(k-1) \end{bmatrix} + \overline{\sigma}((P_{Hs}^T)^{-1} H_{c,lu} P_{Hs}^{-1})(\lambda_s - \zeta_s) + \zeta_c \\
&\quad + \begin{bmatrix} \overline{x}_{RO}(k) \\ u_a(k-1) \end{bmatrix}^T Z_a \begin{bmatrix} \overline{x}_{RO}(k) \\ u_a(k-1) \end{bmatrix} + \lambda_c \\
&\leq \rho_c + h_c \left(\begin{bmatrix} \overline{x}_{RO}(k) \\ u_a(k-1) \end{bmatrix} \right).
\end{aligned}
$$

The first inequality is from Equation (3.9), and the second inequality is from Equation (3.16) and (3.17).

Since in both cases, equation (3.13) holds, we conclude that

$$J_c(\{a_s(k)\}_{k=0}^{\infty}, \{a_c(k)\}_{k=0}^{\infty}) \leq \rho_c.$$

□

3.5.3 An Upper Bound on The Total Suboptimal Cost

From the results in Lemma 3.3.2, 3.5.2 and 3.5.6, we have the following theorem.

Theorem 3.5.7. *Given the event trigger a_s in the sensor subsystem defined in equation (3.9) and the event trigger a_c in the controller subsystem defined in equation (3.14), the average cost $J(\{a_s(k)\}_{k=0}^{\infty}, \{a_c(k)\}_{k=0}^{\infty})$ given by the two weakly coupled triggering sets satisfies*

$$J(\{a_s(k)\}_{k=0}^{\infty}, \{a_c(k)\}_{k=0}^{\infty}) \leq \rho_s + trace(QZ) + \rho_c.$$

3.6 Simulation Results

This section uses an example to demonstrate Theorem 3.5.7. We first calculate the triggering sets S_s and S_c according to equation (3.9) and (3.14), and search for the controller gain K such that inequality (3.16) is satisfied. The system, then, is run using three different transmission rules: weakly coupled event triggered transmission, synchronized event triggered transmission and periodic transmission. The average costs are compared. We also show that the number of transmission times in sensor subsystem, the number of transmission times in controller subsystem, and the number of times when both sensor and controller transmit (concurrent transmission times) to illustrate that the transmission in the sensor subsystem doesn't necessarily trigger the transmission in the controller subsystem, or vice versa.

Let's consider the following system

$$x(k) = \begin{bmatrix} 0.4 & 0 \\ 0 & 1.01 \end{bmatrix} x(k-1) + \begin{bmatrix} 1 \\ 1 \end{bmatrix} u_a(k-1) + w(k-1)$$
$$y(k) = \begin{bmatrix} 0.1 & 1 \end{bmatrix} x(k) + v(k).$$

The variances of the system noises are $W = \begin{bmatrix} 0.2 & 0.1 \\ 0.1 & 0.2 \end{bmatrix}$, and $V = 0.3$. The weight matrix Z is chosen to be an identity matrix.

Given $\delta_s^2 = 1.5$, $\lambda_s = 3$, $\delta_c^2 = 1.02$ and $\rho_c = 0.3$, we can obtain the event trigger a_s in sensor subsystem as

$$a_s(k) = \begin{cases} 1, & \text{if } e_{KF,RO}^{-T} \begin{bmatrix} 2.5641 & 0 \\ 0 & 4.0543 \end{bmatrix} e_{KF,RO}^{-} \leq 0.8414 \text{ or } \|e_{KF,RO}^{-}(k)\| > \theta_s, \\ 0, & \text{otherwise.} \end{cases} \tag{3.19}$$

and the triggering set in controller subsystem S_c as

$$a_c(k) = \begin{cases} 1, & \text{if } \begin{bmatrix} \overline{x}_{RO}(k) \\ u_a(k-1) \end{bmatrix}^T \begin{bmatrix} 1.3315 & -0.2836 & -0.3512 \\ -0.2836 & 3.6377 & 2.6808 \\ -0.3512 & 2.6808 & 13.7606 \end{bmatrix} \begin{bmatrix} \overline{x}_{RO}(k) \\ u_a(k-1) \end{bmatrix} \\ & \leq 0.9008\lambda_c \text{ or } \|[\overline{x}_{RO}(k)\ u_a(k-1)]^T\| > \theta_c, \\ 0, & \text{otherwise.} \end{cases} \tag{3.20}$$

and the controller gain $K = [-0.1967\ \ -0.3133]$.

The closed loop system was run for 3000 steps using different transmission rules with the communication price from controller to actuator varying from 0 to 200.

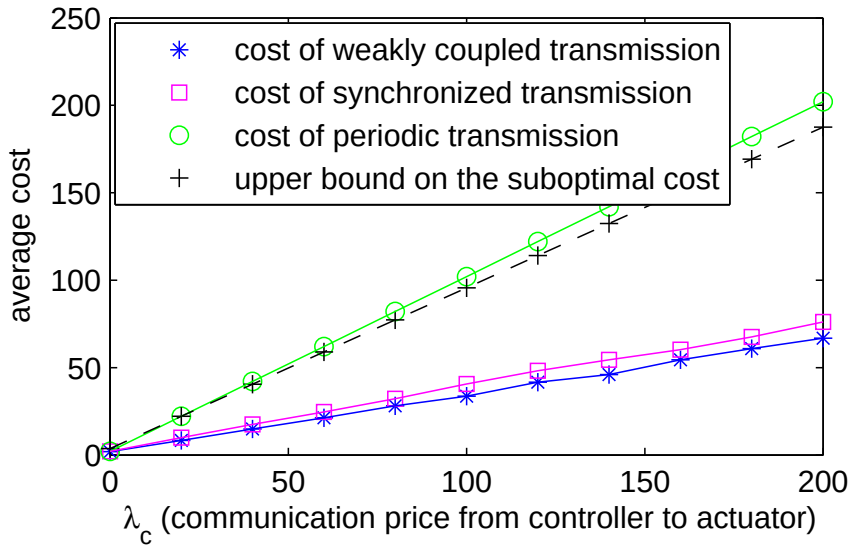

Figure 3.2. Average costs using weakly coupled transmission, synchronized transmission and periodic transmission which different communication price from controller to actuator.

When we run the system, there was one step delay in the communication network. We first run the system with the communication rules defined in (3.19) and (3.20). After that, the system was run using a synchronized transmission rule, with which the transmissions from sensor to controller were only triggered by $e^{-}_{KF,RO}(k) \notin S_s$, and the transmissions from controller to actuator were triggered by either $[\overline{x}_{RO}(k)\ u_a(k-1)]^T \notin S_c$ or transmissions from sensor to controller. Finally, we used the average periods in weakly coupled event triggered transmission experiment as the periods to run the system using periodic transmission. The average costs are given in Figure 3.2.

Figure 3.2 describes the average costs with respect to λ_c, the communication price from controller to actuator. Stars indicate the average cost using weakly coupled transmission rule which gives the least average cost during the costs using different triggering rules. Squares denote the average cost using synchronized transmission

rule which gives the second least average cost, and its difference from the average cost of weakly coupled transmission increases as λ_c increases. That's because when λ_c is small, with synchronized transmission, most transmissions from controller to actuator were triggered by the event $[\overline{x}_{RO}(k)\ u_a(k-1)]^T \notin S_c$, and hence synchronized transmission had similar cost as the weakly coupled transmission. Figure 3.2 also shows that the average cost using periodic transmission (circles) is always greater than the average cost using event triggered transmission no matter whether the transmission is weakly coupled (stars) or synchronized (squares). Crosses are the upper bounds on the average cost of weakly coupled transmission calculated according to Theorem 3.5.7. These crosses are always above the average cost of weakly coupled transmission (stars), which demonstrates Theorem 3.5.7. We also notice that both the upper bound (crosses) and the actual cost (stars) increases linearly with respect to λ_c, and the ratio of the upper bound (crosses) to the actual cost (stars) is about 3.

Figure 3.3 shows that the transmission in the sensor subsystem doesn't always trigger the transmission in controller subsystem, or vice versa. The x-axis of this plot is the communication price from controller to actuator λ_c, and the y-axis indicates the transmission times. We can see that the number of concurrent transmission times (circles) is always less or equal to both the numbers of transmission times in sensor subsystem (stars) and controller subsystem (crosses), which indicates that the transmission in sensor subsystem doesn't always trigger the transmission in controller subsystem, or vice versa.

3.7 Conclusion

This paper presents weakly coupled triggering events in event triggered output feedback system with the whole control loop closed over wireless network. By 'weakly coupled', we mean that the triggering events in both sensor and controller only use

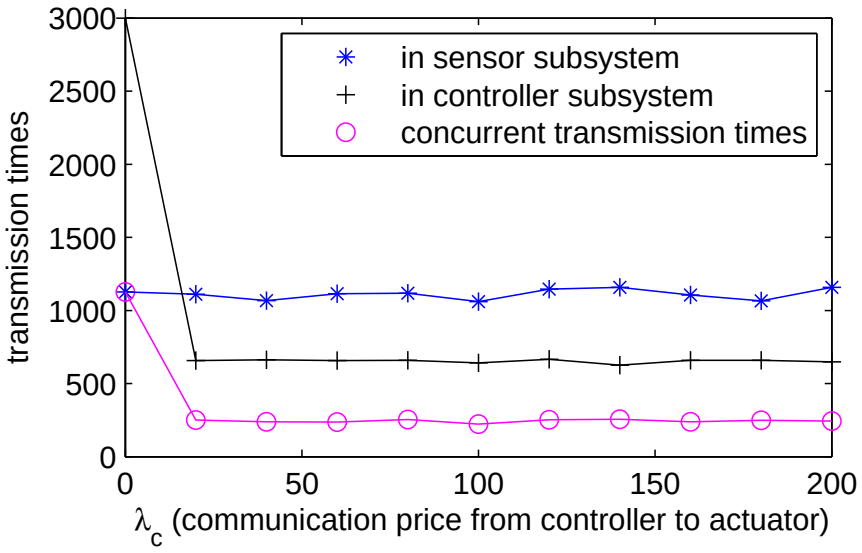

Figure 3.3. Average costs using weakly coupled transmission, synchronized transmission and periodic transmission which different communication price from controller to actuator.

local information to decide when to transmit data, and the transmission in one link doesn't necessarily trigger the transmission in the other link. We also show that with the triggering events and controller we designed, the cost of the closed loop system is bounded from above, and an explicit upper bound on the cost is obtained. Our simulation results show that the proposed triggering events are weakly coupled and the upper bound on the cost of the closed loop system is relatively tight when the communication price λ_s from the sensor subsystem to the controller subsystem is low.

CHAPTER 4

EFFICIENTLY ATTENTIVE AND ISS EVENT TRIGGERED CONTROL SYSTEMS WITH LIMITED TRANSMISSION FREQUENCY AND INSTANTANEOUS BIT-RATE

Chapter 2 and 3 study the minimum system performance cost with limited transmission frequency. The network delay and quantization error, however, are neglected in Chapter 2 and 3. This chapter explicitly considers the influence of network latency and quantization error, and derives a bound on an event-triggered system's stabilizing 'instantaneous' bit-rate when the sampled signal is dynamically quantized. This instantaneous bit-rate is a time-varying function whose average value can be made small by requiring the instantaneous bit-rate get smaller as the system state approaches the origin. This property is referred as *efficient attentiveness*. This chapter provides sufficient conditions guaranteeing the instantaneous bit-rate's efficient attentiveness. Our numerical example illustrates the results, and indicates a tradeoff between inter-sampling interval and instantaneous bit-rate.

4.1 Introduction

Wireless sensor-actuator networks are networked control systems whose actuators/controllers and sensors communicate over a wireless communication network. These communication networks are digital networks with finite capacity. This means that transmitted packets consist of a finite number of bits and always arrive at their destination with a non-negligible delay. The resulting quantization error and mes-

sage latency has a negative impact on overall closed-loop system performance [61] and hence must be considered when designing any wireless sensor-actuator network.

Event triggering is a recent approach to sampled-data control in which sampled feedback measurements are transported over the feedback channel in a sporadic manner. In event-triggered systems, the system state is sampled and transmitted back to the actuator or controller when the difference between the current state and the last transmitted state exceeds a specified threshold. It has been experimentally demonstrated [5, 6, 59, 64, 16, 48, 42] that event-triggered system can greatly reduce the average rate at which the control system accesses the feedback channel over periodically-sampled systems with comparable performance levels.

While event-triggered systems have the *potential* to reduce the inter-sampling rate, they can also increase that rate if improperly designed. The following example illustrates this issue. Consider a cubic system

$$\dot{x} = x^3 + u; \quad x(0) = x_0$$

where $u = -3\hat{x}_k^3$ for $t \in [s_,s_{k+1})$ where s_k is the kth consecutive sampling instant and $\hat{x}_k = x(s_k)$. Let us now consider two different event-triggers. The trigger $\mathbf{E}_1$ generates a sampling instant s_{k+1} when $|x(t) - \hat{x}_k| = 0.5|x(t)|$ and the second trigger $\mathbf{E}_2$ generates a sampling instant when $|x(t) - \hat{x}_k| = 0.5|x^4(t)|$. For both event-triggers we find the system is locally asymptotically stable for all $|x_0| \leq 1$. But if one examines the inter-sampling intervals for these systems in Figure 4.1, it should be apparent that the inter-sampling intervals generated by trigger $\mathbf{E}_1$ get longer as the system approaches its equilibrium. On the other hand, the trigger $\mathbf{E}_2$ results in a sequence of inter-sampling times that get shorter as the system approaches the origin.

Since the above example focuses on regulation about the origin, one would clearly

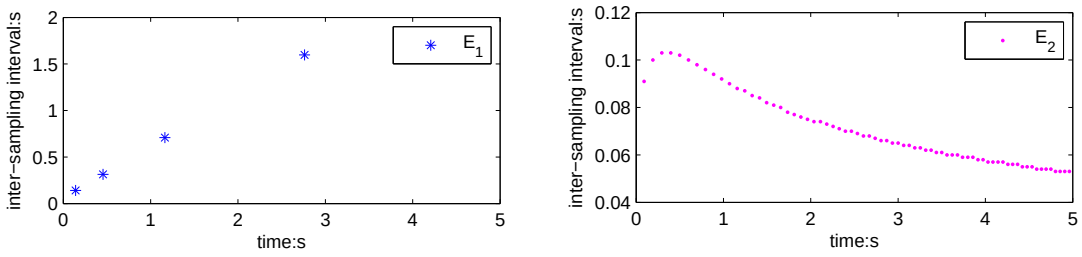

Figure 4.1. Inter-sampling intervals for two different types of event-triggers

want the inter-sampling interval to be longest when the system is close to the origin. The 'interesting' feedback information that mandates use of the feedback channel should occur when the system is perturbed away from the origin, not when the system is resting in the neighborhood of the origin. This "desired" behavior is exhibited by event-trigger $\mathbf{E}_1$, but as shown in Figure 4.1, the opposite trend is exhibited by event-trigger $\mathbf{E}_2$. Event trigger $\mathbf{E}_1$ is said to be *efficiently attentive* because the control system is more efficient in its use of the channel when the system state is close to the origin.

One reason why there has been such great interest in the inter-sampling interval is that it can be taken as a measure of channel usage. Much of this prior work, however, [59, 24, 44, 46] has ignored delays or quantization errors. For this reason, results bounding the inter-sampling interval only provide a partial picture of an event-triggered system's network usage. Recent work has begun to consider constant bounded delays [71, 72, 20, 33], but this chapter shows that delays preserving input-to-state stability (ISS) are state-dependent, thereby suggesting that the 'bit-rates' required to support event-triggered systems are time-varying. If, in fact, one can assure that these 'instantaneous' bit-rates are efficiently attentive, then one reduces the average bit rate over systems using constant bounded delays. The main results in this chapter establish sufficient conditions for an event-triggered system's instantaneous bit-rate to be efficiently attentive. We then provide simulation examples to illus-

trate the value of these results. In the examples, we also see a tradeoff between the inter-sampling interval and the instantaneous bit-rate. This tradeoff indicates that we should not only focus on lengthening the inter-sampling interval, but also need to guarantee the channel bandwidth satisfies the required instantaneous bit-rate.

4.2 Notation and Background on Input-to-State Stability

4.2.1 Notation

Throughout this chapter, the n dimensional real space will be denoted as $\mathbb{R}^n$ and the set of non-negative reals will be denoted as $\mathbb{R}^+$. The infinity (supremum) norm of a vector $x \in \mathbb{R}^n$ will be denoted as $\|x\|$. The $\mathcal{L}$-infinity norm of a function $x(\cdot) : \mathbb{R}^+ \to \mathbb{R}^n$ is defined as $\|x\|_{\mathcal{L}_\infty} = \operatorname{ess\,sup}_{t\geq 0} \|x(t)\|$. This function is said to be essentially bounded if $\|x\|_{\mathcal{L}_\infty} < \infty$ and the linear space of all essentially bounded real-valued functions will be denoted as $\mathcal{L}_\infty$. A subset $\Omega \subset \mathbb{R}^n$ is said to be compact if it is closed and bounded.

A function $\alpha(\cdot) : \mathbb{R}^+ \to \mathbb{R}^+$ is class $\mathcal{K}$ if it is continuous, strictly increasing and $\alpha(0) = 0$. It is said to be of $\mathcal{K}_\infty$, if $\alpha(s) \to \infty$ as $s \to \infty$. A function $\beta : \mathbb{R}^+ \times \mathbb{R}^+ \to \mathbb{R}^+$ is class $\mathcal{K}L$ if $\beta(\cdot, t)$ is class $\mathcal{K}$ for each fixed $t \geq 0$ and $\beta(r, t)$ decreases to 0 as $t \to \infty$ for each fixed $r \geq 0$.

Lemma 4.2.1. *Let $g : [0, \sigma] \to \mathbb{R}^+$ be a continuous, positive definite function satisfying $\lim_{s\to 0} < \infty$. There must exist continuous, positive definite, increasing functions $\underline{h}$ and $\overline{h}$ defined on $[0, \sigma]$ such that*

$$\underline{h}(s) \leq g(s) \leq \overline{h}(s), \forall s \in [0, \sigma],$$
$$\lim_{s\to 0} g(s) = \lim_{s\to 0} \underline{h}(s) = \lim_{s\to 0} \overline{h}(s).$$

Proof. See Lemma 4.3 in [32]. □

Let Ω be a compact subset of $\mathbb{R}^n$. We say $f(\cdot) : \Omega \to \mathbb{R}^n$ is locally Lipschitz on Ω if for any $x, y \in \Omega$, there exists a constant $L \geq 0$ such that

$$\|f(x) - f(y)\| \leq L\|x - y\|$$

4.2.2 Background on Input-to-State Stability

Consider a system whose state trajectory $x(\cdot) : \mathbb{R}^+ \to \mathbb{R}^n$ satisfies the initial value problem,

$$\dot{x}(t) = f(x(t), w(t)), \quad x(0) = x_0 \tag{4.1}$$

where $w(\cdot) : [0, \infty) \to \mathbb{R}^m$ is an essentially bounded signal. Let $x = 0$ be an equilibrium point for (4.1) with $w(t) \equiv 0$, and $\Upsilon \subset \mathbb{R}^n$ be a domain containing $x = 0$. Let $V : \Upsilon \to \mathbb{R}$ be a continuously differentiable function such that

$$\underline{\alpha}(\|x\|) \leq V \leq \overline{\alpha}(\|x\|), \tag{4.2}$$

$$\frac{\partial V}{\partial x} f(x, w) \leq -\alpha(\|x\|) + \gamma(\|w\|), \tag{4.3}$$

for all $(x, w) \in \Upsilon \times \mathbb{R}^m$, where $\underline{\alpha}$, $\overline{\alpha}$ are class $\mathcal{K}_\infty$ functions, and α, γ are class $\mathcal{K}$ functions, then the system (4.1) is input-to-state stable (ISS). The function V is called *ISS-Lyapunov* function.

4.3 Problem Statement

The system under study is a wireless networked event-triggered control system with quantization shown in Figure 4.2.

Consider the following plant whose state satisfies the following differential equa-

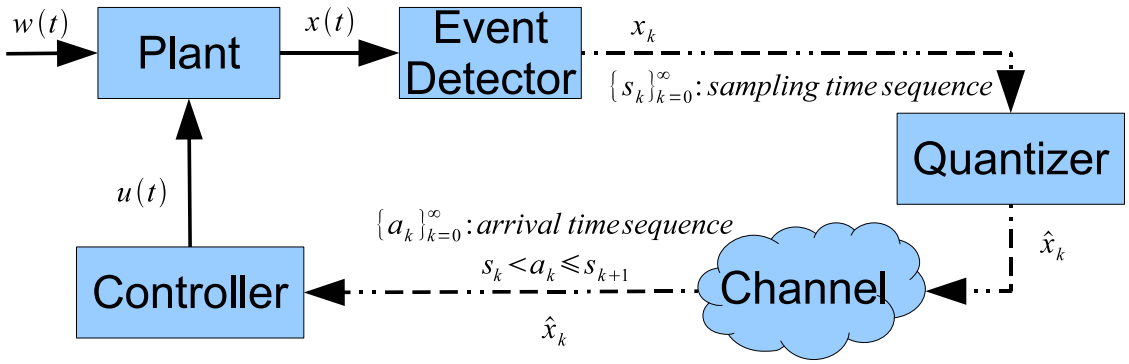

Figure 4.2. Event-triggered control system with quantization

tion.

$$\dot{x}(t) = f(x(t), u(t), w(t)), \quad x(0) = x_0 \tag{4.4}$$

where $f : \mathbb{R}^n \times \mathbb{R}^m \times \mathbb{R}^q \to \mathbb{R}^n$ is locally Lipschitz in all three variables with $f(0,0,0) = 0$. The disturbance $w(\cdot) : \mathbb{R}^+ \to \mathbb{R}^q$ is an $\mathcal{L}_\infty$ disturbance with $\|w\|_{L_\infty} = \bar{w}$. The control signal $u(\cdot) : \mathbb{R}^+ \to \mathbb{R}^m$ is generated by the *controller* in Figure 4.2.

The system state, $x(t)$, at time t is measured by the *event detector* which triggers the transmission once upon the violation of an event $\mathbf{E}$. Formally, event $\mathbf{E}(\cdot) : \mathbb{R}^n \to \{\text{true, false}\}$ maps the current state onto either "TRUE" or "FALSE". The kth transmission time s_k satisfies

$$s_k = \min\{t : \mathbf{E}(x(t)) \text{ is false and } t > s_{k-1}\}, \tag{4.5}$$

and the inter-sampling interval τ_k is defined as $\tau_k = s_{k+1} - s_k$. Let x_k indicate the system state $x(s_k)$ at s_k. Once the event detector decides to transmit, the *quantizer* converts this continuous valued state x_k into N_k bit representation $\hat{x}_k$ with quantization error to be $\Delta_k = |\hat{x}_k - x(s_k)|$. Notice that both N_k and Δ_k can be time

varying and state dependent. The quantized state $\hat{x}_k$ is, then, transmitted to the controller with delay d_k. The *instantaneous bit-rate* r_k is, then, defined as $r_k = \frac{N_k}{d_k}$, and the arrival time a_k of the kth transmission, then, satisfies $a_k = s_k + d_k$. We say that the transmission and arrival sequences are admissible if $s_k < a_k \leq s_{k+1}$ for $k = 0, 1, \ldots, \infty$.

Upon the arrival of the kth quantized state, $\hat{x}_k$, at the controller, a control input is computed and then held until the next quantized state is received. In other words, the control signal takes the form

$$u(t) = u_k = K(\hat{x}_k) \tag{4.6}$$

for $t \in [a_k, a_{k+1})$. The function $K(\cdot) : \mathbb{R}^n \to \mathbb{R}^m$ is locally Lipschitz, and satisfies $K(0) = 0$. As has been done in [59], this chapter assumes that K is chosen so the system

$$\dot{x}(t) = f(x(t), K(x(t) + e(t)), w(t)), \tag{4.7}$$

is locally input-to-state stable with respect to the signals $e, w \in \mathcal{L}_\infty$. This means, of course, that there exists a function $V(\cdot) : \Upsilon \to \mathbb{R}^+$ satisfying

$$\underline{\alpha}(\|x\|) \leq V \leq \overline{\alpha}(\|x\|) \tag{4.8}$$

$$\frac{\partial V}{\partial x} f(x, w) \leq -\alpha(\|x\|) + \gamma_1(\|e\|) + \gamma_2(\|w\|), \tag{4.9}$$

for all $x \in \Upsilon$ where $\Upsilon \subseteq \mathbb{R}^n$ is a domain containing the origin, $\underline{\alpha}$, $\overline{\alpha}$, α, γ_1 and γ_2 are class $\mathcal{K}$ functions.

Our objective is to design the event detector and the quantizer such that the system defined in (5.1), (4.5) and (4.6) is ISS and efficiently attentive.

Definition 4.3.1. *The system defined in (5.1), (4.5) and (4.6) is said to be* efficiently

attentive *if there exists a continuous, positive definite function* $\underline{h}(s_1, s_2)$ *satisfying* $\lim_{s\to 0} \underline{h}(s_1, s_2) > 0$ *and decreasing with respect to both variables, and a continuous, positive definite function* $\bar{h}(s_1, s_2)$ *satisfying* $\lim_{s\to 0} \bar{h}(s_1, s_2) < \infty$ *and increasing with respect to both variables such that*

- *the inter-sampling interval* τ_k *is bounded from below by* $\underline{h}(\|\hat{x}_{k-1}\|, \|\hat{x}_k\|)$*, i.e.*

$$\tau_k \geq \underline{h}(\|\hat{x}_{k-1}\|, \|\hat{x}_k\|). \tag{4.10}$$

- *the instantaneous bit-rate* r_k *is bounded from above by* $\bar{h}(\|\hat{x}_{k-1}\|, \|\hat{x}_k\|)$*, i.e.*

$$r_k \leq \bar{h}(\|\hat{x}_{k-1}\|, \|\hat{x}_k\|). \tag{4.11}$$

Remark 4.3.2. *The bounds on* τ_k *and* r_k *depend on both* $\hat{x}_{k-1}$ *and* $\hat{x}_k$*, because* $\hat{x}_k$ *is transmitted with some delay, and both* $\hat{x}_{k-1}$ *and* $\hat{x}_k$ *are used to produce control input and hence influence the system dynamic during intervals* $[s_k, a_k)$ *and* $[a_k, s_{k+1}]$*, respectively.*

Remark 4.3.3. *The requirement (4.10) on* τ_k *indicates how often the event-triggered control system uses communication resources. Once requirement (4.10) is satisfied, the event-triggered control system will use the communication less frequently as the system state get closer to the origin.*

Remark 4.3.4. *The requirement (4.11) on* r_k *indicates how much communication resources (i.e. bandwidth) is used by the event-triggered control system in each transmission. Equation (4.11) requires the event-triggered control system uses fewer communication resources as the system state gets closer to the origin.*

To guarantee ISS and efficient attentiveness, we first provide the event detector and quantizer guaranteeing ISS assuming there is no delay, then study the acceptable delay based on the designed event detector and quantizer, and finally give the sufficient condition of efficient attentiveness.

Let us first look at the dynamic behavior of the closed loop system. Let $e_k(t) = x(t) - \hat{x}_k$ be the *gap* between the current state and the kth quantized state. From equation (4.8) and (4.9), it is easy to get the following lemma.

Lemma 4.4.1. *Given the event-triggered system in (5.1-4.5) whose controller (4.6) satisfies is locally ISS and satisfies (4.8-4.9). If for all $t \in [a_k, a_{k+1})$ and all $k = 0, 1, \cdots, \infty$,*

$$\|e_k(t)\| \leq \xi(\|x(t)\|, \bar{w}) = \gamma_1^{-1}(c\alpha(\|x(t)\|) + \gamma_3(\bar{w})), \tag{4.12}$$

where $c \in (0, 1)$ and γ_3 is a $\mathcal{K}$ function, then the system is locally ISS.

Proof. Apply equation (4.12) into equation (4.9), we have

$$\frac{\partial V}{\partial x} f(x, w) \leq -(1 - c)\alpha(\|x\|) + \gamma_2(\bar{w}) + \gamma_3(\bar{w}), \forall t \geq 0.$$

Since $c \in (0, 1)$ and $\gamma_2(\bar{w}) + \gamma_3(\bar{w})$ is a class $\mathcal{K}$ function of $\bar{w}$, the system is ISS. □

Suppose that $\xi(s, \bar{w})$ in (4.12) is locally Lipschitz for all $s \in \Upsilon$ with the Lipschitz constant L^ξ. Let

$$\underline{\xi}(s, \bar{w}) = \frac{1}{L^\xi + 1}\xi(s, \bar{w}). \tag{4.13}$$

It can be shown that

Corollary 4.4.2. *Given the event-triggered system in (5.1-4.5) whose controller (4.6) satisfies is locally ISS and satisfies (4.8-4.9). If $\|e_k(t)\| \leq \underline{\xi}_k = \underline{\xi}(\|\hat{x}_k\|, \bar{w})$ in (4.13) , for all $t \in [a_k, a_{k+1})$ and all $k = 0, 1, \cdots, \infty$, then the event-triggered system is ISS.*

Proof.

$$\begin{aligned}\|e_k(t)\| &\leq \frac{1}{L^\xi+1}\xi(\|\hat{x}_k\|,\bar{w}) \\ &\leq \frac{1}{L^\xi+1}\xi(\|x(t)\|+\|e_k(t)\|,\bar{w}). \\ &\leq \frac{1}{L^\xi+1}\xi(\|x(t)\|,\bar{w})+\frac{L^\xi}{L^\xi+1}\|e_k(t)\| \\ \Rightarrow \|e_k(t)\| &\leq \xi(\|x(t)\|,\bar{w})\end{aligned}$$

According to lemma 4.4.1, the above equation implies the system is ISS. □

Now, let us choose our event-trigger as

$$\mathbf{E}: \ \|e_k(t)\| < \theta_k = \theta(\|\hat{x}_k\|,\bar{w}) = \rho_\theta \underline{\xi}(\|\hat{x}_k\|,\bar{w}), \tag{4.14}$$

where $\rho_\theta \in (0,1)$ is a given constant. Let Δ_k be the quantization error at the kth transmission time. To make sure the inter-sampling interval is strictly positive, we need to guarantee $\Delta_k < \theta_k$, so Δ_k is chosen as

$$\Delta_k = \rho_\Delta \theta(|\|\hat{x}_{k-1}\| - \theta_{k-1}|,\bar{w}), \tag{4.15}$$

where $\rho_\Delta \in (0,1)$ is a given constant. The proof of the following Lemma 4.4.3 shows that (4.15) implies $\Delta_k < \theta_k$. We assume that the controller knows the event-trigger and the quantization error. So, when the controller receives the kth packet, it knows that the state x satisfies $\|x-\hat{x}_{k-1}\| = \theta_{k-1}$. The set $\{x : \|x-\hat{x}_{k-1}\| = \theta_{k-1}\}$ is then uniformly quantized such that $\|x-\hat{x}_k\| \leq \Delta_k$, and the number of bits N_k transmitted at s_k satisfies

$$N_k = \lceil \log_2 2n \rceil + \left\lceil \log_2 \left\lceil \frac{\theta_{k-1}}{\Delta_k} \right\rceil^{n-1} \right\rceil. \tag{4.16}$$

Lemma 4.4.3. *Suppose there is no delay. The system defined in (5.1-4.6) with the event-trigger and quantization error defined as (4.14) and (4.15) is ISS.*

Proof. From equation (4.12-4.14), we see that $\theta(s, \bar{w})$ is a increasing function of s. Since $\|\hat{x}_k - \hat{x}_{k-1}\| = \theta_{k-1} \Rightarrow \|\hat{x}_k\| \geq |\|\hat{x}_{k-1}\| - \theta_{k-1}|$, we have

$$\|e_k(s_k)\| \leq \Delta_k < \theta(|\|\hat{x}_{k-1}\| - \theta_{k-1}|, \bar{w}) \leq \theta(\|\hat{x}_k\|, \bar{w}) = \theta_k.$$

Since $\|e_k(s_{k+1})\| = \theta_k$, according to the continuity of e_k, $\|e_k\| < \underline{\xi}_k$ for all $t \in [s_k, s_{k+1})$ and all $k = 0, 1, \cdots, \infty$. From Corollary 4.4.2, the system is ISS. □

4.5 Acceptable Delays Preserving Input-to-State Stability

Corollary 4.4.2 indicates that bounding $e_k(t)$ during interval $[a_k, a_{k+1})$ is essential to preserve the input-to-state stability of the closed loop system. A typical trajectory of $\|e_k(t)\|$ is shown in Figure 4.3. At time s_k, system state is quantized and transmitted with the initial gap $\|e_k(s_k)\| \leq \Delta_k$. This gap gradually increases and finally hits θ_k, which generates the $k+1$-st sampling instant. Before the $k+1$-st quantized state arrives at the controller, the gap $\|e_k(t)\|$ keeps increasing. To guarantee ISS, the gap $\|e_k(t)\|$ should be bounded by $\underline{\xi}_k$.

The gap $e_k(t)$ has the following dynamic behavior.

$$\dot{e}_k(t) = f(\hat{x}_k + e_k(t), u_k, w(t)), \forall t \in [a_k, a_{k+1}). \tag{4.17}$$

Let L_k^x be the Lipschitz constant of f with respect to x during interval $[s_k, a_k]$. $\|f\|$ is bounded from above by

$$\|f(\hat{x}_k + e_k(t), u_k, w)\| \leq \bar{f}(\hat{x}_k, u_k, \bar{w}) + L_k^x \|e_k\|, \tag{4.18}$$

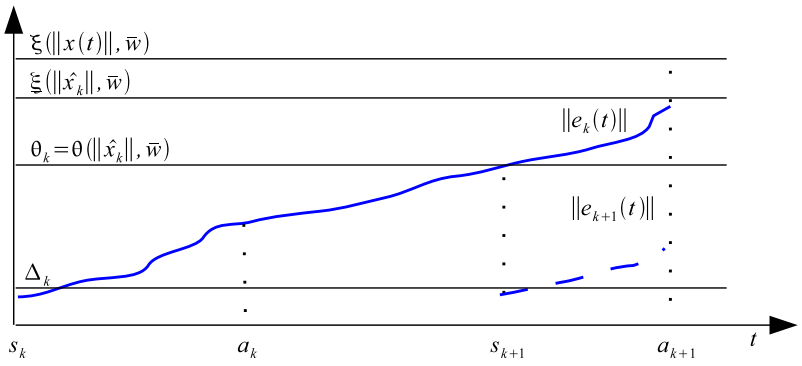

Figure 4.3. A typical trajectory of $\|e_k(t)\|$

where

$$\bar{f}(\hat{x}_k, u_k, \bar{w}) = \|f(\hat{x}_k, u_k, 0)\| + L_k^w \bar{w}.$$

If the transmission and arrival sequences are admissible, the norm of the gap $\|e_k(t)\|$, then, satisfies

$$\frac{d\|e_k(t)\|}{dt} \leq \|\dot{e}_k(t)\| \leq \bar{f}(\hat{x}_k, u_{k-1}, \bar{w}) + L_k^x \|e_k(t)\|, \forall t \in [s_k, a_k).$$
$$\frac{d\|e_k(t)\|}{dt} \leq \|\dot{e}_k(t)\| \leq \bar{f}(\hat{x}_k, u_k, \bar{w}) + L_k^x \|e_k(t)\|, \forall t \in [s_{k+1}, a_{k+1}).$$

With comparison principle, $\|e_k(t)\|$ satisfies

$$\|e_k(t)\| \leq \frac{\bar{f}(\hat{x}_k, u_{k-1}, \bar{w})}{L_k^x}(e^{L_k^x(t-s_k)} - 1) + \Delta_k e^{L_k^x(t-s_k)}, \forall t \in [s_k, a_k). \tag{4.19}$$
$$\|e_k(t)\| \leq \frac{\bar{f}(\hat{x}_k, u_k, \bar{w})}{L_k^x}(e^{L_k^x(t-s_{k+1})} - 1) + \theta_k e^{L_k^x(t-s_{k+1})}, \forall t \in [s_{k+1}, a_{k+1}). \tag{4.20}$$

First, let us assume the transmission and arrival sequences are admissible. The acceptable delay preserving ISS is given by the following lemma.

Lemma 4.5.1. *If the transmission and arrival sequences are admissible, i.e.* $d_k \leq \tau_k$

for all $k = 0, 1, \ldots, \infty$, and the transmission delay d_{k+1} satisfies

$$d_{k+1} \leq \bar{d}_{k+1} = \frac{1}{L_k^x} \ln \left(1 + \frac{L_k^x (\underline{\xi}_k - \theta_k)}{\bar{f}(\hat{x}_k, u_k, \bar{w}) + L_k^x \theta_k} \right), \tag{4.21}$$

then the system defined in (5.1), (4.5) and (4.6) with the event-trigger and quantization error defined as (4.14) and (4.15) is ISS.

Proof. We assume $a_k \leq s_{k+1} \leq a_{k+1}$ for all $k = 0, 1, \ldots, \infty$.

It is easy to see that during interval $[a_k, s_{k+1}]$, $\|e_k(t)\| \leq \theta_k < \underline{\xi}_k$.

For interval $[s_{k+1}, a_{k+1})$, from equation (4.20), we have

$$\|e_k(t)\| \leq \|e_k(a_{k+1})\| \leq \frac{\bar{f}(\hat{x}_k, u_k, \bar{w})}{L_k^x} (e^{L_k^x d_{k+1}} - 1) + \theta_k e^{L_k^x d_{k+1}}, \forall t \in [s_{k+1}, a_{k+1})$$

So, equation (4.13) is guaranteed by

$$\frac{\bar{f}(\hat{x}_k, u_k, \bar{w})}{L_k^x} (e^{L_k^x d_{k+1}} - 1) + \theta_k e^{L_k^x d_{k+1}} < \underline{\xi}_k \Leftrightarrow d_{k+1} \leq \bar{d}_{k+1}$$

Therefore, $\|e_k(t)\| < \underline{\xi}_k$ holds for all $t \in [a_k, a_{k+1})$ and all $k = 0, 1, \ldots, \infty$. According to Corollary 4.4.2, the closed loop system is ISS. □

Next, we would like to find an upper bound on the delay such that the transmission arrival sequences are admissible.

Lemma 4.5.2. *If the transmission delay d_k satisfies*

$$d_k \leq T_k = \frac{1}{L_k^x} \ln \left(1 + \frac{L_k^x (\theta_k - \Delta_k)}{\bar{f}(\hat{x}_k, u_{k-1}, \bar{w}) + L_k^x \Delta_k} \right), \tag{4.22}$$

then the transmission arrival sequences are admissible, i.e. $d_k \leq \tau_k$ for all $k = 0, 1, \ldots, \infty$.

Proof. First, we realize that $d_0 = 0 \leq \tau_0$.

Now, let us assume that $d_{k-1} \leq \tau_{k-1}$ holds, i.e. $a_{k-1} \leq s_k$. If $d_k > \tau_k$, then we have $a_{k-1} \leq s_k \leq s_{k+1} < a_k$. For interval $[s_k, s_{k+1}]$, from equation (4.19), we have

$$\|e_k(s_{k+1})\| \leq \frac{\bar{f}(\hat{x}_k, u_{k-1}, \bar{w})}{L_k^x}(e^{L_k^x \tau_k} - 1) + \Delta_k e^{L_k^x \tau_k}.$$

Since $\|e_k(s_{k+1})\| = \theta_k$, together with the equation above, we have $\tau_k \geq T_k$. From equation (4.22), we further have $\tau_k \geq d_k$. This contradicts the assumption $d_k > \tau_k$.

Therefore, $d_k \leq \tau_k$ for all $k = 0, 1, \ldots, \infty$. □

Corollary 4.5.3. *If $d_k \leq T_k$, then the inter-sampling interval τ_k is bounded from below by T_k, i.e.*

$$\tau_k \geq T_k, \tag{4.23}$$

where T_k is defined in (4.22).

Proof. The contrapositive of Lemma 4.5.2 is

$$d_k > \tau_k \Rightarrow d_k > T_k. \tag{4.24}$$

Assume $T_k > \tau_k$. It is easy to see that

$$d_k > T_k \Rightarrow d_k > \tau_k. \tag{4.25}$$

From equation (4.24) and (4.25), we have

$$d_k > \tau_k \Leftrightarrow d_k > T_k,$$

which implies $\tau_k = T_k$. This contradicts the assumption $T_k > \tau_k$. So, $\tau_k \geq T_k$ □

From Lemma 4.5.1 and 4.5.2, the main theorem is obtained.

Theorem 4.5.4. *If the transmission delay d_k satisfies*

$$d_k \leq D_k = \min\{\bar{d}_k, T_k\}, \tag{4.26}$$

where $\bar{d}_k$ and T_k are given by (4.21) and (4.22) respectively, then the transmission and arrival sequences are admissible and the system defined in (5.1-4.6) with the event-trigger and quantization error defined as (4.14) and (4.15) is ISS.

Remark 4.5.5. *Theorem 4.5.4 indicates that when transmission delays are not negligible, we should not choose θ_k as large as possible to obtain as large as possible inter-sampling interval. Because as θ_k gets closer and closer to $\underline{\xi}_k$, $\bar{d}_k$ dominates the bound on the acceptable delay, and gets smaller and smaller according to (4.21).*

Remark 4.5.6. *The results in Corollary 4.5.3 and Theorem 4.5.4 provide a basis to study the scheduling problem in large scale event-triggered control systems. Let us assume that there are several control systems which share a communication channel, and there is a scheduler which schedules the transmissions of all the control systems. Every time when a control system decides to transmit, from the results in Corollary 4.5.3 and Theorem 4.5.4, it tells the scheduler that N_k bits need to be transmitted in D_k seconds, and the next transmission time will be at least T_k seconds later. The scheduler, then, makes use of the information from all control systems to decide whether all transmission requirements are schedulable.*

This section uses the technique that we used in [64] to derive bounds on acceptable delay and inter-sampling interval. These results are further analyzed in the next section to explain how efficient attentiveness is achieved.

4.6 Efficient Attentiveness

This section studies the sufficient condition achieving efficient attentiveness. For the convenience of the rest of this section, we first define $\bar{f}_c(s)$ as a class $\mathcal{K}$ function

satisfying

$$\|f(\hat{x}_k, K(\hat{x}_k), 0)\| \leq \bar{f}_c(\|\hat{x}_k\|), \tag{4.27}$$

and we have the following corollary which is a direct result from Lemma 4.2.1.

Corollary 4.6.1. *If*

$$\lim_{s\to 0} \frac{\bar{f}_c(s)}{\theta(s,0)} < \infty, \tag{4.28}$$

then there exist continuous, positive definite, increasing functions $h_1(s)$, $h_2(s)$ *such that* $\lim_{s\to 0} h_i(s) < \infty$ *for* $i = 1, 2$ *and*

$$\frac{\theta(s,\bar{w})}{\Delta(s,\bar{w})} \leq h_1(s) \tag{4.29}$$

$$\frac{\bar{f}_c(s) + L_k^w \bar{w}}{\theta(s,\bar{w})} \leq h_2(s). \tag{4.30}$$

Proof. If $\bar{w} \neq 0$, it is easy to show that

$$\lim_{s\to 0} \frac{\theta(s,\bar{w})}{\Delta(\theta(s,\bar{w}))} < \infty$$
$$\lim_{s\to 0} \frac{\bar{f}_c(s) + L_k^w \bar{w}}{\theta(s,\bar{w})} < \infty.$$

According to Lemma 4.2.1, there must exist h_1 and h_2 which are continuous, positive definite, increasing and $\lim_{s\to 0} h_i(s) < \infty$ for $i = 1, 2$ such that equation (4.29) and (4.30) hold.

If $\bar{w} = 0$, we have

$$\lim_{s\to 0} \frac{\theta(s,0)}{\Delta(\theta(s,0))} = \lim_{s\to 0} \frac{\theta(s,0)}{\rho_\Delta \theta(|s - \theta(s,0)|, 0)}$$

From (4.12) and (4.13), we know that $\theta(s,0)$ is a continuous function satisfying

$\theta(0,0) = 0$. There must exist a constant c such that for all $s \in [0, c]$, $\theta(s, 0)$ is either greater or equal to $0.5s$, or less than $0.5s$. If $\theta(s, 0) \leq 0.5s$, then

$$\lim_{s\to 0} \frac{\theta(s,0)}{\rho_\Delta \theta(|s - \theta(s,0)|, 0)} \leq \lim_{s\to 0} \frac{\theta(s,0)}{\rho_\Delta \theta(0.5s, 0)} < \infty.$$

If $\theta(s, 0) > 0.5s$, then

$$\lim_{s\to 0} \frac{\theta(s,0)}{\rho_\Delta \theta(|s - \theta(s,0)|, 0)} \leq \lim_{\theta(s,0)\to 0} \frac{\theta(s,0)}{\rho_\Delta \theta(3\theta(s), 0)} < \frac{2}{3\rho_\Delta} < \infty.$$

Together with (4.28), according to Lemma 4.2.1, equation (4.29) and (4.30) still hold. □

4.6.1 Efficiently Attentive Inter-Sampling Interval

Now, we are ready to present a sufficient condition to achieve efficiently attentive inter-sampling interval.

Lemma 4.6.2. *If the assumption (4.28) is satisfied, then the inter-sampling interval τ_k is efficiently attentive, i.e. there exists a continuous, positive definite, decreasing function $\underline{h}(s_1, s_2)$ such that $\lim_{s\to 0} \underline{h}(s_1, s_2) > 0$ and equation (4.10) is satisfied.*

Proof. From Corollary 4.5.3, we have $\tau_k \geq T_k$. Since $\ln(1 + x) \geq \frac{x}{1+x}$, it is easy to show that

$$\begin{aligned} T_k \geq & \frac{\theta_k - \Delta_k}{\bar{f}(\hat{x}_k, u_{k-1}, \bar{w}) + L_k^x \theta_k} \\ = & \frac{1 - \Delta_k/\theta_k}{\bar{f}(\hat{x}_k, u_{k-1}, \bar{w})/\theta_k + L_k^x}. \end{aligned}$$

From the proof of Lemma 4.4.3, we know that $\Delta_k < \rho_\Delta \theta_k$. We further have

$$\tau_k \geq T_k \geq \frac{1 - \rho_\Delta}{\bar{f}(\hat{x}_k, u_{k-1}, \bar{w})/\theta_k + L_k^x}.$$

$\bar{f}$ is locally lipschitz with respect to $\hat{x}_k$, so

$$\begin{aligned}\frac{\bar{f}(\hat{x}_k, u_{k-1}, \bar{w})}{\theta_k} \leq & \frac{\bar{f}(\hat{x}_{k-1}, u_{k-1}, \bar{w}) + L_k^x \|\hat{x}_k - \hat{x}_{k-1}\|}{\theta_k} \\ \leq & \frac{\bar{f}_c(\|\hat{x}_{k-1}\|) + L_k^w \bar{w} + L_k^x \theta_{k-1}}{\Delta_k} \\ \leq & \frac{\bar{f}_c(\|\hat{x}_{k-1}\|) + L_k^w \bar{w}}{\theta_{k-1}} \frac{\theta_{k-1}}{\Delta_k} + L_k^x \frac{\theta_{k-1}}{\Delta_k}\end{aligned}$$

According to Corollary 4.6.1, there must exist continuous, positive definite, and increasing functions $h_1(\|\hat{x}_{k-1}\|)$ and $h_2(\|\hat{x}_{k-1}\|)$ such that

$$\frac{\bar{f}(\hat{x}_k, u_{k-1}, \bar{w})}{\theta_k} \leq h_1(\|\hat{x}_{k-1}\|) + L_k^x h_2(\|\hat{x}_{k-1}\|),$$

and hence we have

$$\tau_k \geq T_k \geq \frac{1 - c_1}{h_1(\|\hat{x}_{k-1}\|) + L_k^x h_2(\|\hat{x}_{k-1}\|) + L_k^x}.$$

Since h_1 and h_2 are increasing with respect to $\|\hat{x}_{k-1}\|$, L_k^x is increasing with respect to $\|\hat{x}_k\|$, and h_1, h_2 and L_k^x are all bounded from above as x approaches 0, we say that there exists a continuous, positive definite, decreasing function $\underline{h}(\|\hat{x}_{k-1}\|, \|\hat{x}_k\|)$ such that $\lim_{\|\hat{x}_{k-1}\|, \|\hat{x}_k\| \to 0} \underline{h}(\|\hat{x}_{k-1}\|, \|\hat{x}_k\|) > 0$, and equation (4.10) is satisfied. □

4.6.2 Efficiently Attentive Instantaneous Bit-Rate

Since the instantaneous bit-rate r_k is defined as N_k/D_k, it is easy to see that the instantaneous bit-rate r_k is efficiently attentive if N_k is bounded from above by an increasing function, and D_k is bounded from below by a decreasing function. Both N_k and D_k will be studied in this subsection.

First, let us look at the number of bits N_k transmitted at step k.

Lemma 4.6.3. *There exists a continuous, positive definite increasing function* $h'(\|\hat{x}_{k-1}\|)$

such that

$$\lim_{s\to 0} h'(s) < \infty \tag{4.31}$$

$$N_k \leq h'(\|\hat{x}_{k-1}\|). \tag{4.32}$$

Proof. N_k satisfies

$$N_k = \lceil \log_2 2n \rceil + \left\lceil \log_2 \left\lceil \frac{\theta_{k-1}}{\Delta_k} \right\rceil^{n-1} \right\rceil.$$

According to Corollary 4.6.1, there exists a continuous, positive definite, increasing function $h_1(\|\hat{x}_{k-1}\|)$ such that

$$\lim_{s\to 0} h_1(s) < \infty$$
$$\frac{\theta_{k-1}}{\Delta_k} \leq h_1(\|\hat{x}_{k-1}\|).$$

Therefore, there must exist a continuous, positive definite increasing function $h'(\|\hat{x}_{k-1}\|)$ such that equation (4.31) and (4.32) hold. □

Next, we would like to study D_k. Since $D_k = \min\{T_k, \bar{d}_k\}$ and T_k has be analyzed in Lemma 4.6.2, only $\bar{d}_k$ is examined here.

Lemma 4.6.4. *If the assumption (4.28) is satisfied, then there exists a continuous, positive definite decreasing function $h''(\|\hat{x}_{k-1}\|, \|\hat{x}_k\|)$ such that*

$$\lim_{s_1,s_2\to 0} h''(s_1, s_2) > 0 \tag{4.33}$$

$$\bar{d}_k \geq h''(\|\hat{x}_{k-1}\|, \|\hat{x}_k\|). \tag{4.34}$$

Proof. Since $\theta_k = \rho_\theta \underline{\xi}_k$, with the same steps in the proof of Lemma 4.6.2, we show

that

$$\bar{d}_k \geq \frac{1-\rho_\theta}{\bar{f}(\hat{x}_{k-1}, u_{k-1}, \bar{w})/\underline{\xi}_k + L_k^x},$$

where

$$\frac{\bar{f}(\hat{x}_{k-1}, u_{k-1}, \bar{w})}{\underline{\xi}_k} \leq \frac{\bar{f}_c(\|\hat{x}_{k-1}\|) + L_k^w \bar{w}}{\theta_{k-1}}.$$

According to Corollary 4.6.1, there exist a continuous, positive definite, increasing function $h_2(\|\hat{x}_{k-1}\|)$ such that

$$\begin{aligned} \lim_{s\to 0} h_2(s) <& \infty, \\ \frac{\bar{f}(\hat{x}_{k-1}, u_{k-1}, \bar{w})}{\underline{\xi}_k} \leq& h_2(\|\hat{x}_{k-1}\|). \end{aligned}$$

Together with the fact that L_k^x is increasing with respect to $\|\hat{x}_k\|$ and $\lim x \to 0 L_k^x < \infty$, we conclude that there exists a continuous, positive definite decreasing function $h''(s_1, s_2)$ such that equation (4.33) and (4.34) hold. □

From Lemma 4.6.2, 4.6.3 and 4.6.4, we have the following corollary.

Corollary 4.6.5. *If equation (4.28) are satisfied, the instantaneous bit-rate r_k is efficiently attentive, i.e. there exists a continuous, positive definite, increasing function $\bar{h}(s_1, s_2)$ such that $\lim_{s\to 0} \bar{h}(s_1, s_2) < \infty$ and equation (4.11) is satisfied.*

4.6.3 Efficiently Attentive and ISS Event Triggered Control System

Now, we are at the step to make a conclusion. Event triggered control systems should be designed to achieve not only a desired system performance but also attention efficiency. To this purpose, we have the following theorem which is easily derived from Theorem 4.5.4, Lemma 4.6.2, and Corollary 4.6.5.

Theorem 4.6.6. *If the transmission delay d_k is bounded from above by D_k given by (4.26), and the threshold function θ satisfy equation (4.28), then the system defined in (5.1-4.6) with the event-trigger and quantization error defined as (4.14) and (4.15) is input-to-state stable and efficiently attentive.*

Remark 4.6.7. *Equation (4.28) indicates that as the system state approaches* 0*, the threshold function θ decreases more slowly than the closed loop dynamic behavior of the state trajectory. Therefore, when x get closer to* 0*, it takes more time for the gap $e_k(t)$ to hit the threshold θ_k and $\underline{\xi}_k$, which leads to longer inter-sampling interval and acceptable delay.*

4.7 A Case Study

This section uses an example to explain how to design an event-triggered control system to achieve ISS and attention efficiency. After the event-triggered control system is well established, we will try different threshold functions to study the tradeoff between the inter-sampling interval and the instantaneous bit-rate.

Our experiment shows that the threshold function should be chosen as large as possible while the instantaneous bit-rate is lower than the channel capacity. It is also found that the event-triggered control system with its threshold function to be $0.6\underline{\xi}$ can tolerate 25 times of the delay tolerated by the system with the threshold function to be $0.99\underline{\xi}$, while only transmitting 2 times as frequently as the system with the threshold function to be $0.99\underline{\xi}$.

4.7.1 Design of event-triggered control systems

Consider the following nonlinear dynamic system.

$$\dot{x}_1 = -2x_1^3 + x_2^3 + w_1 \tag{4.35}$$

$$\dot{x}_2 = x_2^3 + u + w_2, \tag{4.36}$$

with $x_0 = [1\ 1]^T$. w is an L_∞ disturbance with $\|w\|_{L_\infty} = 0.1$. The control input u is chosen such that

$$u_k = -3\hat{x}_2^3, \forall t \in [a_k, a_{k+1}).$$

First, the input-to-state stability is studied for the dynamic system described in equation (4.35) and (4.36). Let $V = \frac{1}{4}x_1^4 + \frac{1}{4}x_2^4$ be a Lyapunov candidate function. Its derivative satisfies

$$\dot{V} = -2x_1^6 + x_1^3x_2^3 - 2x_2^6 + x_1^3w_1 + x_2^3w_2 + 3(3x_2^2e_2 - 3x_2e_2^2 + e_2^3)x_2^3,$$

where $e_i = x_i(t) - \hat{x}_i(s_k)$ for $i = 1, 2$. Let $\Omega = \{x : \|x\| \leq 1\}$.

$$\dot{V} \leq -1.5x_1^6 - 1.5x_2^6 + 2\bar{w} + 3x_2^3(3x_2^2e_2 - 3x_2e_2^2 + e_3^3), \forall x \in \Omega.$$

If

$$\|e\| \leq \epsilon\|x\|^l + \bar{w}, \text{for all } l \geq 1,$$

we have

$$\begin{aligned}\dot{V} \leq & -1.5x_1^6 - 1.5x_2^6 + 2\bar{w} + 3(3\epsilon + 3\epsilon^2 + \epsilon^3)\|x\|^6 \\ & + 3\|x\|^5\bar{w} - 6\epsilon\|x\|^5\bar{w} - 3\|x\|^4\bar{w}^2 + 3\epsilon^2\|x\|^5\bar{w} + 3\epsilon\|x\|^4\bar{w}^2 + \|x\|^3\bar{w}^3 \\ \leq & -1.5x_1^6 - 1.5x_2^6 + 3(3\epsilon + 3\epsilon^2 + \epsilon^3)\|x\|^6 \\ & + 3(\bar{w}^3 + 3|\epsilon - 1|\bar{w}^2 + 3|\epsilon - 1|^2\bar{w}) + 2\bar{w}, \forall x \in \Omega.\end{aligned}$$

Let $\epsilon = 0.14$, and $\gamma(\bar{w}) = 3(\bar{w}^3 + 3|\epsilon - 1|\bar{w}^2 + 3|\epsilon - 1|^2\bar{w}) + 2\bar{w}$. We have

$$\dot{V} \leq -0.055\|x\|^6 + \gamma(\bar{w}).$$

Therefore, the system is input-to-state stable if

$$\|e_k(t)\| \leq \xi(\|x(t)\|) = 0.14\|x(t)\|^l + \bar{w}, \text{for all } l \geq 1. \tag{4.37}$$

According to equation (4.13), (4.14) and (4.15), we have

$$\theta(\|\hat{x}_k\|) = \rho_\theta(0.12\|\hat{x}_k\|^l + 0.87\bar{w}), \text{for some } \rho_\theta \in (0, 1). \tag{4.38}$$

$$\Delta(s) = \rho_\Delta\rho_\theta(0.12(s - \theta(s))^l + 0.87\bar{w}), \text{for some } \rho_\Delta \in (0, 1).$$

4.7.2 Efficient attentiveness

This subsection will design an experiment to demonstrate Theorem 4.6.6. According to this theorem, if $l \leq 3$, then the system is efficiently attentive. So, in this experiment, we will fix $\rho_\theta = 0.6$ and $\rho_\Delta = 0.6$, vary $l = 1, 4$, and run the system for 50 seconds to see how inter-sampling interval and instantaneous bit-rate change.

When $\bar{w} = 0$, the system performance, inter-sampling interval, and instantaneous

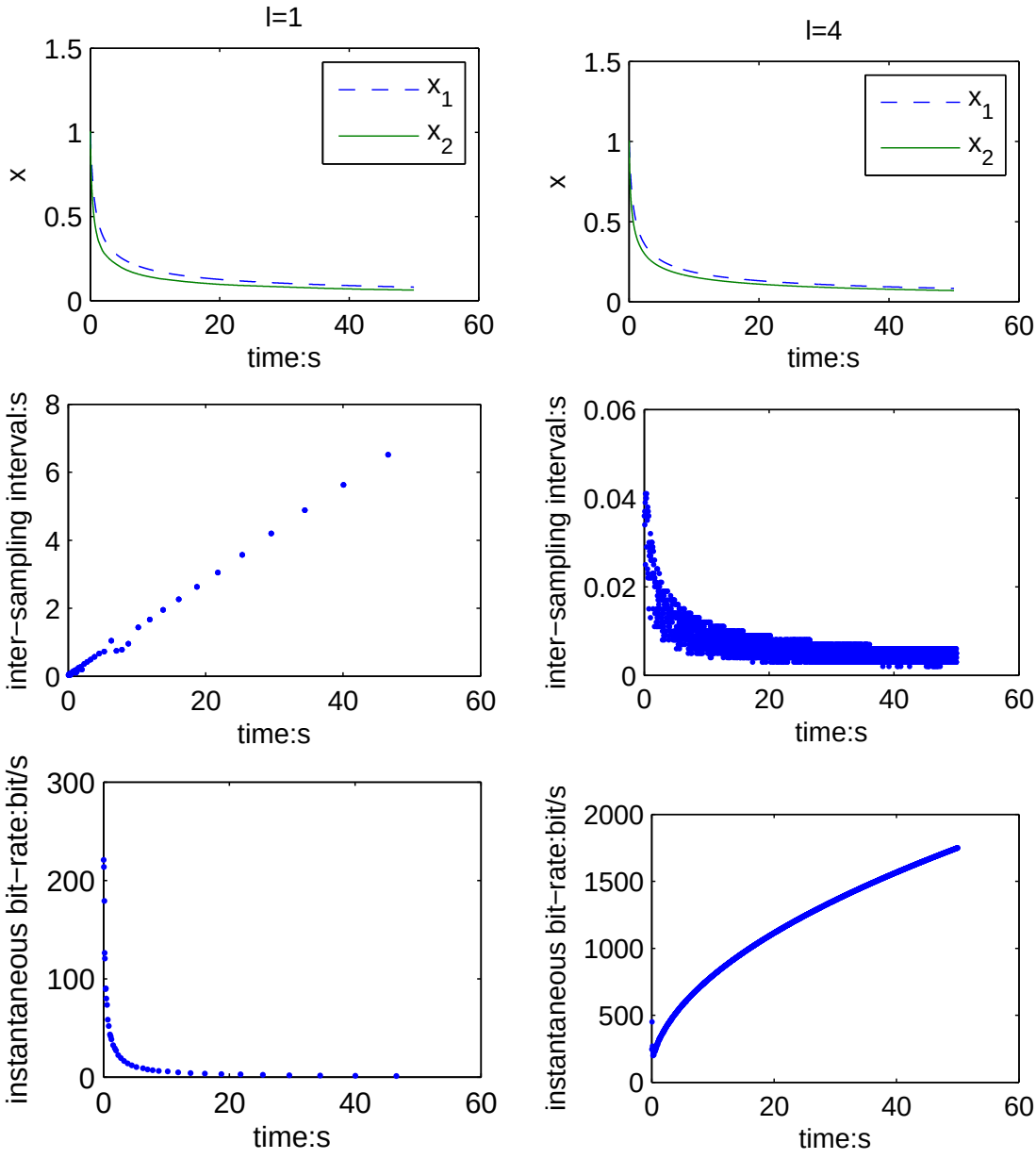

Figure 4.4. Performance, inter-sampling interval and instantaneous bit-rate with $\rho_\theta = \rho_\Delta = 0.6$ and $l = 1, 4$ for the noise free case.

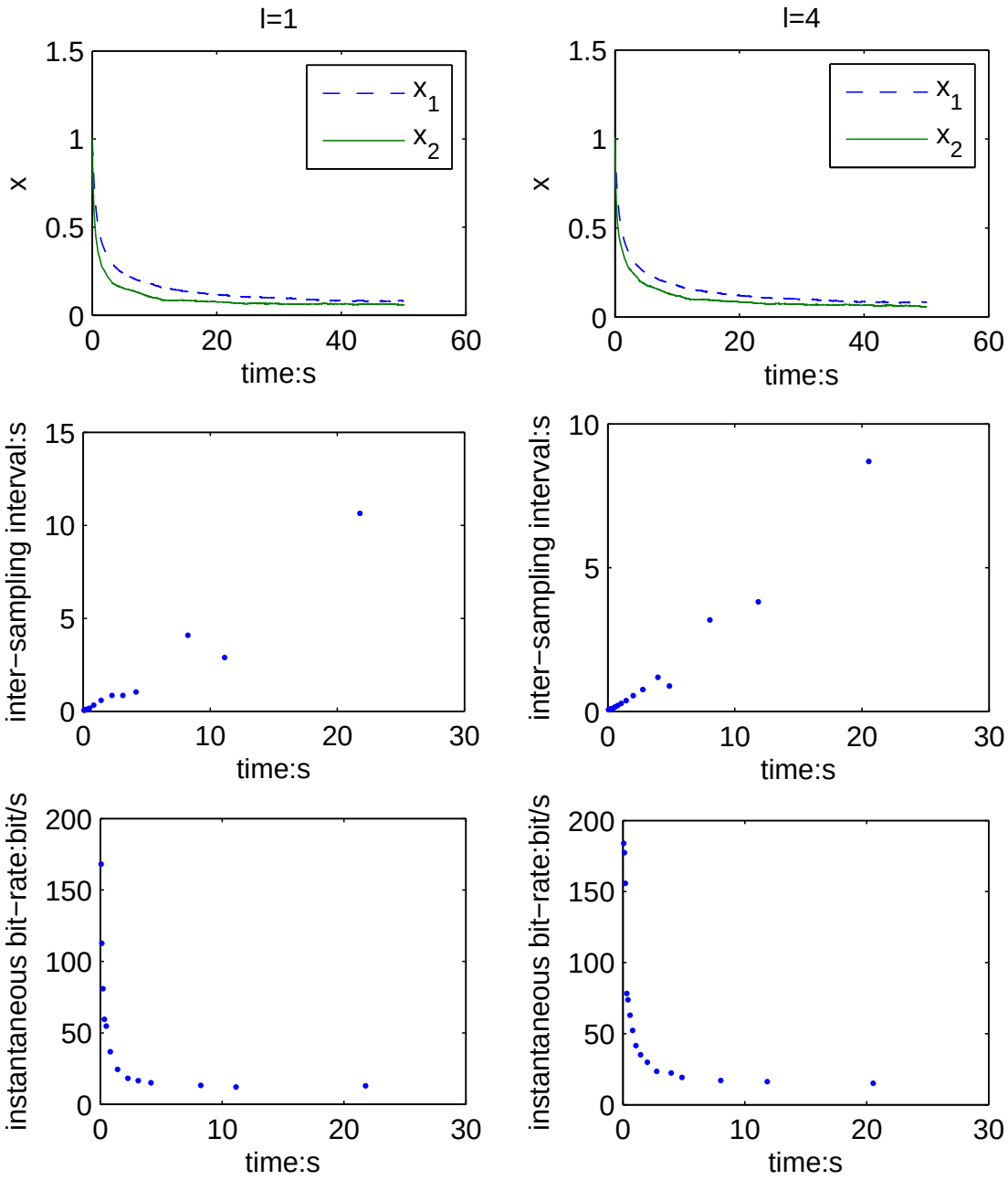

Figure 4.5. Performance, inter-sampling interval and instantaneous bit-rate with $\rho_\theta = \rho_\Delta = 0.6$, and $l = 1, 4$ for noisy case.

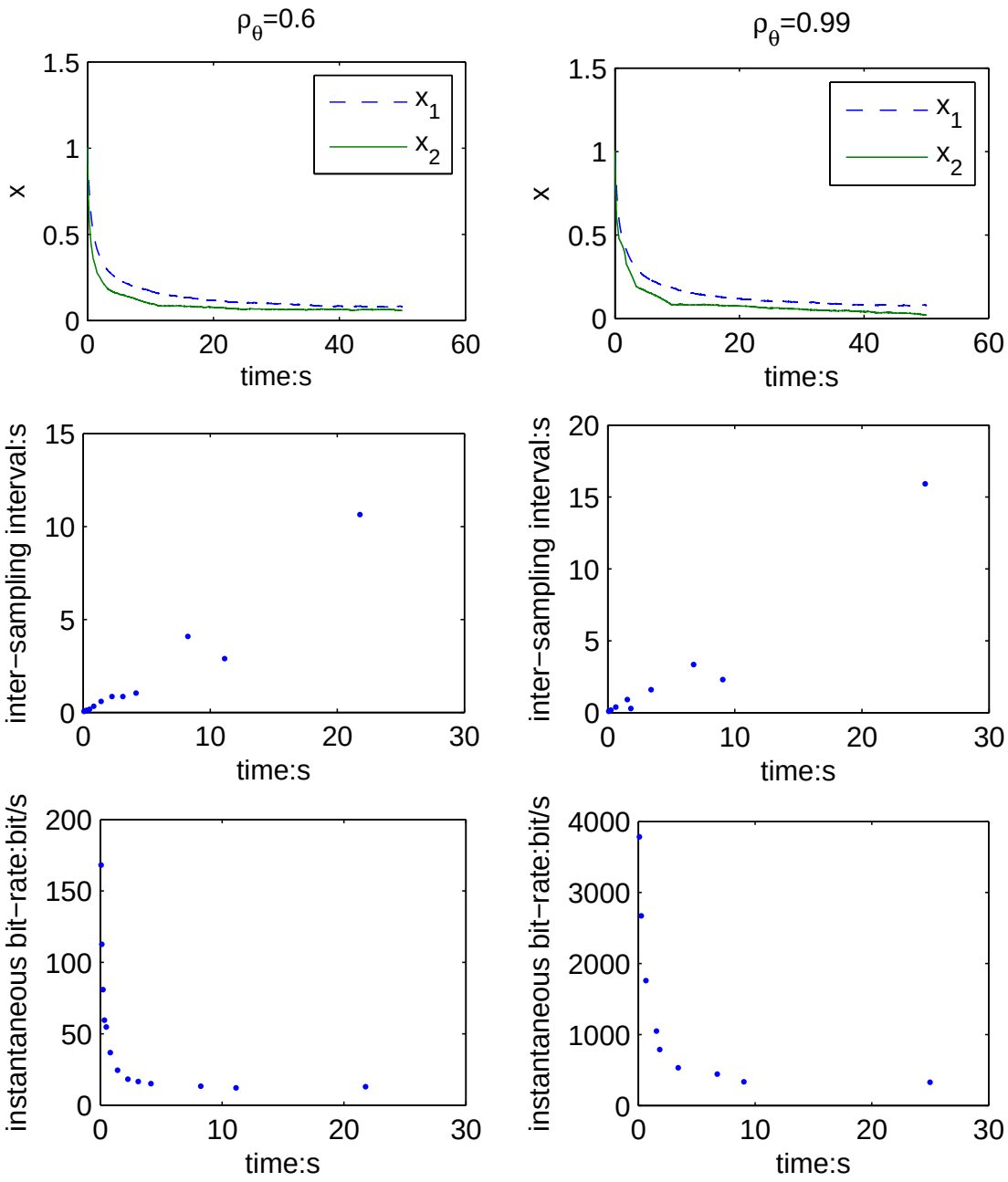

Figure 4.6. Performance, inter-sampling interval and instantaneous bit-rate with $\rho_\theta = 0.6, 0.99$, $\rho_\Delta = 0.6$ and $l = 1$ for noisy case.

bit-rate are shown in Figure 4.4. The left plots are the simulation results for $l = 1$. The top plot gives the system performance, and the system is asymptotically stable. The middle plot shows the inter-sampling interval which got longer and longer as the system state approached 0. The bottom plot shows the instantaneous bit-rate which was smaller and smaller as the state went to 0. So, we say the system is efficiently attentive. The right plots are the simulation results for $l = 4$. We see that the system is still ISS, but the inter-sampling interval became shorter and shorter and the instantaneous bit-rate got larger and larger as the system state went to the origin. Therefore, when $l = 4$, the system is not efficiently attentive.

When $\bar{w} = 0.1$, the system performance, inter-sampling interval, and instantaneous bit-rate are shown in Figure 4.5. Comparing the left plots ($l = 1$) with the right plots($l = 4$), we find that for both cases, the systems had similar system performances, inter-sampling intervals, and instantaneous bit-rates, and both are ISS and efficiently attentive. This is because when $\bar{w} \neq 0$, and x is small, for both cases, the term associated with $\bar{w}$ dominated the threshold and the quantization error, and hence for both cases, the systems had similar performances, inter-sampling intervals, and instantaneous bit-rates.

4.7.3 The inter-sampling interval and the instantaneous bit-rate

In this section, we will fix $l = 1$ and $\rho_\Delta = 0.6$. By varying $\rho_\theta = 0.6, 0.99$, we want to explore the tradeoff between the inter-sampling interval and the instantaneous bit-rate. The simulation results are shown in Figure 4.6. The left plots are the results for $\rho_\theta = 0.6$, and the right plots are the results for $\rho_\theta = 0.99$. The top plots give the system performance. we see that both of them are ISS. The middle plots show the inter-sampling intervals. We see that the inter-sampling interval of the system with $\rho_\theta = 0.99$ is about 2 times of the inter-sampling interval of the system with $\rho_\theta = 0.6$. The bottom plots show the instantaneous bit-rates. we find

that the instantaneous bit-rate of the system with $\rho_\theta = 0.99$ is about 20 times of the instantaneous bit-rate of the system with $\rho_\theta = 0.6$. This experiment showed the tradeoff between inter-sampling interval and instantaneous bit-rate. When we increased the threshold, while the inter-sampling interval increased, the required instantaneous bit-rate also increased. Therefore, for bandwidth limited systems, we should not only focus on lengthening the inter-sampling interval, but also need to guarantee the channel bandwidth satisfies the required instantaneous bit-rate.

4.8 Conclusion

This chapter studies the input-to-state stability and efficient attentiveness for bandwidth limited event-triggered control systems. A system is said to be efficiently attentive, if the inter-sampling interval gets longer and the required instantaneous bit-rate gets smaller when the system state goes to the origin. We first talk about how to design the event-trigger and the quantization map, then provide the acceptable delay preserving ISS, and finally gives a sufficient condition of efficient attentiveness. Our simulation results demonstrated these main results, and indicates that for bandwidth limited systems, we should not only focus on lengthening the inter-sampling interval, but also need to guarantee the channel bandwidth satisfies the required instantaneous bit-rate.

CHAPTER 5

RESILIENT EVENT TRIGGERED SYSTEMS WITH LIMITED TRANSMISSION FREQUENCY AND INSTANTANEOUS BIT-RATE

Chapter 4 shows that if the event trigger is properly designed, the inter-sampling interval is longer and longer as the system state approaches the origin. From the simulation results, we see that for a cubic system, the inter-sampling interval is even longer than 10 seconds, when the system state is close to 0. Such a long inter-sampling interval raises a concern about resilience of event triggered systems. By 'resilience', we mean the system maintains state awareness and an accepted level of operational normalcy in response to unexpected disturbances. This chapter examines the bit-rates needed to realize event-triggered systems that are resilient to transient faults. Using techniques from dynamically quantized control, we derive sufficient resilient bit-rates for nonlinear scalar systems with affine controls and disturbances. The results in this chapter suggest that, at least for transient faults, resilient control is indeed achievable using event-triggered feedback.

5.1 Introduction

Resilient operation of critical systems is of great societal importance. Failures of critical civil infrastructure, such as the power grid or transportation network, will result in economic losses and societal disruptions. The scale of these disruptions will grow larger and larger as more systems are integrated over public networks. These public systems also become more vulnerable to malicious attacks as system

size increases. It is therefore crucial that the control strategies used for these systems be resilient to these threats.

A resilient control system is one that maintains state awareness of threats and anomalies [56]. In particular, we expect such control systems to provide guarantees on a system's return to operational normalcy in the presence of disturbances generated by such threats and anomalies. The impact of such threats can be modeled as *stop faults* which change the structure of the system [73]. Such threats may also be modeled as *transient faults* that result in a discontinuous step change in the plant's state. This chapter examines resilience to such transient faults. We consider a nonlinear scalar system whose operation can be divided into a *safe* and an *unsafe* regime. The safe operating regime is an interval of time over which the controller ensures a pre-specified performance objective. Disturbances due to threats are impulses of *unknown magnitude* that may drive a system into its unsafe regime. Within the unsafe regime it is no longer possible to guarantee system performance levels. One may, however, be able to use an *emergency* control action that guarantees the system's return to the safe regime in finite time. The main result of this chapter characterizes lower bounds on those bit rates ensuring resilient operation of *quantized event-triggered* control systems.

Event triggered systems have shown their potential to conserve communication resources while preserving system performance. Many embedded system engineers, however, favor the use of time-triggered over event-triggered control architectures. A major objection to the use of event-triggered control is that it tends to generate *sporadic* information streams. In these sporadic streams, the time between consecutive transmissions changes in a time-varying manner. This lack of predictability is seen as an obstacle to resilient operation. This concern may appear valid on the surface, but in fact event-triggered systems do provide some degree of predictability in that the minimum time between successive transmissions is usually bounded away from zero.

In this regard, event-triggering can be seen as providing a minimum level of feedback connectivity, with additional information being transmitted over the channel when the system is driven away from its equilibrium point. A key question is how small this feedback information rate can be made while still assuring resilient operation?

The main results in this chapter characterize an upper bound on the minimum bit-rates required for resilient behavior. These results are obtained for scalar nonlinear systems whose control and disturbance enter in an affine manner. The control input, u, is an impulse train whose impulses are applied when sensor data is transmitted over a communication channel to the system's actuator. Disturbance inputs are also impulses that force a jump in the plant's state as the result of some transient fault. We assume that the magnitude of these faults is *unknown*. The occurrence of such a fault forces the system out of its safe operating regime and into an unsafe regime. The main result of this chapter establishes upper bounds on the information bit rate between sensor and actuator required to 1) eventually force an unsafe system back into its safe operating regime and 2) maintain a specified performance level within the safe regime.

5.2 System Setup

The system structure is shown as in Figure 5.1. The plant is a nonlinear scalar system whose state trajectory $x : \mathbb{R}^+ \to \mathbb{R}$ satisfies the following initial value problem,

$$\dot{x}(t) = f(x(t)) + u(t) + w(t) \tag{5.1}$$

for all $t \geq 0$ with $x(0) = x_0$. We assume that $f(\cdot) : \mathbb{R} \to \mathbb{R}$ is locally Lipschitz about the origin with Lipschitz constant L with $f(0) = 0$. The input signal u is a train of control impulses and the input signal w is a train of exogenous disturbance impulses generated by transient system faults.

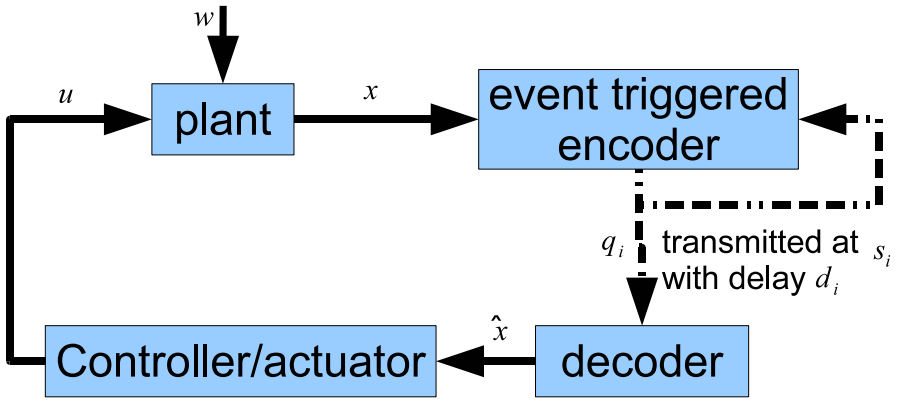

Figure 5.1. System structure of resilient event triggered system

The disturbance signal, w, is an impulse train of the form,

$$w(t) = \sum_{i=1}^{\infty} \omega_i \delta(t - h_i)$$

where h_i denotes the ith consecutive *fault* time and $\omega_i \in \mathbb{R}$ represents the *magnitude* of the ith fault. The main feature of this fault model is that ω_i is not known or bounded in an *a priori* manner.

The control input, u, is generated by the controller shown in Figure 5.1. In this system, a subsystem called the *encoder* samples the plant's state at discrete time instants s_i for $i = 1, 2, \ldots, \infty$. The ith consecutive sampled state, $x(s_i)$, is encoded as a codeword $q_i \in \{1, 2, \ldots, Q\}$. The event-triggered encoder then transmits this codeword over the channel at time s_i with a delay $d_i \geq 0$. The transmitted codeword is received at time instant $a_i = s_i + d_i$. Upon receiving this codeword, the decoder generates the control update, $\hat{x}_i \in \mathbb{R}$. The controller/actuator then takes this update and applies it to the plant through an impulse at time a_i. The final control signal

input therefore takes the form of an impulse train,

$$u(t) = -\sum_{i=1}^{\infty} \hat{x}_i \delta(t - a_i)$$

where $\hat{x}_i$ is the ith consecutive control command applied at time instant a_i.

It will be convenient to restrict the system function, f, so that

$$f(-x) = -f(x) \text{ for all } x \in \mathbb{R}, \tag{5.2}$$

$$f(|x|) \text{ is class } \mathcal{K} \tag{5.3}$$

The second assumption can be relaxed at the cost of degrading the bit-rate bounds derived below. Finally, we assume there exists a real number x_a such that for all $|x| > x_a$ we can uniformly bound $|f(x)|$. In other words, we assume there exist positive constants L and $\bar{L}$ such that

$$|f(x)| \leq \begin{cases} L|x| & \text{if } |x| \leq x_a \\ \bar{L} & \text{if } |x| > x_a \end{cases} \tag{5.4}$$

We refer to the set $\Omega_a \equiv \{x \in \mathbb{R} : |x| \leq x_a\}$ as the *absorbing region*. The motivation for this terminology is as follows. For the absorbing region, the Lipschitz constant, L, provides an accurate upper bound on the system's rate of growth. Outside of this region, however, this Lipschitz approximation is too conservative because the plant's open-loop rate of change begins to saturate due to physical limitations within the system.

The safe regime is a regime under which a desired level of performance is guaranteed (as shown in the right part of Figure 5.2). In this chapter, we specify this desired performance as exponential stability. Let t_0 be the initial time when the system switches to the safe regime, and t_f be the terminal time when the system exits

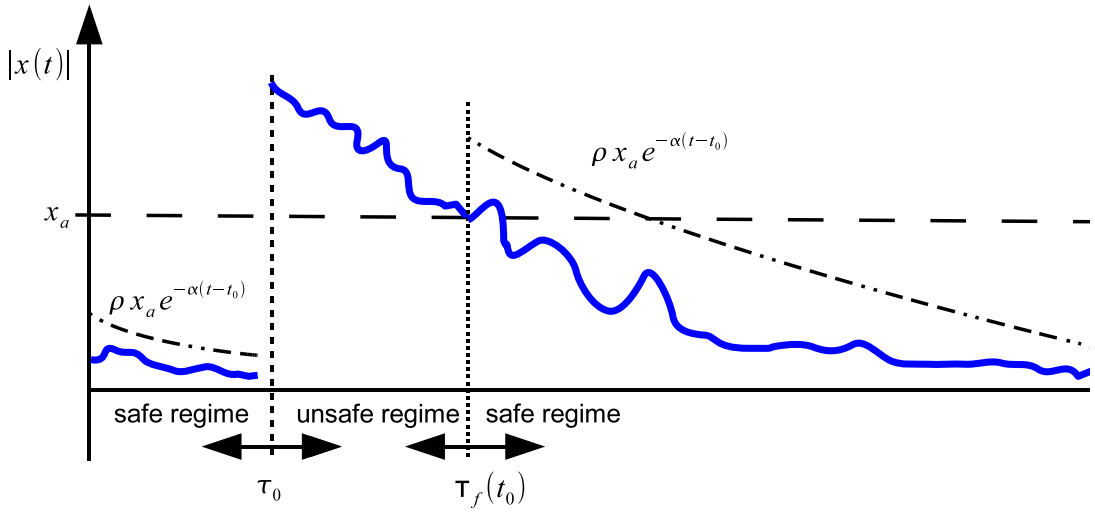

Figure 5.2. Safe regime, unsafe regime and resilience

the safe regime. For all $t \in [t_0, t_f]$, the system state $x(t)$ satisfies

$$|x(t)| \leq \rho x_a e^{-\alpha(t-t_0)}, \text{for some } \alpha \geq 0 \text{ and } \rho \geq 1 \tag{5.5}$$

Equation (5.5) represents a desired level of exponential stability. So when the constraint in equation (5.5) is violated, the system is operating in its unsafe regime. Let T_0 and T_f be the initial time and terminal time of the unsafe regime. There must exist some time $t \in [T_0, T_f]$ such that

$$|x(t)| > \rho x_a e^{-\alpha(t-T_0)}.$$

To be resilient, we require that the system is able to come back to the safe regime from unsafe regime in finite time. To be more specific, we define the resilience of a system as below.

Definition 5.2.1. *A system is resilient if for all state $x(T_0)$ satisfying $|x(T_0)| \in$*

(x_a, ∞), *there is a finite time* $T_f \in (0, \infty)$ *such that*

$$|x(T_f)| \leq x_a. \tag{5.6}$$

We use the term *resilience* to refer to a system's ability to return to the safe regime in *finite* time. What makes resilience distinct from *robustness* is that the transient faults have an arbitrarily large magnitude, rather than just a bounded magnitude. Because the magnitude of the fault can be arbitrarily large, the controller/actuator doesn't know exactly what control level is needed to return the state to the origin. So we propose having the controller apply an *emergency* or *unsafe* control step. The main result of this chapter characterizes the rate at which this emergency control must be applied to assure that the system is resilient; i.e. that it returns to its safe regime in finite time.

5.2.1 Necessary Bit-Rate under Safe Regime

Let's assume that at time t_0, the system enters the safe regime. Define $\phi(x_0, t-t_0)$ as the zero-input behavior of plant (5.1), where x_0 and t_0 are the initial state and initial time. With the assumptions in (5.2) and (5.3), the zero-input behavior of plant (5.1) has some nice properties which are given in the following lemma.

Lemma 5.2.2. *If equations (5.2) and (5.3) hold, then for some small enough time interval* $\epsilon > 0$, *we have*

$$\phi(-x, \epsilon) = -\phi(x, \epsilon), \tag{5.7}$$

$$\phi(x_1, \epsilon) \geq \phi(x_2, \epsilon), \textit{if } x_1 \geq x_2 \geq 0. \tag{5.8}$$

This lemma can be easily justified by noticing that for a small enough time interval

$\epsilon > 0$, the state at time $t + \epsilon$ is

$$\phi(x(t), \epsilon) = x(t) + \int_t^{t+\epsilon} f(x(\tau))d\tau + o = x(t) + f(x(t))\epsilon + o,$$

where o indicates a negligible bias.

Next theorem gives us the necessary bit-rate to maintain exponential stability under safe regime. The basic idea is similar to the idea used in dynamic quantization area [69, 60].

Theorem 5.2.3. *Let t_0 be the initial time when the system enters its safe regime, and $\beta(t) = \rho x_a e^{-\alpha(t-t_0)}$. If the performance level in equation (5.5) is guaranteed for all $t \geq t_0$, then the instantaneous bit-rate $r(t)$ at time t satisfies*

$$r(t) \geq \underline{r}_s(t) = \max\left\{\frac{1}{\ln 2}\left(\frac{f(\beta(t))}{\beta(t)} + \alpha\right), 0\right\}. \tag{5.9}$$

$\underline{r}_s$ is called the necessary stabilizing bit-rate under safe regime.

Proof. Since performance level (5.5) is guaranteed for any $t \geq t_0$, we know that for any t, $x(t)$ is within interval $[-\beta(t), \beta(t)]$. From Lemma 5.2.2, we know that after a small enough time interval ϵ, $x(t + \epsilon)$ should lie in another interval $\mathcal{R} = [-\phi(\beta(t), \epsilon) + \mu, \phi(\beta(t), \epsilon) + \mu]$, where μ is the total amount of control input applied during interval $[t, t + \epsilon]$. So the volume of $\mathcal{R}$ is

$$V(\mathcal{R}) = 2\phi(\beta(t), \epsilon). \tag{5.10}$$

We divide the interval $\mathcal{R}$ into N parts, and let $\mathcal{L}_j$ indicate the jth part. so the total volume of these parts satisfies

$$\sum_{j=1}^{N} V(\mathcal{L}_j) = V(\mathcal{R}). \tag{5.11}$$

By dividing $\mathcal{R}$ into N subintervals, the encoder determines which subinterval the current state rests in and assigns a unique codeword to that interval. So N represents the total number of codewords used to encode the sampled state.

Since the performance level (5.5) is guaranteed for all $t \geq t_0$, we know that

$$V(\mathcal{L}_j) \leq 2\beta(t+\epsilon). \tag{5.12}$$

Therefore, from equation (5.10), (5.11) and (5.12), we arrive at the inequality that

$$N \geq \frac{\phi(\beta(t),\epsilon)}{\beta(t+\epsilon)}.$$

The above inequality means we need at least $\log_2\left(\frac{\phi(\beta(t),\epsilon)}{\beta(t+\epsilon)}\right)$ bits to represent the codeword for the sampled state. This means that the average bit-rate during this interval is

$$r(t,t+\epsilon) \geq \frac{\log_2\left(\frac{\phi(\beta(t),\epsilon)}{\beta(t+\epsilon)}\right)}{\epsilon}.$$

To obtain the instantaneous bit-rate at time t, we let ϵ to be infinitely close to 0, i.e.

$$r(t) = \lim_{\epsilon\to 0} r(t,t+\epsilon) \geq \frac{1}{\ln 2}\left(\frac{f(\beta(t))}{\beta(t)} + \alpha\right).$$

Since $r(t)$ is always non-negative, we have equation (5.9). □

Remark 5.2.4. *The term $\frac{f(\beta(t))}{\beta(t)}$ in equation (5.9) is proportional to the fastest increasing speed of the system. Our necessary stabilizing bit-rate is proportional to this speed.*

Theorem 5.2.3 is then applied to linear systems, and we have the following corollary.

Corollary 5.2.5. *If the plant (5.1) is linear, then the necessary bit-rate $\underline{r}_s$ to maintain the performance level (5.5) under safe regime is $\frac{L+\alpha}{\ln 2}$, i.e.*

$$\underline{r}_s = \frac{L+\alpha}{\ln 2}. \tag{5.13}$$

Remark 5.2.6. *The necessary bit-rate of continuous system given in [27] is recovered by our result in equation (5.13) with $\alpha = 0$, since [27] only considered uniform boundedness.*

5.2.2 Sufficient Bit-Rate under Safe Regime

This section first proposes an event triggered encoding and decoding algorithm under safe regime, and then analyze the bit-rate of this algorithm. Finally, we would like to discuss how to choose the parameters to achieve the necessary bit-rates for linear systems.

Before giving the algorithm, we would like to introduce some variables to make the algorithm easier to read. Let M_e and M_d, stored in encoder and decoder respectively, indicate which regime the system is running in. To be more specific,

$$M_e, M_d = \begin{cases} 0, & \text{under safe regime;} \\ 1, & \text{under unsafe regime,} \end{cases}$$

The algorithm presented using a programmable timer whose variable, t, is reset by the program and updated in real-time

We're assuming the encoder and decoder both know what the triggering event is. With this assumption, once a sampling event is triggered, then both encoder and decoder know the magnitude of the sampled state. So, one only needs to transmit a single bit to indicate the sign of the state. The details of this algorithm are given below.

Algorithm 5.2.7. *Event triggered encoding and decoding under safe regime.*

Encoder algorithm

If system enters safe regime, i.e. $M_e \neq 0$ *and* $|x(t)| \leq x_a$*, then*

1. *Initialization*

   - *Update system regime to be safe, i.e.* $M_e = 0$.
   - *set timer variable,* $t \equiv 0$*, and start the timer.*
   - *Quantize* $x(0)$ *as* $q = \begin{cases} 00, & \text{if } x(0) \geq 0; \\ 01, & \text{if } x(0) < 0. \end{cases}$
   - *Send* q_0 *to decoder.*
   - *Wait for the acknowledgement from the decoder and set* $d_0 = t$.

2. *while* $(t > d_0)$

   - *If* $|x(t)| = \theta(x_a, t - d_0) = x_a e^{-\alpha(t-d_0)}$,
     - *Quantize* $x(t)$ *as* $q = \begin{cases} 0, & \text{if } x(t) \geq 0; \\ 1, & \text{if } x(t) < 0. \end{cases}$
     - *Send* q *to decoder.*
   - *If system enters unsafe regime, go to encoder algorithm under unsafe regime*

Decoder algorithm

If system enters safe regime, i.e. $q = 00$ *or* 01*, then*

1. *Initialization*

   - *Update system regime to be safe, i.e.* $M_d = 0$.
   - *Reset timer variable* $t \equiv 0$ *and restart the timer.*
   - *Estimate state as* $\hat{x}(0) = \begin{cases} \frac{x_a}{2}, & \text{if } q = 00; \\ -\frac{x_a}{2}, & \text{if } q = 01. \end{cases}$
   - *Send an acknowledgement to encoder.*

2. *while* $(M_d = 0)$,

   - *If received packet is quantized data then update state estimate,*

$$\hat{x}(t) = \begin{cases} \theta(x_a, t), & \text{if } q = 0; \\ -\theta(x_a, t), & \text{if } q = 1. \end{cases}$$

   - *If received packet signals regime change, then go to unsafe regime decoder algorithm.*

Given the encoding and decoding algorithm, let's analyze the sufficient bit-rate to guarantee the system performance. Since the number of bits transmitted at each time is fixed (2 bits for regime changing and 1 bit otherwise), one only needs to bound the maximum acceptable delay for each packet where 'acceptable' means the system satisfies the performance bound in (5.5).

The safe regime can be divided into 2 time intervals. The first time interval $[0, d_0)$ is the one during which the 'regime changing' packet is transmitted. The second time interval $[d_0, t_f)$, where t_f indicates the terminal time of this safe regime, is the interval over which the threshold function θ is used to trigger transmission.

For time interval $[0, d_0]$, we need to guarantee that the performance level (5.5) is satisfied and the state trajectory comes back to the absorbing region after q_0 is received and the control is applied, i.e. $|x(d_0)| \leq x_a$. The next lemma gives an upper bound on the initial delay d_0.

Lemma 5.2.8. *If*

$$d_0 \leq \min\left\{\frac{\ln\left(\frac{3}{2}\right)}{L}, \frac{\ln\rho}{L+\alpha}\right\}, \tag{5.14}$$

then $|x(d_0)| \leq x_a$ and equation (5.5) is satisfied for all $t \leq d_0$.

Proof. Let x_0 indicate the initial state when the state enters the safe regime. From equation (5.4), we have

$$|x(d_0)| = \left||\phi(x_0, d_0)| - \frac{x_a}{2}\right| \leq \left||x_0|e^{Ld_0} - \frac{x_a}{2}\right|.$$

To make sure $|x(d_0)| \leq x_a$, we have $d_0 \leq \frac{\ln(3x_a/(2|x_0|))}{L}$. Since the inequality holds for any $x_0 \in [-x_a, x_a]$, we have the first term of equation (5.14).

Besides, we also need to guarantee that the performance level is satisfied, i.e. $|x(t)| \leq \rho x_a e^{-\alpha t}$ for all $t \in [0, d_0]$. To guarantee this, we force $|x_0|e^{Ld_0} \leq \rho x_a e^{-\alpha d_0}$,

and have the following solution $d_0 \leq \frac{\ln(\rho x_a/|x_0|)}{L+\alpha}$. To make sure that the inequality holds for any $|x_0| \leq x_a$, we have the second term of equation (5.14). □

With the upper bound on the initial delay given by Lemma 5.2.8, we assure that the system state is bounded by the threshold θ at time d_0. For the second time interval $[d_0, t_f)$, we require not only that the state is bounded by the threshold function after packet is received and the control input is applied, i.e. $|x(a_i)| \leq \theta(x_a, a_i - d_0)$, but also that the performance level indicated by equation (5.5) is guaranteed, i.e $|x(t)| \leq \beta(x_a, t)$ for all $t \in [s_i, a_i]$. To do that, we provide an upper bound on the delay d_i in the next lemma.

Lemma 5.2.9. *During time interval $[d_0, t_f)$, if*

$$d_i \leq \min\left\{\frac{\ln 2}{L+\alpha}, \frac{\ln(\rho e^{-\alpha d_0})}{L+\alpha}\right\}, \tag{5.15}$$

where ρ satisfies $\rho e^{-\alpha d_0} > 1$ for any d_0 satisfies (5.14), then $|x(a_i)| \leq \theta(x_a, a_i - d_0)$ and $|x(t)| \leq \beta(x_a, t)$ for all $t \in [s_i, a_i]$.

Proof. Using the same technique as in the proof of Lemma 5.2.8, we have

$$|x(a_i)| \leq |x(s_i)|e^{Ld_i} - x_a e^{-\alpha(s_i - d_0 + d_i)}.$$

To make sure $|x(a_i)| \leq \theta(x_a, a_i - d_0)$, and realizing that $|x(s_i)| = x_a e^{-\alpha(s_i - d_0)}$, we get $d_i \leq \frac{\ln 2}{L+\alpha}$.

To guarantee $|x(t)| \leq \rho x_a e^{-\alpha t}$ for all $t \in [s_i, a_i]$, we first notice that $|x(t)| \leq |x(s_i)|e^{Ld_i}$ for all $t \in [s_i, a_i]$. If

$$|x(s_i)|e^{Ld_i} \leq \rho x_a e^{-\alpha(s_i + d_i)},$$

then $|x(t)| \leq \beta(x_a, t)$. Solving the equation above with $|x(s_i)| = x_a e^{-\alpha(s_i - d_0)}$, we

have $d_i \leq \frac{\ln(\rho e^{-\alpha d_0})}{L+\alpha}$. □

Remark 5.2.10. *The requirement on ρ, i.e. $\rho e^{-\alpha d_0} > 1$, indicates that after time d_0, the threshold function is always below the performance level.*

From Lemma 5.2.9, we see that if we properly choose parameter ρ, we can minimize the sufficient stabilizing bit-rate. The next corollary tells us what we should pick.

Corollary 5.2.11. *Suppose the ith transmission occurs during the time interval $[d_0, t_f)$. If we choose ρ such that*

$$\rho \leq 2^{\frac{\alpha+L}{L}},$$

then as long as the delay satisfies

$$d_i \leq \frac{\ln 2}{L+\alpha},$$

$|x(a_i)| \leq \theta(x_a, a_i - d_0)$ *and* $|x(t)| \leq \beta(x_a, t)$ *for all* $t \in [s_i, a_i]$.

Proof. This corollary is true, if $\frac{\ln 2}{L+\alpha} \leq \frac{\ln(\rho e^{-\alpha d_0})}{L+\alpha}$, i.e. $d_0 \leq \frac{\ln \frac{\rho}{2}}{\alpha}$. To make sure that the initial delay in (5.14) still works, we force $\frac{\ln \frac{\rho}{2}}{\alpha} \geq \frac{\ln \rho}{L+\alpha}$, and have $\rho \leq 2^{\frac{\alpha+L}{L}}$. □

Using Lemma 5.2.8 and corollary 5.2.11, one obtains the following theorem characterizing the sufficient stabilizing bit-rate under the safe regime.

Theorem 5.2.12. *Under safe regime, if q_0 is transmitted with bit-rate $r(0)$ satisfying*

$$r(0) \geq \bar{r}_s(0) = \frac{2}{\min\left\{\frac{\ln\left(\frac{3}{2}\right)}{L}, \frac{\ln \rho}{L+\alpha}\right\}},$$

and q_i for $i = 1, 2, \cdots$ is transmitted with bit-rate $r(i)$ satisfying

$$r(i) \geq \bar{r}_s(i) = \frac{L + \alpha}{\ln 2},$$

then the performance level (5.5) is guaranteed with $\rho \geq 2^{\frac{\alpha+L}{L}}$.

Remark 5.2.13. *If the system is nonlinear, it's easy to verify that $\underline{r}_s \leq \bar{r}_s$. If the system is linear, the equality holds, i.e. $\underline{r}_s = \bar{r}_s$. Therefore, for linear system, we can say that after the initial delay, the performance level (5.5) is guaranteed with the necessary stabilizing bit-rate under safe regime.*

5.3 Sufficient Bit-Rate under Unsafe Regime

This section first proposes an algorithm for unsafe regime to assure the resilience, and then analyzes the bit-rate of this algorithm.

The basic idea of our algorithm under the unsafe regime is very simple. For each transmission, the encoder asks the decoder to move towards the origin by $2x_a$. This step movement guarantees that the plant's state does not move across the absorbing region in a single step. Once the packet is received and the control input is applied, the encoder checks the state again. If the state is still out of the absorbing region, i.e. $|x(t)| \geq x_a$, the encoder asks the decoder to move towards the origin by $2x_a$ again. Otherwise, the system enters the safe regime, and uses the safe regime's algorithm instead.

Algorithm 5.3.1. *Event triggered encoding and decoding under unsafe regime*

Encoder algorithm

If system enters unsafe regime, then

1. Initialization

- *Update system regime to be unsafe, i.e. $M_e = 1$.*

- *If* $|x(t)| \leq x_a$*, go to encoder algorithm under safe regime.*
- *Reset timer variable,* $t \equiv 0$ *and restart timer.*
- *Quantize* $x(0)$ *as* $q = \begin{cases} 10, & \text{if } x(0) \geq 0; \\ 11, & \text{if } x(0) < 0. \end{cases}$
- *Send* q *to decoder.*
- *Wait for the acknowledgement from decoder*

2. while $|x(t)| > x_a$

- *Quantize* $x(t)$ *as* $q = \begin{cases} 0, & \text{if } x(0) \geq 0; \\ 1, & \text{if } x(0) < 0. \end{cases}$
- *send* q *to decoder*
- *wait for acknowledge*

3. Go to encoder's safe-regime algorithm.

Decoder algorithm

If the system enters the unsafe regime, i.e. $q = 10$ *or* 11*, then*

1. Initialization.

- *Update system regime to be unsafe, i.e.* $M_d = 1$.
- *Estimate state as* $\hat{x}(0) = \begin{cases} 2x_a, & \text{if } q = 10; \\ -2x_a, & \text{if } q = 11. \end{cases}$
- *Send an acknowledgement to encoder.*
- *Wait for quantized data from encoder.*

2. while $M_d = 1$

- *If system enters safe regime, set* $M_d = 0$ *and go to decoder algorithm under safe regime.*
- *Estimate state as* $\hat{x}(t) = \begin{cases} 2x_a, & \text{if } q = 0; \\ -2x_a, & \text{if } q = 1. \end{cases}$
- *Send an acknowledgement to encoder.*

Remark 5.3.2. *Under unsafe regime, the zoom out idea in [9] can also be applied. However, in this zoom out strategy, the controller is assumed to have unlimited power to drive the system state back to the neighborhood. This is not practical in most cases. Considering this limitation, we propose algorithm 5.3.1. With this algorithm,*

for each time, only $2x_a$ amount of control is applied for each time, so the control effort is uniformly bounded.

Since the number of bits is fixed in each packet, one only needs to bound the delay to determine a sufficient bit-rate for resilience.

Lemma 5.3.3. *Under unsafe region, if the delay of the jth transmission, d_j, satisfies*

$$d_j < \frac{2x_a}{\bar{L}} \tag{5.16}$$

then there exist a pair of encoder and decoder that guarantee the system's resilience, i.e. for any $|x(0)| > x_a$, there exists a finite time T_f such that $|x(T_f)| \leq x_a$.

Proof. If for every transmission, the magnitude of the state is decreased, i.e.

$$|x(s_{j+1})| < |x(s_j)|, \forall j = 0, 1, 2, \cdots \tag{5.17}$$

then there must exist a constant $\sigma_j \in (0, 1)$ such that $|x(s_{j+1})| \leq \sigma_j |x(s_j)|$, for all $j = 0, 1, 2, \ldots$. Hence, we have $|x(s_N)| \leq (\sigma^*)^N |x(0)|$, where $\sigma^* = \max_{j=0,1,\cdots,N-1} \sigma_j$. Since $\sigma_j \in (0, 1)$ for all $j = 0, 1, \cdots, N$, $\sigma^* \in (0, 1)$. So, for any $x(0)$ and x_a, one can always find a finite integer N such that

$$|x(s_N)| \leq (\sigma^*)^N |x(0)| \leq x_a.$$

In other words, the system is resilient.

From equation (5.4), we have

$$|x(s_{j+1})| \leq |x(s_j)| + \bar{L} d_j - 2x_a.$$

To make sure that (5.17) is true, we have $d_j < \frac{2x_a}{\bar{L}}$ □

With Lemma 5.3.3, we give the sufficient bit-rate to guarantee resilience under unsafe regime in the next theorem.

Theorem 5.3.4. *Under unsafe regime, if q_0 is transmitted with bit-rate*

$$r(0) > \bar{r}_u(0) = \frac{\bar{L}}{x_a},$$

and the bit-rate of the jth transmission for $j = 1, 2, \cdots, N$, $r(j)$, satisfies

$$r(j) > \bar{r}_u(j) = \frac{\bar{L}}{2x_a},$$

where N indicates the last transmission index under unsafe regime, then there exists a pair of encoder and decoder to guarantee that the system is resilient, i.e. for any $|x(0)| > x_a$, there exists a finite time T_f such that $|x(T_f)| \leq x_a$. $\bar{r}_u$ is called the sufficient resilience bit-rate.

Remark 5.3.5. *Notice that the sufficient resilience bit-rate $\bar{r}_u$ is independent with the initial state $x(0)$. It means that no matter how far away the system state is from the origin, the state can always be pushed back into the absorbing region with the same bit-rate.*

5.4 Simulation Results

In this section, we first use a nonlinear case to demonstrate Theorem 5.3.4 which says that the system is resilient against any state jump with a bit-rate that is only slightly higher than the sufficient resilience bit-rate. Besides, we also show that a certain performance level is guaranteed under safe regime. A linear case is presented to show that our algorithm achieves the necessary stabilizing bit-rate in the safe regime.

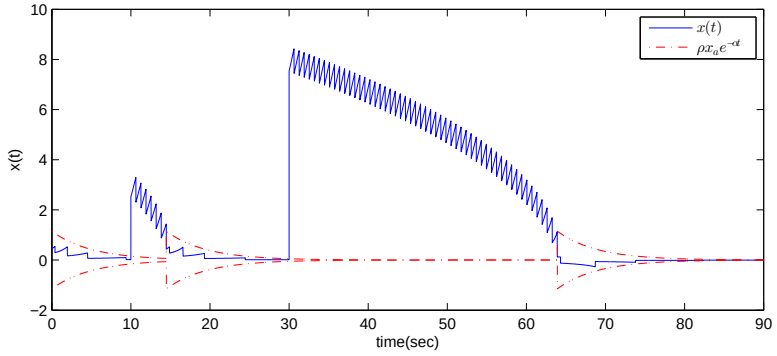

Figure 5.3. System performance for the nonlinear system

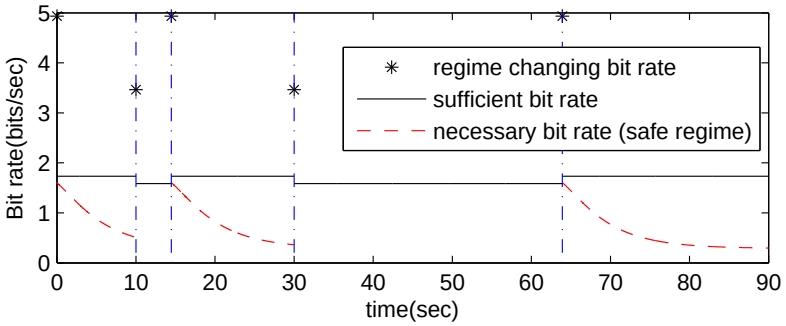

Figure 5.4. Necessary and sufficient bit-rates for the nonlinear system

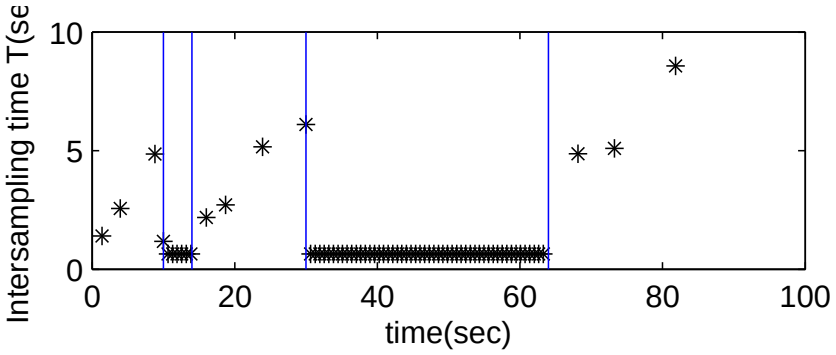

Figure 5.5. Inter-sampling interval for the nonlinear system

Consider the following nonlinear system:

$$\dot{x} = \begin{cases} |x|sin(x) + u + w, & \text{if } |x| \leq \rho x_a; \\ \arctan(x) + u + w, & \text{if } |x| > \rho x_a. \end{cases}$$

with $-0.9x_a$ as the initial state. $x_a = 0.5$ is the magnitude of absorbing region. We choose our performance level to be $\beta(t) = \rho x_a e^{-0.2(t-t_0)}$ with $\rho = 2^{\frac{0.2+L}{L}}$, where $L = 1$ is the Lipschitz constant under safe regime. $\bar{L} = \pi/2$ is the uniform bound of $|f(x)|$ when $|x| > \rho x_a$. When the system is under unsafe regime, we choose the maximum delay to be 1.01 of the sufficient resilience bit rate.

The system is run for 90 seconds with maximum delay, and two impulsive disturbances hit the system with magnitude $5x_a$ and $15x_a$ at time 10s and 30s, respectively. The system performance is given in Figure 5.3 with x-axis and y-axis indicating time and state, respectively. At time 10s and 30s, the state (solid line) jumps to 2.5 and 7.8, respectively. With the same maximum delay, which is 0.99 of the sufficient resilience delay, we see from the plot that the system state comes back to the absorbing region in 5 seconds for the first attack and 34 seconds for the second attack, which shows that as long as the bit-rate is higher than the sufficient resilience bit-rate, no matter how far away the state is, the system is resilient, i.e. comes back to the absorbing region in finite time. Examining the system behavior in the safe regimes (time intervals $[0, 8]$, $[42, 50]$ and $[58, 75]$) one sees that the performance level (dot dashed line) is guaranteed.

Figure 5.4 gives the bit-rates of the system. x-axis is time, and y-axis is bit-rate. Since the regime changing packet has 2 bits, the corresponding bit-rate (stars) is higher than the other packets. We also notice that there is a gap between the necessary stabilizing bit-rates (dashed line) and the sufficient stabilizing bit-rates (solid line) under safe regimes (intervals $[0, 8]$, $[42, 50]$ and $[58, 75]$). That is because our sufficient stabilizing bit-rates are calculated from a global Lipschitz constant.

This global Lipschitz constant becomes more conservative as the state goes to 0.

The inter-sampling interval $s_{i+1} - s_i$ is given in Figure 5.5 with x-axis indicating time and y axis indicating inter-sampling interval. In unsafe regimes, the inter-sampling intervals are constant since we always set our delay to be the maximum delay. In safe regimes, we can see that the inter-sampling intervals are increasing with respect to time, or in other words, increasing as x goes to the origin, which implies that our system is efficiently attentive [65].

To test how tight our sufficient resilience bit-rate is, we use 0.9 of the sufficient resilience bit-rate to run the system when the system is under unsafe regime. Figure 5.6 gives the system performance with the same disturbances that we use in Figure 5.3. We can see that for the first disturbance with magnitude of $5x_a$, the system is still resilient, but for the second disturbance with magnitude of $15x_a$, the system can't come back to the absorbing region again. That's because when $x = 5x_a$, $\bar{L}$ doesn't bound $|f(x)|$ tight enough, but when $x = 15x_a$, $\bar{L}$ is a very close upper bound on $|f(x)|$.

To verify our necessary stabilizing bit-rate, we use 0.9 of this bit-rate to run the system under safe regime. Figure 5.7 gives the system performance with initial state to be x_a. we see that the state trajectory (solid line) becomes unbounded. That's because the delay is so long that after the control input is applied, the state is still above the threshold (dashed line), the event $|x(t)| = \theta(x_a, t)$ will never occur, and there is no transmission anymore. This verifies that the system can't be stabilized with a bit-rate lower than this necessary rate.

Now, let's consider a linear system as below.

$$\dot{x} = \begin{cases} 2x + u + w, & \text{if } |x| \leq \rho x_a; \\ 4\arctan(x) + u + w, & \text{if } |x| > \rho x_a, \end{cases}$$

with initial state to be 2. The magnitude of absorbing region x_a is 3, and the

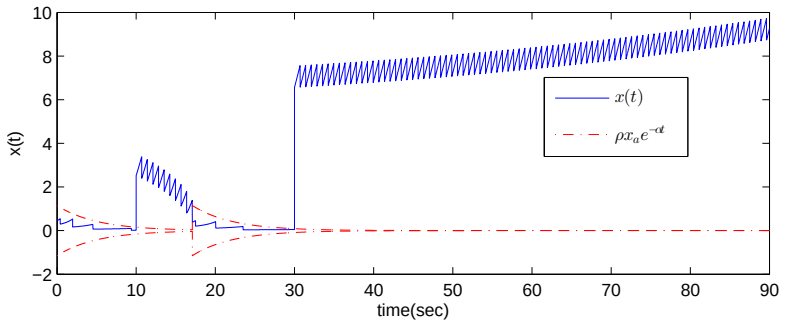

Figure 5.6. System performance for nonlinear system with 0.9 of $\bar{r}_u$

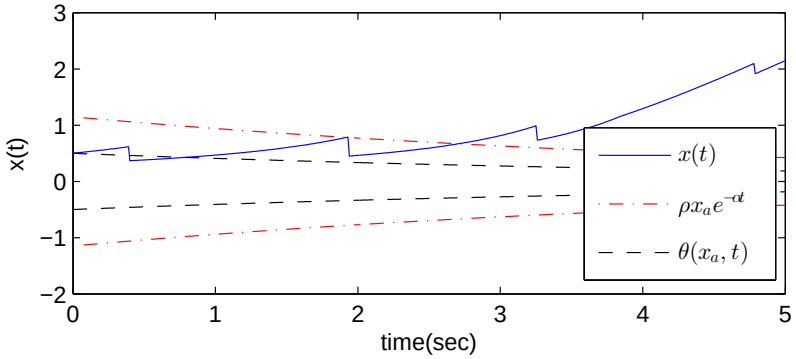

Figure 5.7. System performance for nonlinear system with 0.9 of necessary bit-rate under safe regime

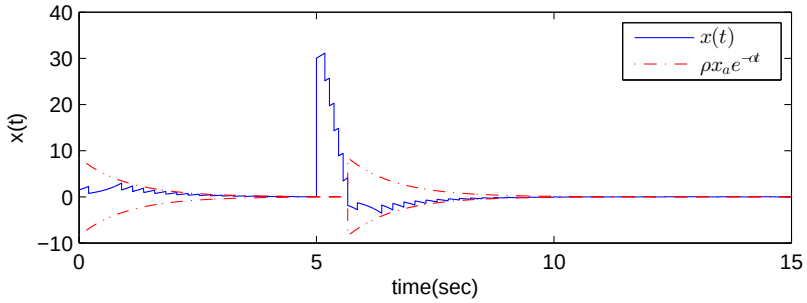

Figure 5.8. System performance for the linear system

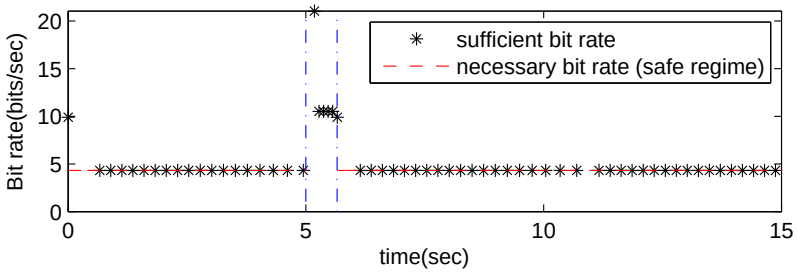

Figure 5.9. Necessary and sufficient bit-rates for the linear system

performance level is chosen to be $\beta(t) = \rho x_a e^{-\alpha}$ with $\rho = 2^{\frac{1+2}{2}}$. When $|x| > \rho x_a$, the uniform bound on $|f(x)|$ is $\bar{L} = \pi/2$. The maximum delay under unsafe regime is chosen to be $0.1\frac{2x_a}{\bar{L}}$.

We ran the system for 15 seconds. Figure 5.8 shows the performance of the system. x-axis indicates time, and y-axis indicates state. The system is attacked at time 5s with the state (solid line) jumping to 30. We can see that the state comes back to the absorbing region in about 2 seconds, which demonstrates that our system is resilient. Under safe regimes, which are intervals $[0, 5]$ and $[7, 15]$, the performance level (dashed line) is always guaranteed. The necessary and sufficient bit-rates are shown in Figure 5.9 with x-axis to be the time, and y-axis indicating bit-rate. We notice that under safe regimes, the gap between the sufficient stabilizing bit-rate (stars) and the necessary bit-rate (dashed line) is 0 (except the first packet indicating 'regime change'). It demonstrates our assertion that for linear systems, we achieve the necessary stabilizing bit-rate.

5.5 Conclusions and Future Works

This chapter studies the resilience of event triggered systems against impulsive disturbances with unknown magnitude. An even triggered strategy is provided to achieve the resilience, and the sufficient resilience bit-rate is derived. This sufficient

resilience bit-rate is independent with the initial state, which means that no matter how far away the system state is driven to, we can always use the same bit-rate to move the state back to the absorbing region.

CHAPTER 6

CONCLUSION

The integration of networking and information technology (NIT) into control systems has the potential to make control systems less expensive, more efficient, and more sustainable. There are, however, two challenges to apply NIT in control systems: limited transmission frequency and limited instantaneous bit-rate. Both challenges can destroy or degrade control systems. To address these two challenges, event triggered transmission, with which a transmission is triggered by the advent of an event, was raised, and it was shown in many experiments that event triggered systems transmitted less often than periodic triggered systems with comparable system performance [5, 6, 59, 64, 15, 3, 44, 67, 63]. But in the prior work, analytical tradeoff between system performance and transmission frequency was missing, and the influence of limited instantaneous bit-rate was totally ignored.

This dissertation examines the tradeoff among system performance, transmission frequency, and instantaneous bit-rate in event triggered state estimation and control systems. We first study the optimal transmission rule which minimizes mean square state estimation error with limited transmission frequency in Chapter 2. It is shown that the optimal transmission rule is event triggered. Because of the computational complexity of the optimal event trigger, a computationally efficient suboptimal event trigger and an upper bound on the suboptimal cost are provided. Moreover, to characterize how far away the suboptimal cost is, a computationally efficient lower bound on the optimal cost is also given. Our simulation results show that we provide tighter lower bound on the optimal cost, and tighter upper bound on the suboptimal

cost than prior work [14, 12, 35], while guaranteeing similar actual cost.

The same idea is, then, extended to output feedback system in Chapter 3. In this chapter, the whole feedback loop is closed over network, and we study the optimal transmission rules for both sensor and controller such that the mean square state is minimized with limited transmission frequency. The optimal transmission rules for both sensor and controller, again, are event triggered and difficult to compute. Therefore, computationally efficient and weakly coupled suboptimal event triggers are proposed. By 'weakly coupled', we mean that both the event trigger in sensor, and the event trigger in controller are based on local information only, the transmission in controller does not necessarily trigger the transmission in sensor, and vice versa. This weakly coupled event trigger design represents an advance over the synchronized transmissions in [16].

All the work above only considers limited transmission frequency. But to fully characterize the usage of communication, we need to know not only how often the channel is used, i.e. transmission frequency, but also how much bandwidth is used for each transmission, i.e. instantaneous bit-rate. Therefore, Chapter 4 and 5 examine both the minimum inter-sampling interval and the sufficient instantaneous bit-rate required to achieve ISS and resilience, respectively.

Chapter 4 provides not only the minimum inter-sampling interval and the sufficient instantaneous bit-rate to guarantee ISS, but also a sufficient condition of efficient attentiveness. An event triggered system is efficiently attentive if its inter-sampling interval gets longer and the required sufficient instantaneous bit-rate gets lower when the system state is closer to the origin. Meanwhile, our simulation results show that there is a tradeoff between the inter-sampling interval and the instantaneous bit-rate, which indicates that while maximizing the inter-sampling interval, we need to guarantee that the channel bandwidth can support the required instantaneous bit-rate.

One of the advantages of efficiently attentive event triggered control systems is

that long inter-sampling interval can be achieved when the system state is close to its equilibrium. A concern about this long inter-sampling interval is whether event triggered system is resilient to unexpected disturbances between two consecutive transmissions. Chapter 5 addresses this concern by considering a train of transient unknown magnitude disturbances in a scalar nonlinear system. The system is analyzed under two operational regimes: safe and unsafe. Under safe regime, a necessary instantaneous bit-rate and a sufficient instantaneous bit-rate are presented to guarantee uniform boundedness, and the necessary bit-rate meets the sufficient bit-rate when the system is linear. Under unsafe regime, a sufficient instantaneous bit-rate is given to guarantee resilience, i.e. returning to a neighborhood of the origin in a finite time. Moreover, detailed algorithms under both safe and unsafe regime are provided, and our simulation results demonstrate that event triggered systems are indeed resilient to transient unknown magnitude disturbances.

APPENDIX A

Proofs

Lemma A.0.1. *The filtered state error, $\overline{e}_{KF}(k)$ is orthogonal to $e_{KF,RO}(k)$.*

Proof. Since Kalman filter is the minimum mean square estimate of the state based on all history measurements $\{y(0), \ldots, y(k)\}$, the estimation error $\overline{e}_{KF}(k)$ is orthogonal to any function of the history measurements $\{y(0), \ldots, y(k)\}$. Since both $\overline{x}_{KF}(k)$ and $\overline{x}_{RO}(k)$ (see equation (2.11) and (2.12)) are functions of history measurements $\{y(0), \ldots, y(k)\}$, $\overline{e}_{KF}(k)$ is orthogonal to $e_{KF,RO}(k)$. □

Lemma A.0.2. *Let $l(k) = \max\left\{l : \tau_s^l \leq k\right\}$ indicate the latest transmission time from the sensor subsystem to the controller subsystem. The a posteriori history information $\mathbf{H}(k)$ is*

$$\begin{aligned}\mathbf{H}(k) = \big\{&\tau_s^1, \tau_s^2, \cdots, \tau_s^{l(k)}, \overline{x}_{KF}(\tau_s^1), \overline{x}_{KF}(\tau_s^2), \cdots, \overline{x}_{KF}(\tau_s^{l(k)}),\\ &u_a(0), u_a(1), \ldots, u_a(k-1)\big\},\end{aligned}$$

for $k = 0, 1, \ldots$. Correspondingly, we also define the a priori history information, the history information known by the controller subsystem before the event detector in sensor subsystem decides whether to transmit at step k, $\mathbf{H}^-(k)$ as

$$\begin{aligned}\mathbf{H}^-(k) = \big\{&\tau_s^1, \tau_s^2, \cdots, \tau_s^{l(k-1)}, \overline{x}_{KF}(\tau_s^1), \overline{x}_{KF}(\tau_s^2), \cdots, \overline{x}_{KF}(\tau_s^{l(k-1)}),\\ &u_a(0), u_a(1), \ldots, u_a(k-1)\big\}.\end{aligned}$$

for $k = 0, 1, \ldots$ *with* $\mathbf{H}^-(0) = \emptyset$. *The a posteriori remote state estimate in equation (3.2) satisfies*

$$\overline{x}_{RO}(k) = E(x(k)|\mathbf{H}(k)),$$

and the a priori remote state estimate $\overline{x}_{RO}^-(k)$ *in equation (3.1) satisfies*

$$\overline{x}_{RO}^-(k) = E(x(k)|\mathbf{H}^-(k)).$$

Proof. Now, let's examine how the remote state estimate evolves. The initial condition is

$$\overline{x}_{RO}^-(0) = E(x(k)|\mathbf{H}^-(0)) = \mu_0.$$

If information is transmitted from sensor to controller at step k, the history information at step k is $\mathbf{H}(k) = \{\mathbf{H}^-(k), \overline{x}_{KF}(k)\}$, and the a posteriori remote state estimate is

$$\begin{aligned}
\overline{x}_{RO}(k) &= E(x(k)|\mathbf{H}^-(k), \overline{x}_{KF}(k)) \\
&= E(\overline{x}_{KF}(k) + \bar{e}_{KF}(k)|\mathbf{H}^-(k), \overline{x}_{KF}(k)) \\
&= \overline{x}_{KF}(k),
\end{aligned}$$

where the second equality holds because $\bar{e}_{KF}(k)$ is uncorrelated with $\mathbf{H}(k)$.

If information is not transmitted from sensor to controller at step k, the history information at step k is $\mathbf{H}(k) = \mathbf{H}^-(k)$, and the a posteriori remote state estimate is

the same as the a priori remote state estimate, i.e.

$$\begin{aligned}\overline{x}_{RO}(k) &= E(x(k)|\mathbf{H}(k)) = E(x(k)|\mathbf{H}^{-}(k)) \\ &= \overline{x}^{-}_{RO}(k).\end{aligned}$$

The a priori state estimate evolves as the following:

$$\begin{aligned}\overline{x}^{-}_{RO}(k) &= E(x(k)|\mathbf{H}^{-}(k)) \\ &= E(Ax(k-1) + Bu_a(k-1) + w(k-1)|\mathbf{H}^{-}(k)) \\ &= AE(x(k-1)|\mathbf{H}^{-}(k)) + Bu_a(k-1) \\ &= A\overline{x}_{RO}(k-1) + Bu_a(k-1),\end{aligned}$$

where the third equality holds because $w(k-1)$ is independent from $\mathbf{H}^{-}(k)$.

To conclude, we say that the minimum mean square remote state estimate based on $\mathbf{H}(k)$ takes the form of equation (3.1) and (3.2). □

BIBLIOGRAPHY

1. H. Alemdar and C. Ersoy. Wireless sensor networks for healthcare: A survey. *Computer Networks*, 54(15):2688–2710, 2010.

2. G. Anastasi, M. Conti, M. Di Francesco, and A. Passarella. Energy conservation in wireless sensor networks: A survey. *Ad Hoc Networks*, 7(3):537–568, 2009.

3. A. Anta and P. Tabuada. To sample or not to sample: Self-triggered control for nonlinear systems. In *Automatic Control, IEEE Transactions on*, volume 55, pages 2030–2042. IEEE, 2010.

4. A. Arapostathis, V. Borkar, E. Fernández-Gaucherand, M. Ghosh, and S. Marcus. Discrete-time controlled markov processes with average cost criterion: a survey. *SIAM Journal on Control and Optimization*, 31(2):282–344, 1993.

5. K. Arzen. A simple event-based pid controller. In *Proc. 14th IFAC World Congress*, volume 18, pages 423–428, 1999.

6. K. Astrom and B. Bernhardsson. Comparison of Riemann and Lebesgue sampling for first order stochastic systems. In *Decision and Control, 2002, Proceedings of the 41st IEEE Conference on*, volume 2, pages 2011–2016. IEEE, 2002. ISBN 0780375165.

7. S. Bayraktar. *Aggressive landing maneuvers for unmanned aerial vehicles*. PhD thesis, Massachusetts Institute of Technology, 2006.

8. S. Boyd and L. Vandenberghe. *Convex optimization*. Cambridge university press, 2004.

9. R. Brockett and D. Liberzon. Quantized feedback stabilization of linear systems. *Automatic Control, IEEE Transactions on*, 45(7):1279–1289, 2000.

10. M. Cardei and D.-Z. Du. Improving wireless sensor network lifetime through power aware organization. *Wireless Networks*, 11(3):333–340, 2005.

11. M. Choi, T. Lam, and B. Reznick. Sums of squares of real polynomials. In *Proceedings of Symposia in Pure Mathematics*, volume 58, pages 103–126. American Mathematical Society, 1995.

12. R. Cogill. Event-based control using quadratic approximate value functions. In *Decision and Control, 2009 held jointly with the 2009 28th Chinese Control Conference. CDC/CCC 2009. Proceedings of the 48th IEEE Conference on*, pages 5883–5888. IEEE, 2009.

13. R. Cogill and S. Lall. Suboptimality bounds in stochastic control: A queueing example. In *American Control Conference, 2006*, pages 1642–1647. IEEE, 2006.

14. R. Cogill, S. Lall, and J. Hespanha. A constant factor approximation algorithm for event-based sampling. In *American Control Conference, 2007. ACC'07*, pages 305–311. IEEE, 2007.

15. D. V. Dimarogonas and K. H. Johansson. Event-triggered control for multi-agent systems. In *Decision and Control, 2009 held jointly with the 2009 28th Chinese Control Conference. CDC/CCC 2009. Proceedings of the 48th IEEE Conference on*, pages 7131–7136. IEEE, 2009.

16. M. Donkers and W. Heemels. Output-based event-triggered control with guaranteed L8-gain and improved event-triggering. In *Proceedings of the 49th IEEE Conference on Decision and Control*, 2010.

17. E. Dynkin and A. Juškevič. *Controlled markov processes*, volume 235. Springer New York, 1979.

18. H. Farhangi. The path of the smart grid. *Power and Energy Magazine, IEEE*, 8 (1):18–28, 2010.

19. D. Finkel. Direct optimization algorithm user guide. *Center for Research in Scientific Computation, North Carolina State University*, 2, 2003.

20. E. Garcia and P. J. Antsaklis. Model-based event-triggered control with time-varying network delays. In *Decision and Control and European Control Conference (CDC-ECC), 2011 50th IEEE Conference on*, pages 1650–1655. IEEE, 2011.

21. E. Gordienko and O. Hernández-Lerma. Average cost markov control processes with weighted norms: value iteration. *Appl. Math*, 23:219–237, 1995.

22. X. Guo and Q. Zhu. Average optimality for markov decision processes in borel spaces: a new condition and approach. *Journal of Applied Probability*, 43(2): 318–334, 2006.

23. R. A. Gupta and M.-Y. Chow. Networked control system: Overview and research trends. *Industrial Electronics, IEEE Transactions on*, 57(7):2527–2535, 2010.

24. W. Heemels, J. Sandee, and P. Van Den Bosch. Analysis of event-driven controllers for linear systems. In *International Journal of Control*, volume 81, pages 571–590. Taylor & Francis, 2008.

25. O. Hernández-Lerma and J. Lasserre. *Discrete-time Markov control processes: basic optimality criteria*. Springer New York, 1996.

26. O. Hernandez-Lerma and J. Lasserre. Policy iteration for average cost markov control processes on borel spaces. *Acta Applicandae Mathematicae*, 47(2):125–154, 1997.

27. J. Hespanha, A. Ortega, and L. Vasudevan. Towards the control of linear systems with minimum bit-rate. 2002.

28. Y.-F. Huang, S. Werner, J. Huang, N. Kashyap, and V. Gupta. State estimation in electric power grids: Meeting new challenges presented by the requirements of the future grid. *Signal Processing Magazine, IEEE*, 29(5):33–43, 2012.

29. O. Imer and T. Basar. Optimal estimation with limited measurements. In *Decision and Control, 2005 and 2005 European Control Conference. CDC-ECC'05. 44th IEEE Conference on*, pages 1029–1034. IEEE, 2005. ISBN 0780395670.

30. O. Imer and T. Basar. Optimal estimation with scheduled measurements. In *Appl. Comput. Math*, volume 4, pages 92–101, 2005.

31. L. Isserlis. On a formula for the product-moment coefficient of any order of a normal frequency distribution in any number of variables. *Biometrika*, 12(1/2): 134–139, 1918.

32. H. Khalil and J. Grizzle. *Nonlinear systems*, volume 3. Prentice hall, 1992.

33. D. Lehmann and J. Lunze. Event-based control with communication delays. In *Proceedings of the 18th International Federation of Automatic ControlWorld Congress (IFAC'11)*, pages 3262–3267, 2011.

34. L. Li and M. Lemmon. Event-Triggered Output Feedback Control of Finite Horizon Discrete-time Multi-dimensional Linear Processes. In *Proceedings of the 49th IEEE Conference on Decision and Control*, 2010.

35. L. Li and M. Lemmon. Performance and average sampling period of sub-optimal triggering event in event triggered state estimation. In *Conference of decision and control*. IEEE, 2011.

36. L. Li and M. Lemmon. Weakly coupled event triggered output feedback control in wireless networked control systems. In *Communication, Control, and Computing (Allerton), 2011 49th Annual Allerton Conference on*, pages 572–579. IEEE, 2011.

37. L. Li and M. Lemmon. Computationally efficient suboptimal event trigger design for MMSE problem with limited communication. *submitted to IEEE Transaction of Automatic Control*, 2013.

38. L. Li and M. Lemmon. Efficient attentive event triggered control systems with limited bandwidth. *submitted to IEEE Transaction of Automatic Control*, 2013.

39. L. Li and M. Lemmon. Polynomial Approximation of Optimal Event Triggers for State Estimation Problems Using SOSTOOLS. In *American Control Conference (ACC), 2013*, 2013.

40. L. Li, M. Lemmon, and X. Wang. Event-triggered state estimation in vector linear processes. In *American Control Conference (ACC), 2010*, pages 2138–2143. IEEE, 2010.

41. L. Li, M. Lemmon, and X. Wang. Stabilizing bit-rates in quantized event triggered control systems. In *Hybrid Systems: Computation and Control*, 2012.

42. L. L. Li and M. Lemmon. Weakly coupled event triggered output feedback system in wireless networked control systems. *to appear in Discrete Event Dynamic System*, 2013. URL `http://www3.nd.edu/~lli3/publications/deds.pdf`.

43. L. L. Li, X. Wang, and M. Lemmon. Stabilizing bit-rates in disturbed event triggered control systems. In *the 4th IFAC Conference on Analysis and Design of Hybrid Systems*, 2012.

44. J. Lunze and D. Lehmann. A state-feedback approach to event-based control. In *Automatica*, volume 46, pages 211–215. Elsevier, 2010.

45. M. Mazo and P. Tabuada. On event-triggered and self-triggered control over sensor/actuator networks. In *Decision and Control, 2008. CDC 2008. 47th IEEE Conference on*, pages 435–440. IEEE, 2008.

46. M. Mazo and P. Tabuada. Decentralized event-triggered control over wireless sensor/actuator networks. *Automatic Control, IEEE Transactions on*, 56(10): 2456–2461, 2011.

47. S. Meyn. The policy iteration algorithm for average reward markov decision processes with general state space. *Automatic Control, IEEE Transactions on*, 42(12):1663–1680, 1997.

48. A. Molin and S. Hirche. Structural characterization of optimal event-based controllers for linear stochastic systems. In *Proceedings of the 49th IEEE Conference on Decision and Control*, 2010.

49. P. Parrilo. Semidefinite programming relaxations for semialgebraic problems. *Mathematical Programming*, 96(2):293–320, 2003.

50. G. J. Pottie and W. J. Kaiser. Wireless integrated network sensors. *Communications of the ACM*, 43(5):51–58, 2000.

51. V. Powers and T. Wörmann. An algorithm for sums of squares of real polynomials. *Journal of pure and applied algebra*, 127(1):99–104, 1998.

52. S. Prajna, A. Papachristodoulou, P. Seiler, and P. Parrilo. Sostools: Sum of squares optimization toolbox for matlab. *Users guide*, 2004.

53. M. L. Puterman. *Markov decision processes: discrete stochastic dynamic programming*, volume 414. Wiley-Interscience, 2009.

54. M. Rabi, G. Moustakides, and J. Baras. Multiple sampling for estimation on a finite horizon. In *Decision and Control, 2006 45th IEEE Conference on*, pages 1351–1357. IEEE, 2006. ISBN 1424401712.

55. V. Raghunathan, C. Schurgers, S. Park, and M. B. Srivastava. Energy-aware wireless microsensor networks. *Signal Processing Magazine, IEEE*, 19(2):40–50, 2002.

56. C. Rieger, D. Gertman, and M. McQueen. Resilient control systems: next generation design research. In *Human System Interactions, 2009. HSI'09. 2nd Conference on*, pages 632–636. IEEE, 2009.

57. P. Santi. Topology control in wireless ad hoc and sensor networks. *ACM Computing Surveys (CSUR)*, 37(2):164–194, 2005.

58. S. M. L. C. (SMLC). Implementing 21st century smart nanufacturing. *Workshop Summary Report*. URL `https://smart-process-manufacturing.ucla.edu/about/news/Smart%20Manufacturing%206_24_11.pdf`.

59. P. Tabuada. Event-triggered real-time scheduling of stabilizing control tasks. *Automatic Control, IEEE Transactions on*, 52(9):1680–1685, 2007. ISSN 0018-9286.

60. S. Tatikonda and S. Mitter. Control under communication constraints. *Automatic Control, IEEE Transactions on*, 49(7):1056–1068, 2004.

61. M. H. ten Berge, B. Orlic, and J. F. Broenink. Co-simulation of networked embedded control systems, a csp-like process-oriented approach. In *Computer Aided Control System Design, 2006 IEEE International Conference on Control Applications, 2006 IEEE International Symposium on Intelligent Control, 2006 IEEE*, pages 434–439. IEEE, 2006.

62. K. Toh, M. Todd, and R. Tütüncü. Sdpt3 - a matlab software package for semidefinite programming. *Optimization Methods and Software*, 11(1-4):545–581, 1999.

63. P. Wan and M. D. Lemmon. Event-triggered distributed optimization in sensor networks. In *Information Processing in Sensor Networks, 2009. IPSN 2009. International Conference on*, pages 49–60. IEEE, 2009.

64. X. Wang and M. Lemmon. Self-Triggered Feedback Control Systems With Finite-Gain L_2 Stability. In *Automatic Control, IEEE Transactions on*, volume 54, pages 452–467. IEEE, 2009.

65. X. Wang and M. Lemmon. Attentively efficient controllers for event-triggered feedback systems. In *IEEE Conference on Decsion and Control*, 2011.

66. X. Wang and M. Lemmon. Minimum attention controllers for event-triggered feedback systems. In *IEEE Conference on Decision and Control-European Control Conference*, 2011.

67. X. Wang and M. D. Lemmon. Event-triggering in distributed networked control systems. *Automatic Control, IEEE Transactions on*, 56(3):586–601, 2011.

68. T. Wark, P. Corke, P. Sikka, L. Klingbeil, Y. Guo, C. Crossman, P. Valencia, D. Swain, and G. Bishop-Hurley. Transforming agriculture through pervasive wireless sensor networks. *Pervasive Computing, IEEE*, 6(2):50–57, 2007.

69. W. Wong and R. Brockett. Systems with finite communication bandwidth constraints. ii. stabilization with limited information feedback. *Automatic Control, IEEE Transactions on*, 44(5):1049–1053, 1999.

70. Y. Xu and J. Hespanha. Optimal communication logics in networked control systems. In *Proceedings of the IEEE Conference on Decision and Control*, volume 4, pages 3527–3532, Nassau, Bahamas, 2004.

71. H. Yu and P. J. Antsaklis. Event-triggered output feedback control for networked control systems using passivity: Triggering condition and limitations. In *Decision and Control and European Control Conference (CDC-ECC), 2011 50th IEEE Conference on*, pages 199–204. IEEE, 2011.

72. D. Yue, E. Tian, and Q.-L. Han. A delay system method to design of event-triggered control of networked control systems. In *Decision and Control and European Control Conference (CDC-ECC), 2011 50th IEEE Conference on*, pages 1668–1673. IEEE, 2011.

73. Q. Zhu and T. Basar. Robust and resilient control design for cyber-physical systems with an application to power systems. In *Proc. of 50th IEEE Conference on Decision and Control and European Control Conference, Orlando, Florida*, 2011.

This document was prepared & typeset with LaTeX 2$_\varepsilon$*, and formatted with* NDdiss2$_\varepsilon$ *classfile (v3.2013[2013/04/16]) provided by Sameer Vijay and updated by Megan Patnott.*